PRESIDENT CHURE TERAI-MADHESH CONSERVATION DEVELOPMENT BOARD
Lalitpur, Nepal

STOCK MEASUREMENT AND PROJECTION OF HARVESTING RIVER BED MATERIAL FROM THE RIVER SYSTEMS OF CHURE REGION OF PROVINCE NO. 2



FINAL REPORT

Volume-I, Main Report

July 2021

Submitted by:

Center for Applied Research and Development (CARD)
Institute of Engineering, Tribhuvan University in Association with Hydro Lab,
Pulchowk, Lalitpur

Acknowledgement

Center for Applied Research and Development (CARD), Institute of Engineering, Tribhuvan University is grateful to the Nepal government initiative under President Chure Terai-Madhesh Conservation Development Board (PCTMDCB) for the providing an opportunity to conduct a research on “Stock measurement and projection of harvesting river bed material from the river systems of Chure region of Province no. 2”, a relatively less studied topic in Nepal.

We are thankful to Mr. Birendra Yadav, Former Chairman and Mr. Man Bahadur Khadka, Former Member Secretary at PCTMCDB, for the support in formulation and approval of the project as well as co-operation during execution of the project. Likewise, we are grateful to the guidance and support provided by Mr. Rajan Regmi, Under Secretary (Tech), and Mr. Sarad Babu Pangeni, Under Secretary/Spokesperson at PCTMCDB. We are also thankful to Mr. Milan Dhungana, assistant Research Officer for his gracious, support and assistance during the execution of this project. Similarly, we would like to extend our gratefulness to Mr. Sudarsan Prasad Adhikari and Mr. Arbinda Mishra from Groundwater Board Division Office Lahan, and Birgunj respectively, whose support on data collection during field visit were invaluable. The historical data collection and status of river utilization would not have been possible without the gracious support of local people, who proved to be a valuable secondary data collection source. Last but not least, we would like to thank the current members at PCTMCDB Dr. Kiran Paudel (Chairperson), Dr. Krishna Prasad Acharya (Member-Secretary), Ms. Kamala Oli Siwakoti (Member), Mr. Sashi Kumar Sharma (Member), Dr. Susmita Dhakal (Member), Mr. Bhesh Raj Acharya (Member) and Mr. Shankar Kumar Giri (Ast. Forest Officer/ Information Officer), whose support, reviews and feedback were invaluable for the final outcome of this report. Lastly, our sincere gratitude to all the personnel and organization who helped us directly and indirectly during the project period.

Prof. Dr. Bhola Nath Sharma Ghimire
Director
Center for Applied Research and Development (CARD)
Institute of Engineering
Tribhuvan University

अनुसन्धान कार्यको सारांश

विगत दसकौं बर्षदेखि हालसम्म पनि चुरे तराई मधेश अत्यधिक उर्वर भूमि भएका कारणले कृषि र बसोबासको लागि बढ्दो एक आकर्षक स्थान बनेको छ । त्यसैले यस क्षेत्रमा जनसंख्याबृद्धि र बस्ती विस्तार व्यापक रुपमा भएको पाइन्छ । तीव्र शहरीकरण र पूर्वाधार बिकाश का कारण गिटी बालुवाजन्य निर्माण सामग्रीहरू को प्रयोग गर्ने प्रवृत्ति पनि अत्यधिक बढी रहेको छ । द्रुत राजमार्ग, गौतम बुद्ध विमानस्थल, हुलाकी राजमार्ग, पूर्व पश्चिम राजमार्ग विस्तार परियोजना जस्ता ठूला ठूला पूर्वाधार परियोजनाहरू यसै क्षेत्रमा निर्माण भैरहेका छन् । साथै पुर्व - पश्चिम रेल मार्ग आदि जस्ता राष्ट्रिय गौरव परियोजना हरू तथा आवस र स्थानीय पूर्वाधारकों निर्माणले पनि थप निर्माण सामग्रीहरुको मागलाई बढावा दिएका छन् । फलत निर्माण सामग्रीको आवश्यकता पुरा गर्नको लागी चुरे तराईमा रहेको नदी प्रणाली नै प्राथमिक रुपमा नदिजन्य निर्माण सामग्रीहरुको स्रोत हुनु परेको छ । यी नदीजन्य खानीस्रोतहरु स्थानीय सरकारको आम्दानीको प्राथमिक स्रोत पनि हो ।

मुलत यी उत्खननका गतिविधिहरू कुनै बैज्ञानिक अध्ययनको आधार भन्दा पनि कर प्रणाली मा आधारित देखिन्छन् र जसको कारण नदिप्रणालिको बातावरणमा नराम्रो असर परेको छ । यस्तो अस्थिर अबैज्ञानिक उत्खनन को अभ्यास ले खोलाको बातावरणिय प्रकोप र बाढी जन्य जोखिम बढाउने गर्दछ । बैज्ञानिक अध्ययन र विश्लेषण का आधारमा दिगो उत्खनन गर्न सके ति समस्याहरु धेरै हदसम्म अल्पिकरण (mitigation) गर्न सकिन्छ । अर्को तर्फ जलाधार क्षेत्रमा अध्ययन विनाको अबैज्ञानिक विकास निर्माण कार्य तथा बस्तिबस्ने परिपाठीले कतै नदी किनारामा क्षयीकरण हुन गयको छ भने कतै नदीको प्राकृतिक सतह बढ्न गई पुर्वाधारहरुलाई क्षति पुग्न गएको देखिन्छ । त्यसैले बैज्ञानिक अध्ययनका आधारमा ति प्रत्येक खोला प्रणालि बाट अधिकतम परिमाणमा निर्माण सामग्रीको रुपमा गेग्रान (sediment) उत्खनन गर्न सकिन्छ भन्ने सिमा निर्धारण गर्नु आवश्यक छ । यसै प्रसंगमा चुरे, दुन, भावर को प्राकृतिक श्रोत को व्यवस्थापन तथा संरक्षण को जिम्मेवार संस्था रास्ट्रपति चुरे तराइ मधेश संरक्षण विकास समिति (PCTMCDB) ले त्रिभुवन बिश्वबिद्यालय अन्तर्गतको इ.अ.स. मातहतको अनुसन्धान केन्द्र व्यबहारिक अनुसन्धान तथा बिकाश केन्द्र (CARD) लाई प्रदेश नं. दुईको खोलाप्रणालिमा रहेको निर्माण सामाग्रीको परिमाण नाप जांच तथा अनुमान गर्न र उत्खनन को प्रक्षेपण गरी अनुसन्धानात्मक प्रतिवेदन पेश गर्न जिम्मेवारी दिएको थियो । त्यसै प्रसंगमा उक्त अध्ययन कार्य गर्न रास्ट्रपति चुरे तराइ मधेश संरक्षण विकास समिति र व्यबहारिक अनुसन्धान केन्द्र बिचमा मिति २०२० जनवरी १९ मा एक सम्झौता भएको थियो । प्रदेश दुइ भित्र का चुरेका नदी प्रणालीहरुमा जम्मा हुने गेग्रान (Sediment) को परिमाण र यसको प्रकृतिको अवस्था पत्ता लगाउनका लागि ईन्जिनियरिङ्ग अध्ययन संस्थान अनुसन्धान तथा बिकाश केन्द्र,(CARD) लाइ दिईएको जिम्वेवारी अनुसार अनुसन्धानको लागी भौगोलिक पक्षको एकीकृत दृष्टिकोण प्रयोग गरि अध्यन कार्य गरीएको छ । भूगर्भीय अध्ययनमा नदी प्रणालीको भूगर्भीय बनावट र उत्पत्ति, साथसाथै जलस्रोत, गेग्रान Sediment) को गुणहरू र उनीहरूको वर्गीकरणबाट गेग्रानको असर र भूभौतिकी (ERT) अनुसन्धान का आधारमा

नदीको प्राकृतिक बेड तहमा जम्मा हुने गेग्रान को गहिराईको अवस्थाको वर्णन गरिएको छ । त्यसैगरि ईन्जिनियरिङ्ग अध्ययनमा प्रमुख नदीहरु को मार्ग रेखांकन गरि तथ्यांकित गर्ने, नदिप्रणालीको भिरालोपन हेर्न लम्बाई को निश्चित अन्तरालमा उचाइ नाँप गरि प्रोफाइल तयार गर्न ईन्जिनियरिङ्ग सर्वेक्षण गर्ने, जलबिज्ञान को अध्यन गर्ने , जलाधार क्षेत्रको भुक्षयको अध्यन गर्ने र जलबिज्ञानको आधारमा अवस्था अध्यन गरि गेग्रान (Sediment) को परिमाण अनुमान गरिएको छ । त्यस्तै वातावणिय अध्ययनको आधारमा भविष्यमा हुन जाने सम्भावित वातावरणिय आसर र वातारण मैत्री उत्खनन गर्ने अभ्यासहरुको पुनरावोलोकन गरिएको छ । विषयमा गेग्रान (Sediment) को परिमाण अनुमान गर्दा क्षयिकरण हुने, बगेर आउने र जम्मा हुने गेग्रान (Sediment) को परिमाण को दर (rate) हिसाब गर्दा दुइ बर्षको बहाबको अवधि (2 years return period) को पानीको वहावलाई लिएर क्षेत्रीय प्रचलित सुत्रका का आधारमा अनुमान गरीएको छ । थेग्रिने र क्षयिकरण को हिसाब गर्दा त्यस क्षेत्रको औसत बाढी हुने अवधिको गणना गरि नजिकको जलाधार क्षेत्रको अत्यधिक वर्षा को औसत लाइ आधार मानि गरिएको छ । चुरेबाट बग्ने प्राय जसो नदीहरु केहि समय मात्र बहने (ephemeral) प्रकारका हुन्छन् र बर्षाको बेला ठूलो बहाव हुने र ठूलो बहाव भएका बेला गेग्रानहरु तलतीर सर्ने काम हुन्छ । त्यसैले ईन्जिनियरिंग हिसाबका लागी औसत बहावको बिधि अनुसार गेग्रान सराइको हिसाब गणना गरिएको छ । अध्ययन क्षेत्रमा तथ्यांक को अभाव हुनुले यस अध्ययनमा अनुभवजन्य दृष्टिकोण (emperical approach) र पुनर्गमन र सहसम्बन्धको आधारमा तथ्यांकको विश्लेषण गरी विभिन्न हिसाब गणनाका चरणहरू प्रयोग भएको छ । नदीको गेग्रान ओसार्ने हिसाब अत्यधिक जटिल प्रकृया हो र हाल सम्म को भौतिकज्ञान मा अनिश्चितता अन्तर्निहित छ भने जलबिज्ञान को अनिश्चितता पनि थपिंदै आउँछ । त्यसैले उत्खननको परिमाणको हिसाब गर्दा उपरोक्त अनिश्चितता र दिगो सुरक्षाको हिसाबले नदीमा बगेर जम्मा हुन आउने गेग्रानको कूल परिमाण लाइ भाग गरेपछि प्राप्त हुने अंसलाइ लिईएको छ । यसै हिसाबले प्रदेश न २ का खोलाबाट बार्षिक दिगो उत्खनन गर्न सकिने परिमाण करिब एघार करोड (110.30 मिलियन) घनमिटर अनुमान गरिएको छ । यो सिफारीस गरिएको बार्षिक परिमाण उपयुक्त प्रविधि तथा वातावरण मैत्रि प्रविधिबाट हुनु जरुरि छ ।

यद्धपी यो अध्ययनको समयमा सुक्ष्म तथ्यांक को अभावले गर्दा त्यस क्षेत्रमा प्राप्त तथ्यांक को आधारमा गरिएकोले बिस्तृत सटिक बिश्लेशन हुन भने सकेको छैन । सुक्ष्म विश्लेषण गर्ने भनेको एक ठुलो चुनौतीको काम हो जसका लागि सरकारले परियोजना क्षेत्रमा उपयुक्त लगानी गरेर गर्नु पर्दछ । त्यस्तै जलवायु को सुचना अनुगमन गर्न पर्याप्त मात्रमा मापन केन्द्रहरु स्थापना गर्नु पर्दछ । तसर्थ यस अध्ययनको निस्कर्षहरु प्रयोग गर्नु अघि उत्खनन क्षेत्रमा मान्य हुनसक्छ वा सक्दैन ठहर गर्नुपर्दछ । सबै नदि प्रणाली बाट दिगो उत्खनन्को परिमाण तय गर्न गेग्रानको उत्खननको प्रभाव (बेग्लाबेग्लै भागमा र समग्रमा) को पूर्वानुमान गरेर मात्र गर्न सकिन्छ । यसको लागि जलाधारको गेग्रान थप गर्ने क्षमता, खोलाको (नदीको) बहाब को चरित्र, गेग्रानको स्थानान्तर हुने चरित्र, नदीको पर्यावरणिय अवस्थितिको बिस्तृत अध्यन आदि हुनु जरुरि छ । यसैले नदी प्रणालीबाट दिगो उत्खनन योग्य गेग्रानको मात्रा निर्धारण गर्नका लागि समग्र नदि

प्रणालि को दीर्घकालीन अनुगमन र नदीको भौतिक स्वरुपको नमुना अध्ययन (morphological modelling) परिक्षण गरिन्छ । प्रदेश २ का खोला प्रणालीबाट वार्षिक रुपमा उत्खनन गर्न सकिने गेग्रान को बिस्तृत बिबरण तल तालिकामा दिइएको छ ।

River Systems	Number of reaches	Harvestable Volume (Mm3/year)
Badahar-Gagan Khola	10	1.60
Bagmati Main	4	12.10
Bagmati Nadi-Chadi Khola	12	4.33
Bagmati Nadi-Mansumara-Bagahi Nadi	8	1.14
Balan Nadi	55	7.80
Baluwa-Bilauti Nadi	4	0.02
Banke Hardi Khola	15	3.78
Bataha Khola	8	1.40
Bhalubahi-Bakhariya Nadi	13	1.95
Bigahi Khola	18	1.74
Bihul Nadi	5	0.00
Dhansar Khola	3	0.40
Dudhaura Khola	17	6.30
Ghurmi Khola	14	2.91
Jaladh Nadi	13	2.23
Jhim Nadi	15	10.35
Kamala Main	5	8.81
Kamala Nadi-Charnath Khola	5	1.02
Khadak Nadi	17	0.07
Khado Khola	18	1.00
Lakhandehi Khola	52	8.00
Lal Bakaiya Nadi	21	6.65
Lamaha-Jhanj Khola	7	4.41
Mahuli Khola	10	0.54
Maraha Khola	24	4.97
Pasaha Khola	9	2.46
Pauda Khola	17	0.91
Paurai	4	0.04
Ratu Khola	22	4.81
Thute Sikhar Bas Khola	34	5.47
Tilabe Nadi	27	1.57
Trijuga Southern	3	0.00
Other Reaches	12	1.53
Grand Total	**501**	**110.29**

Executive Summary

Chure-Terai-Madesh, a valued region for both agriculture and settlement has reported an increased population and expanding settlements in past decades. The demand of construction materials is increasing due to rapid urbanization and infrastructure development. Large scale infrastructure projects like Fast Track Highway, Gautam-Buddha Airport, East-West Highway expansion project, the Postal Higway, East-West Railways, Madan Bhandari Highway – which are located in Chure-Terai-Madhesh region – constitute of the most of the demand. The river systems in Chure-Terai have an important role in fulfilling the construction material demand of the region. The river bed material abstraction have also been the primary sources of income for the local level government through the taxation on natural resources use.

In many cases, the allocated extraction volume are arbitrarily determined, poorly monitored and allocated based on ad-hoc practices. The existing extraction policies are barely based on scientific studies, and coupled with the lax regulations, has created environmental pressure on these river systems. This unsustainable extraction practice increases the risk of environmental hazards such as flooding, damage to the existing infrastructures (e.g., highways, bridges, dams), lowering of the ground water levels, loss of aquatic biodiversity to name a few. On the other hand unplanned developmental activities and unsustainable livelihood practices have resulted in severe erosion as well as depletion of some catchments. Because of this depletion and erosion, the river systems originating from these catchments are under acute stress due to high sediment yield from the region. This has resulted in morphodynamic changes in river such as channel migration, avulsion, and bank erosion/accretion which has significantly affected the agricultural areas, infrastructure and settlement in the Terai region.

It is evident that, a proper scientific study quantifying the available riverbed materials in the river systems of Chure region is required for the sustainable management of the river resources. So, Chure-Terai Madhesh Conservation Development Board (PCTMDCB) – an institution responsible for the management of the natural resources in Chure Hill, Bhavar, Terai Madhesh and Dun regions as a single landscape was requested to Center for Applied Research and Development (CARD) of Institute of Engineering (IOE), Tribhuvan University to carry out a study on "*Stock Measurement and Projection of Harvesting River Bed Material from the River Systems of Chure Region of Province No. 2*". Accordingly a contract agreement was signed between PTCMB and CARD on 19th January 2020 for conducting the study.

A unified approach involving geological, engineering and environmental assessments were used for the quantification of sediment and its nature in the rivers systems of Chure inside Province 2. The geological assessment involved the study on geological settings and origin of river system as well as the sediment source from the watershed, sediment properties and their classification, effects of slope stabilities on the sediment generation and characterization of the depth of river bed deposits based on geophysical investigation (i.e., ERT Surveys). The engineering assessment involved the delineation of river corridors, hydrology of the river systems, sediment yield, the sediment characterization along the longitudinal profile of the rivers, hydraulic properties of the classified river reach, sediment transport based on the hydraulic methods and estimation of erosion-deposition of sediment on the river reaches. The environmental assessment involved prediction of the potential impacts to the environment and reviewing the good practices of river bed material abstraction.

The annual harvestable sediment volume was determined based on sediment balance approach. The annual erosion and deposition rates were computed based on assumed formative discharge of the 2-year return period flow - derived from regional empirical method. Since, most of the rivers in study area are ephemeral type, major sediment transport occurs during rainfall events. The paucity of data in study area means, the duration of the rainfall events were determined based on the observation in the vicinity of the study area. A separate analysis of sediment transport for perennial rivers, Kamala and Bagmati were carried out, as these rivers differ from the ephemeral rivers in sediment transport phenomenon. Sediment transport is a highly complex phenomenon and current physical understanding has inherent uncertainty in sediment transport calculation in addition to uncertainty in hydrology. So the factor of 0.5 is used to incorporate such uncertainties. Thus, the annual harvestable volume from the River Systems of Province 2 is estimated as 110.30 Mm^3/ year and its distribution within the river systems is provided in the table below. The annual harvestable volume represents the annual replenishable rate of the deposits. The recommended volume needs to be extracted from the river systems using the well-established good river sediment extraction practices.

The computed volume of harvestable river bed material (sediments/aggregate) is a theoretical value. Although, the study used survey data and other data of the area, a fine resolution data is still absent for more accurate analysis of Individual river reaches. So, the results obtained from this study should be validated in the field before its application. The sustainable harvestable amount can only be estimated after prediction of the impacts of the sediment mining (individual and the cumulative) in the river reaches. This will require in depth study and monitoring of

sediment yield from the catchments, river flow, and sediment transport characteristics of the river reaches and ecological setting of the river, which is beyond the scope of the present study. So detailed studies involving long-term field monitoring and morphological modelling are recommended for determining the sustainable harvestable sediment volume from the River Systems.

River Systems	Number of reaches	Harvestable Volume (Mm3/year)
Badahar-Gagan Khola	10	1.60
Bagmati Main	4	12.10
Bagmati Nadi-Chadi Khola	12	4.33
Bagmati Nadi-Mansumara-Bagahi Nadi	8	1.14
Balan Nadi	55	7.80
Baluwa-Bilauti Nadi	4	0.02
Banke Hardi Khola	15	3.78
Bataha Khola	8	1.40
Bhalubahi-Bakhariya Nadi	13	1.95
Bigahi Khola	18	1.74
Bihul Nadi	5	0.00
Dhansar Khola	3	0.40
Dudhaura Khola	17	6.30
Ghurmi Khola	14	2.91
Jaladh Nadi	13	2.23
Jhim Nadi	15	10.35
Kamala Main	5	8.81
Kamala Nadi-Charnath Khola	5	1.02
Khadak Nadi	17	0.07
Khado Khola	18	1.00
Lakhandehi Khola	52	8.00
Lal Bakaiya Nadi	21	6.65
Lamaha-Jhanj Khola	7	4.41
Mahuli Khola	10	0.54
Maraha Khola	24	4.97
Pasaha Khola	9	2.46
Pauda Khola	17	0.91
Paurai	4	0.04
Ratu Khola	22	4.81
Thute Sikhar Bas Khola	34	5.47
Tilabe Nadi	27	1.57
Trijuga Southern	3	0.00
Other Reaches	12	1.53
Grand Total	**501**	**110.29**

Contents

Acknowledgement ii
Executive Summary iv
Contents vii
1 Introduction 17
1.1 Background 17
1.2 Objectives 18
1.3 Scope of Works 18
1.4 Methodology 19
1.4.1 Pre-field study works 19
1.4.2 Field Data Collection 19
1.4.3 Data processing and analysis 21
1.4.4 Sediment Yield from the catchment 21
1.4.5 Sediment thickness in the river bed 22
1.4.6 Routing of sediment in the river 22
1.4.7 Estimation of the annual harvest quantity 23
1.5 The Study Area 23
1.5.1 Location and physiography 23
1.5.2 Topography 23
1.5.3 Geology 24
1.5.4 Land cover 25
1.5.5 River systems 26
2 River system and hydrological study 27
2.1 River system 27
2.2 Hydrological analysis 29

2.2.1 Watershed Delineation 30
2.2.2 Flood Estimation using empirical methods 31
2.2.3 Duration of formative events for ephemeral rivers 34
2.2.4 Monthly flow of perennial rivers 34
3 Geological study 36
3.1 Geology of the Himalaya 36
3.1.1 Tectonic division of Nepal Himalaya 36
3.2 Geology of Province-2 42
3.2.1 Terai Plain 42
3.2.2 The Churiya 43
3.2.3 Sediment characteristics 44
3.2.4 Material Sources 45
4 Engineering geological study 55
4.1 Introduction 55
4.2 Landslide: Process and Types 55
4.3 Slope Stability Factors 57
4.4 Methodology 59
4.5 Landslides in Province 2 59
4.5.1 Observed Representative Landslides 62
4.6 Summary and discussion 69
5 Geophysical study 71
5.1 Background 71
5.2 Methodology 72
5.2.1 Electrical Resistivity Tomography 72
5.3 Geology of the study area 80
5.4 2D Electrical Resistivity Tomography Survey 80
5.4.1 Introduction 80

5.4.2 Management and Inversion of ERT data 80
5.4.3 ERT Profiles 81
5.4.4 Summary of the ERT surveys 91
6 Sediment yield from catchment 94
6.1 Rainfall Erosivity 94
6.2 Soil Erodibility Factor 96
6.3 Slope Length Factor (L-Factor) 97
6.4 Slope angle Factor (S-Factor) 97
6.5 Cover and Management Practice Factor (C-Factor) 98
6.6 Conservation Practice Factor (P) 98
6.7 Results 99
7 Topographic analysis 103
7.1 River cross-section survey 103
7.1.1 Methodology 104
7.1.2 River Cross-sections 107
7.2 Longitudinal profile analysis 109
8 Estimation of annual harvestable amount of sediment 112
8.1 Methods 112
8.2 Estimation of the hydraulic parameters of river reaches 113
8.3 Sediment transport of river reaches 118
8.4 Annual harvestable rate of sediment from river reaches 121
9 Impacts of riverbed sediment mining 124
9.1 Physical Environment 124
9.2 Biological Environment 124
9.3 Social Environment 124
9.4 Environmental and social impacts 125
9.4.1 Beneficial impact 125

9.4.2 Adverse impact 125
9.5 Good practices for gravel mining 127
10 Conclusions and Recommendations 130
10.1 Conclusions 130
10.2 Recommendation 130
11 References 132

List of Figures

Figure 1. River systems selected for field work and verifications 19
Figure 2. Location of the Study area 23
Figure 3. Digital Elevation Model of Province 2. 24
Figure 4: Generalized geological map of Province 2, Nepal (modified after DHM, 1987). 25
Figure 5. Land cover map of the study area in the year 2010. (Adapted from Uddin et al., 2014) 25
Figure 6. River systems in the study area 26
Figure 7. Major river systems in the study area 27
Figure 8. Existing Hydro-metrological stations in the study area. Only rain gauge stations are located, mostly in the downstream part of the catchments. 29
Figure 9. GIS based model used to derive watersheds. 31
Figure 10. Average monthly flow of Bagmati and Kamala Rivers. 35
Figure 11: (a) In the process of formation of the Himalaya the Indian Plate subducts below the Eurasian Plate and the Tethys Sea between the Plates shrinks; (b) Collision of the Plates gives birth of the Himalaya in expense of the closure of the Tethys Sea. 36
Figure 12. a) Map of the Himalaya plate boundary showing the important lithological and structural units and the limits of the western, central (Nepal), and eastern segments of the Himalaya (after Rajendran et al., 2017); b) Geological cross-section along the N-S line in Figure 2a. 37
Figure 13: Geological map of Nepal with location of Province 2 (modified after Upreti,1999). ..38
Figure 14: A view of part of the Terai Plain and the Siwalik as seen north from the Terai Plain. MFT=Main Himalayan Thrust. 43
Figure 15: Exposures of the Lower Siwalik mudstone north of Bardibas (left), and the Middle Siwalik sandstone at the Churiya Khola section, Parsa district (right). 44
Figure 16: An exposure of the Upper Siwalik conglomerate beds at the Churiya Khola section, Parsa district. 44
Figure 17: Slope stability states and destabilizing factors (Adopted from Popescu, 1994). 57
Figure 18: An overview of landslide distribution on the Google earth image in the Siwalik watersheds of the 129 river systems mentioned on Table 1. Red marks indicate landslide spots which are more than 40,000. 60
Figure 19: Slope and landslide distribution map of Province 2, Nepal. 61
Figure 20: Distribution of landslides in different slope range of Province 2. 61
Figure 21: Distribution of landslides in different slope range in Province 2 62

Figure 22: Photograph showing a) Rock fall on the Middle Siwalik sandstone on right bank of Churiya Khola, Bara District; b) Rock fall on the Middle Siwalik sandstone cliff on right bank of Churiya Khola adjacent to the E-W Highway, Bara District. 63
Figure 23: Photograph showing a plane rock failure along the bedding plane of the Middle Siwalik sandstone on right bank of Churiya Khola, Bara District (Photograph after TU-CDES, 2016). The slabby nature of the sandstone beds, its dipping parallel to the hill slope, and toe cutting by the Chriya River are the cause of the failure. 63
Figure 24: a) Landslide on Upper Siwalik conglomerate beds on right bank of Churiya Khola, Bara District. The conglomerate is highly-moderately weathered making it easier to develop landslide. The dry tributary stream of Churiya Khola has full of gravels generated from the landslide upstream; b) Landslide on hill face of the highly weathered Upper Siwalik conglomerate as source of river bed material in Churiya Khola valley, Bara District. 64
Figure 25: Google Earth images showing landslide distribution on the catchment of Bagmati River watersheds. Old landslide scars are abundant in the watershed. 64
Figure 26: An upstream view of Bakaiya Khola valley about 7 km north from the E-W Highway at Nijgad. Two landslides seen on the right side are caused by the Fast-track opening (at the bottom of the slides). The hills are made from the Middle Siwalik sandstone. The riverbed materials seen in the front part are of the Siwalik sandstone and Lesser Himalayan Quartzite with the large boulders mostly of sandstone. A belly bridge over the Bakaiya Khola is seen at the toe part of the landslides. 65
Figure 27: Photographs showing a) An example of river bank erosion and remobilization of the old river terrace materials of Bakaiya Khola as source of sediments to the downstream in addition to the materials added to the rivers by landslide from the mountain slope. The site is on the right bank of the Bakaiya Khola about 5 km north from the E-W Highway; b) River bank erosion caused by the Bakaiya Khola in the Terai Plain (when river runs high discharge during summer monsoon) south of the E-W Highway also supply sediments further downstream. The marks on the measuring stick are at 10 cm interval. 65
Figure 28: Photographs showing a) Landslides (white/grey marks) on the hills of Middle Siwalik sandstone on the right bank of the Bagmati River as seen north from about 1 km south from the E-W Highway at Karmaiya. The debris generated from the landslides delivers to the Bagmati River. Bagmati River and extracted riverbed materials are seen on the foreground; b) A close-up view of part of the photograph shown in (a) with the Bagmati River and Barrage on the foreground. 66

Figure 29: A view of Chapini Khola watershed a) With the Middle Siwalik hills and landslides (white/grey marks) on the mountain slopes. The sandstone is moderately-highly weathered. The Chapini riverbed is filled with white sands. View towards north (upstream); b) A distant view of a landslide (white/grey marks) on the Middle Siwalik sandstone further east from Chapini Khola.67
Figure 30: Photograph showing a) An upstream view of Khando Khola (as observed from the E-W Highway) with the Khando Khola itself on the foreground and the Middle Siwalik hills upstream. The Middle Siwalik sandstone has landslides (white/grey marks) of various sizes and that contribute sediments to the stream. The rocks are fresh to moderately weathered. The riverbed materials seen on the photograph is sand and silt. View towards north; b) A view of the Middle Siwalik hills in the catchment of Khando Khola further east with swamps of landslides (white/grey marks) on sandstone beds. The debris derived from the landslides ultimately discharges into the Khado Khola. View towards north from the E-W Highway. 67
Figure 31: Landslides and gully erosion caused huge erosion on the already weathered Lower Siwalik mudstone on the right bank of Ratu Khola north of Bardibas, Mahottari District. This process produces abundant clay to the downstream section.....68
Figure 32: Landslides on the cliff face of the highly weathered Lower Siwalik mudstone and the overlying Quaternary deposits (brown) on the right bank of Ratu Khola north of Bardibas, Mahottari District. The landslides are caused due to the slippery nature of the weathered mudstone, when wet, and toe cutting of the Ratu Khola. 68
Figure 33: Photographs showing landslides (white marks) on Middle Siwalik sandstone on left bank of the Ratu Khola north of Bardibas, Mahottari District. The rocks are moderately weathered. Landslides on the Ratu Khola produces abundant sand which is white in color.....69
Figure 34: Photographs showing a) A landslides (rockfall) on highly weathered sandstone and mudstone beds of the Middle Siwalik north of Lalbandi, Sarlahi District; b) Landslides on the Middle Siwalik sandstone in upstream section of Gagan Khola. 69
Figure 35: Schematic illustrating basic concept of electrical resistivity measurement, (Lowrie & Fichtner, 2020).....74
Figure 36: Conductivities and resistivity of common rocks, soils and ores. 75
Figure 37: The different four-electrode configurations. a) Wenner, b) Schlumberger and c) Dipole-Dipole. 77
Figure 38: Image showing the field setup of the ERT equipment at the surveyed river section..78
Figure 39: ERT profile alignment at the Bakaiya L2 transect. 82
Figure 40: ERT tomogram of Bakaiya-L2-ERT-1 and Bakaiya-L2-ERT-2 presented in the river cross-section profile. 83

Figure 41: Interpretated ERT tomogram of Bakaiya-L2-ERT-1 and Bakaiya-L2-ERT-2 presented in the river cross-section profile.....84
Figure 42 Spatial distribution of annual sediment yield (tonnes/hectare/year) in river systems of draining through Province 2 of Nepal 102
Figure 43 Schematic diagram of functioning of GNSS based Real Time Kinematic survey technique 103
Figure 44 View of Established base points in Bagmati River, Balan River and Bakaiya River .105
Figure 45 View of data collection along river cross-sections of Balan River, Bakaiya River and Ratu River (left to right) 106
Figure 46:Cross-section of the Bakaiya River at section R2 (X= 318,525.02, Y= 3,010,336.81) 107
Figure 47: Cross-section of the Bagmati River at section R2 (X=343,920.71, Y=2,992,497.89) 107
Figure 48: Cross-section of the Ratu River at section R1 (X= 395,527.22, Y= 2,993,859.33)..108
Figure 49:Cross-section of the Balan River at section R2 (X= 451,511.63, Y= 2,944,696.66) .108
Figure 50: Cross-section of the Khado River at section R4 (X= 478,829.28, Y= 2,933,630.33) 109
Figure 51: Longitudinal profile of the Bagmati River with location of field observation points and ERT data collection points 110
Figure 52: Longitudinal profile of the Bakaiya River with location of field observation points and ERT data collection points 110
Figure 53:Longitudinal profile of the Ratu River with location of field observation points and ERT data collection points.....111
Figure 54: Sediment dynamics of a typical river system (Source: Kondolf, 1997).....113
Figure 55: Representative cross-section of river based on their cross-sectional characteristics defined by the cumulative width and depth information 114
Figure 56: Y-Shaped distribution of cumulative river width vs water elevation calculated from field cross-section survey data of the Balan River at R1 115
Figure 57: U-Shaped distribution of cumulative river width vs water elevation calculated from field cross-section survey data of the Khado River at R6 116
Figure 58: W vs K graph plotted for the results obtained from field survey 117
Figure 59:Stream power (P) vs alpha (α) graph plotted for the results obtained from field survey 117
Figure 60: Slope vs D50 relation from selected rivers 120

Figure 61: Multiple Linear Regression for D50, slope and Upper Siwalik.....120
Figure 62: Exner equation describing the mass conservation principle in sediment transport..121
Figure 63: Depiction of erosion and deposition in different reaches.....121
Figure 64: Damage to the East-West Highway bridge over Ratu River Caused by the settlement of the pier. The river bed has lowered by at least 2.5 m due to riverbed sediment mining. A newly constructed bridge can be observed behind the damaged bridge. 126
Figure 65: Commonly adopted gravel mining practices (Source: Kondolf, 1993).....127
Figure 66: Sediment extraction by bar skimming (Source: http://threeissues.sdsu.edu/three_issues_sandminingfacts02.html) 128
Figure 67: The upstream and downstream effects of mining by pit or trench excavation (Source: M. G. Kondolf, 1997). 128
Figure 68: a) Sediment extraction by manual methods near observation point Bakaiya-2; b) Sediment extraction by using machines at the observation point Bakaiya-5. 129

List of Tables

Table 1. Land cover distribution in the study area. 26
Table 2. List of river systems in the study area.....27
Table 3. Values of standard normal variate for different return periods adopted by WECS/DHM method.....32
Table 4. Average monthly flow of Bagmati and Kamala Rivers.....35
Table 5: Geological coverage of Province 2, Nepal. 42
Table 6. River deposits (locations and material characteristics) studied in Province 2.....47
Table 7: Landslide distribution in different slope range in the Siwalik of Province 2.....62
Table 8: Summary of ERT profiles (The coordinate system used is WGS84, UTM, N45).....71
Table 9: Resistivity value with respective lithology 81
Table 10: ERT survey summary table 92
Table 11 Cover And Management Factor For Different Land Use(A. Pandey et al., 2015).....98
Table 12: Sediment yield from Rivers of Chure region of Province 2.....99
Table 13 Details of the base points established at the surveyed cross-sections.....105
Table 14: Estimated annual harvestable sediment volume from river systems of Province-2, Nepal 122

1 Introduction

1.1 Background

Chure region also known as the Siwaliks or the foothills of the Himalayas, is located between the lowland Terai plain and the Middle Mountain range. It was formed by the thrusting up of the deposited erosional debris from the Himalaya some 18 million years ago. The upper part of the region (Upper Siwalik) mainly consists of unconsolidated fine to coarse materials whereas the middle and the lower part (middle and lower Siwalik) is composed of soft and fine grained grey coloured sandstone and siltstone respectively. This region has remained fragile where soil erosion and landslide processes are very active partly due to its location within the zone of active crustal movement and weak geology. The erosion has resulted in loss of significant amount of sediment every year. Thus, the rivers originating from this region are sediment laden and cause significant amount of river bed aggradation further downstream on Lowland: Bhawar and Terai, where the sediment transport capacity of rivers is reduced. Aggradation of river beds have led to widening of the rivers and flooding causing significant damage to the infrastructures and agricultural lands in the Bhawar and Terai region.

River bed materials extraction could be an effective measure to control the river bed aggradation and mitigate associate hazards. The extracted materials such as sand, gravel and cobbles are valuable resources for the development of different infrastructures such as road paving, making concrete blocks, building construction etc. Nepal is picking up the development pace after emerging from decade long period of insurgencies which has increased the demand of construction materials. So, this demand can be partially fulfilled by the extracted river bed material from the Chure region.

There are also diverse effects of riverbed extraction such as depletion and loss of aquatic habitat, lowering of ground water table, bank erosion, river incision, change in river morphology etc. In addition, severe riverbed mining has threatened infrastructures on the rivers (such as bridges, dams and weirs etc.). In order to mitigate these impacts a study is required to determine the sustainable volume and methods of river bed material abstraction from Chure region. So, Chure-Terai Madhesh Conservation Development Board (PCTMDCB)– an institution responsible for the management of the natural resources in Chure Hill, Bhavar, Terai Madhesh and Dun regions as a single landscape – requested Center for Applied Research and Development (CARD) of Institute of Engineering (IOE), Tribhuvan University to carry out a study on “Stock Measurement

and Projection of Harvesting River Bed Material from the River Systems of Chure Region of Province No. 2". Accordingly a contract agreement was signed between PTCMB and CARD on 19th January 2020 for conducting the study.

1.2 Objectives

The main objective of the study is to delineate the reserve of river bed material in the river systems considered in this study and quantify the harvestable materials. The specific objectives of the study are as follows:

- Identify major provenance of construction materials with their geological and structural association
- Delineate areal extent of the deposits and its characterization
- Prepare geomorphic map and associated deposits of the material
- Estimate the volume of material and their types in 32 river systems identified by PCTMCDB
- Estimation of extractable material for the coming five years

1.3 Scope of Works

The scope of the study are as follow:

- Acquire information on distribution of riverbed material on the studied river by means of systematic mapping through remote sensing and field investigation.
- Optimum utilization of aerial photographs, Google images, topographic maps and previously study reports related to the present work.
- Assess the volume of deposits and characterize the material type
- Carry out study on river dynamics from hydraulic engineering perspective
- Geomorphic mapping of the study area linking with river dynamics from engineering and geological perspective
- Carry out longitudinal profile of the selected rivers
- Sampling of the sediments along the river reach
- Assess the source area for riverbed materials and its geological and structural association
- Application of geophysical method at selected rivers to investigate the thickness of deposits
- Recommendation of potential sites for further extraction of the materials.

1.4 Methodology

1.4.1 Pre-field study works

Reports of the similar previous studies, relevant literature and the guidelines and principles of sediment mining from river bed were collected and reviewed. All available topographic maps, satellite imageries, aerial photographs and geological maps of the study were thoroughly studied. The watershed areas of all river systems – referred in the Chure-Terai Madhesh Conservation and Management Master Plan – in the study area were delineated using GIS tools. Similarly, available hydrological and meteorological data from the stations within the study area and its vicinity were also collected. The river systems were grouped/clustered based on the similarities of the catchment properties (i.e topographic, geological and hydrological characteristics). A river system representing each group/cluster was then be selected for the detailed field investigation also including the geographic coverage and the downstream impact. Reaches of river, within the selected representative river systems, were then identified for the field measurements.

1.4.2 Field Data Collection

Five river systems: Bakaiya River, Bagmati River, Ratu River, Balan River and Khado River were selected for field work and verification based on the geological, catchment, geographical coverage and downstream impact criteria.

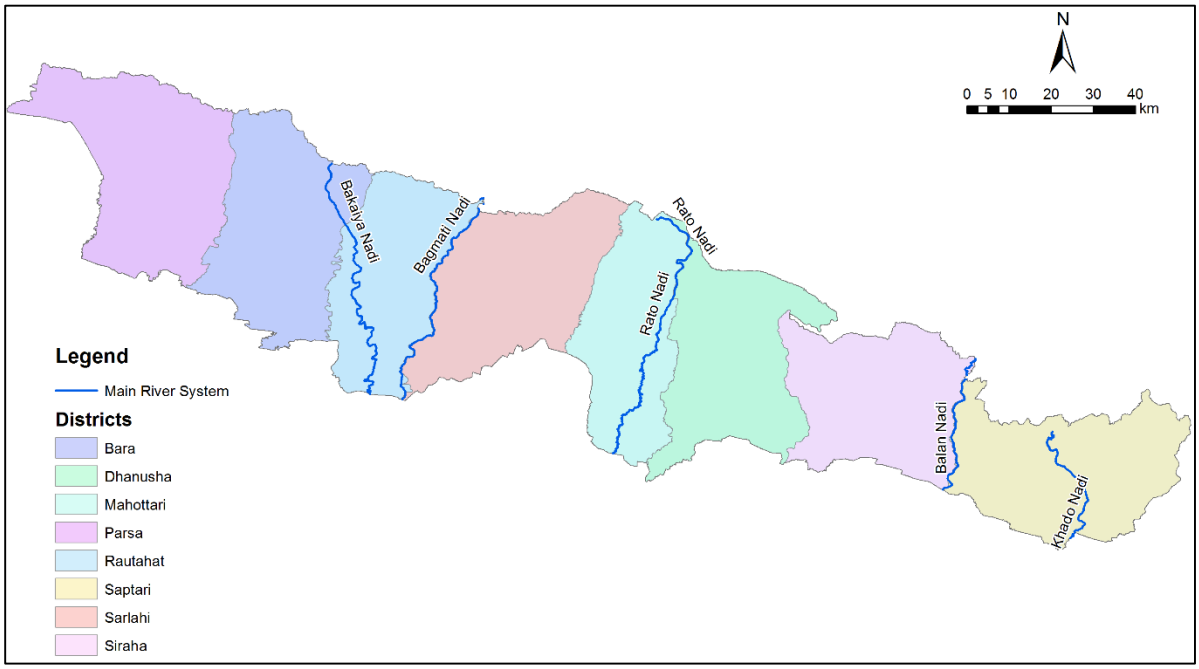


Figure 1. River systems selected for field work and verifications

The location of the river systems selected for the field study are shown in Figure 1. The following activities were carried out in the field.

1.4.2.1 Stakeholder discussion

A stakeholder discussion was carried out with the key informants in the field to understand the current gravel mining practices and supply and demand of the sand and the aggregates. The current situation and trend of ground water in the study area was also discussed with the key informants of the Department of Irrigation in Birgunj and Lahan.

1.4.2.2 Reconnaissance survey

A field reconnaissance survey along the selected river reach were first carried out by the study team. Most of the river cross-section selected for the field data collection were verified in the fiels. Similarly necessary photographs and videos of key geomorphological features and sediment characteristics of the river reach were also taken along with the GPS coordinates.

1.4.2.3 Geological\ engineering geological survey

Out of the 39 river systems in Province 2, Bagmati River, Kamala River and Bakaiya have origin in the Lesser Himalaya and flow to the south through the Siwalik range, carrying materials from both the Lesser Himalaya and the Siwalik. The remaining 36 river systems, on the other hand, originate within the Siwalik in Province 2 and north of it, and have materials derived from the Siwalik Hills. Surface distribution of the river-generated materials were mapped. Based on the field observations and laboratory analysis, engineering geological classification of the river deposits were also made.

1.4.2.4 Geophysical survey

Electrical Resistivity Tomography (2D-ERT) were used for the subsurface geological exploration in the river bed and banks. For carrying out 2D-ERT, electrical current of very low frequency was passed through the geological subsurface. The response of current on geological formations such as clay, silt, sand, gravel, boulders, and bedrock are different. By virtue of different capacity of different material on electrical conductivity, it is possible to separate different materials from each other.

The main scope of 2D-ERT was to explore characteristics of the subsurface riverbed material at different river basins. This allowed estimation of the composition and thickness of construction materials (sand and gravel) in the study area.

1.4.2.5 Cross-section survey

The cross-section surveys were carried out in Bakaiya, Bagmati, Ratu, Balan and Khado river systems, to compute the hydraulics and sediment transport charachteristics of the river reaches. The river reaches were long and the survey cross-sections were spaced at longer intervals. So, cross-section surveys were carried out using Differential GPS (DGPS) Real Time Kinematic (RTK) survey technique. In this technique a base station were placed in the permanent control marks established at the site and rover was used to collect the data. The precision of this method less than 5 cm horizontally and vertically, deemed acceptable for the current study.

1.4.3 Data processing and analysis

The information collected during the pre-field study and the field study will be compiled and analysed. The following parameters were derived:

1.4.3.1 Hydrological parameters

Hydrological parameters mainly floods of different frequency (2 years, 5 years and 10 years) were estimated using the following empirical methods.

- WECS/DHM method (Sharma & Adhikari, 2004)
- Modified Dicken's Method (Pandey et al., 2020)

The available measured rainfall data within the catchment or around the catchment were also used to derive the characteristics of floods. In the case of perennial rivers like Bagmati, the observed flow data was collected for the hydrological analysis. The hydrological parameters Kamala River (another perennial river) was then derived from Bagmati River by transposing using Catchment Area Ratio (Griffiths & McKerchar, 2008). The required catchment characteristics were derived based on the DEM and other relevant data.

1.4.4 Sediment Yield from the catchment

Sediment yield from a catchment is a complex process. It is combined result of the rainfall induced surface erosion and mass wasting phenomena along the hill slopes. Several empirical and semi-empirical models are available in the literature to estimate the sediment yield from the catchment. Empirical models such as Erosion Potential Models (EPM) (Efthimiou et al., 2017) are popular in estimating the sediment yield from the catchment. Gavrilovic initially derived the model in 1969 based on the experience in the mountain region of Balakan region of Europe and generalized to apply to the other parts of the world. These models have not yet been tested in the Chure region. The sediment yield from empirical methods is sensitive to the values of the parameters (because

they are more valid to the region where they were derived). So their values have to be evaluated comparing the results with the field measurements while applying to the other areas.

Semi-empirical methods, which are more physics based, are mostly based on computing the soil loss due to surface erosion, without considering the mass wasting phenomena. It should be noted that this method was originally developed to estimate sediment loss from the farm lands. However some of the parameters have been implemented to incorporate the gully erosions which are prevalent in the catchments. They have also been incorporated in many hydrological models and have been widely used to estimate the sediment yield from the mountainous catchments (Sinha et al., 2019). So, surface erosion models were preferred over the empirical models to estimate the sediment yield from the catchments in the study area. There are different relationships to estimate the sediment yield from the catchment based on surface erosion but Revised Universal Soil Loss Equation (RUSLE) (Renard et al., 1997) is widely used. The practically applicable model which can estimate the sediment yield from the mass wasting phenomena is so far not available.

1.4.5 Sediment thickness in the river bed

The main objectives of the geophysical investigation were as follows:

1. Show different layers of subsurface materials along the given profiles,
2. Find out ground water table along the given profiles,
3. Estimate the composition of construction materials at different depths

The main outcome of the 2D-ERT was a resistivity tomogram showing different electrical layers in the subsurface along the surveyed profile. Based on the resistivity values and geological information gathered during field work interpretative geological section were prepared. Further the content of particular material were estimated from the interpretative section based on surface observations.

1.4.6 Routing of sediment in the river

The channel characteristics as well as the sediment characteristics changes along the length of the river. So the sediment transported from the catchment was routed along the river channel by calculating the hydraulic transport capacity of the river reaches. The cross-section data was first used to compute the hydraulic parameters of the reach. Then sediment transport was estimated using Meyer-Peter & Müller (1948) transport formulation. Sediment continuity equation was then be used to estimate the amount of deposit or scour from the river bed.

1.4.7 Estimation of the annual harvest quantity

The harvest quantity of the river bed material shall be such that it does not cause much degradation of the river bed. The sediment at 2 years return period flood (which was assumed as the formative discharge of the channels) was routed along the channel and the reaches with deposition were identified. The average annual deposition rate will then be determined based on the likely annual deposition rate.

1.5 The Study Area

1.5.1 Location and physiography

The study area is situated in Province No. 2 of Nepal (Figure 2). This province only covers the Chure, Bhawar and Terai Physiography. Parsa, Bara, Rautahat, Sarlahi, Mahottari, Dhanusa, Siraha and Saptari districts lie in this province. So, most of the rivers flowing in the province originate from the Chure region.

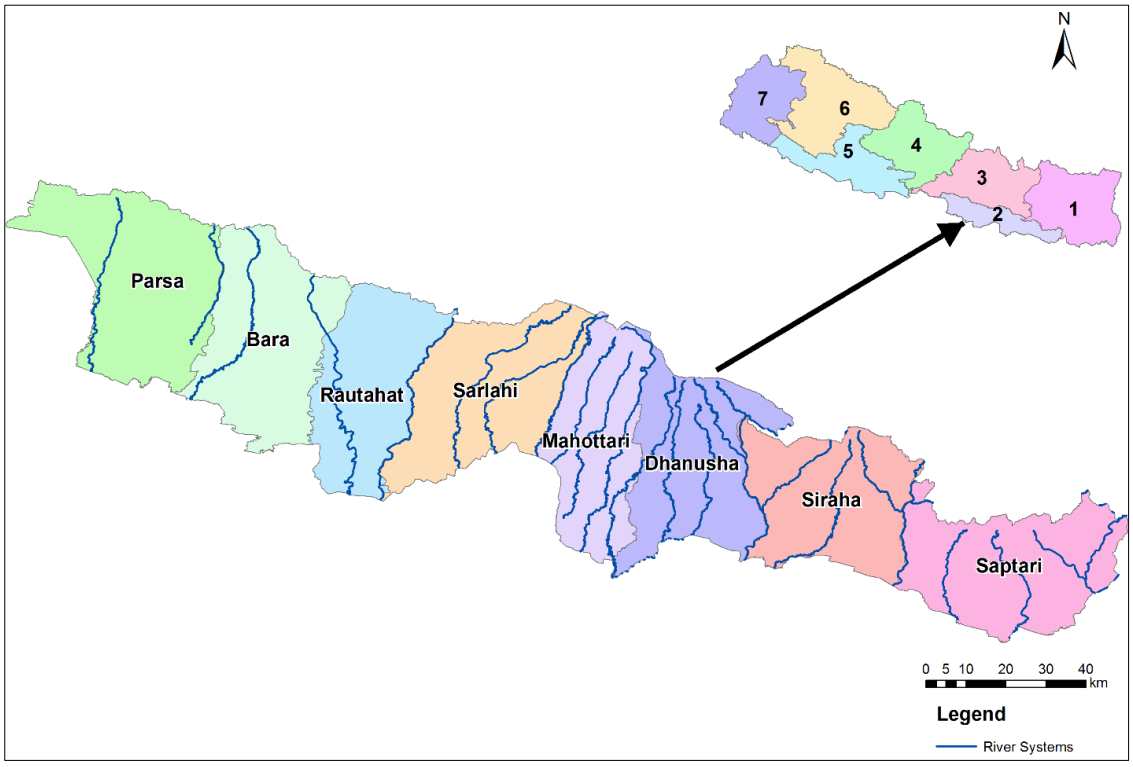


Figure 2. Location of the Study area

1.5.2 Topography

The elevation of the study area varies from about 60 masl in the south to about 870 m in the north(Figure 3). The southern part mainly consists of terai lowland whereas the northern part

consists of the Chure hills having higher elevations. The bhawar region only covers a small area lying in the foothills of Chure region.

1.5.3 Geology

Geologically, the province belongs to the Siwalik and the Terai Plain (Figure 4). The Siwalik zone makes a 5-15 km wide strip along east-west direction in the northern part of the province. It represents about 17% area of the province. The width of the Siwalik is minimum in Bara and Rautahat districts and the widest part lies in the Sarlahi and Dhanusa districts. About 83% area of the province is located south of the Siwalik and is known as the Terai Plain or the Indo-Gangetic plain. The widest part of the plain lies in the Rautahat and Mahottari Districts and is about 35 km.

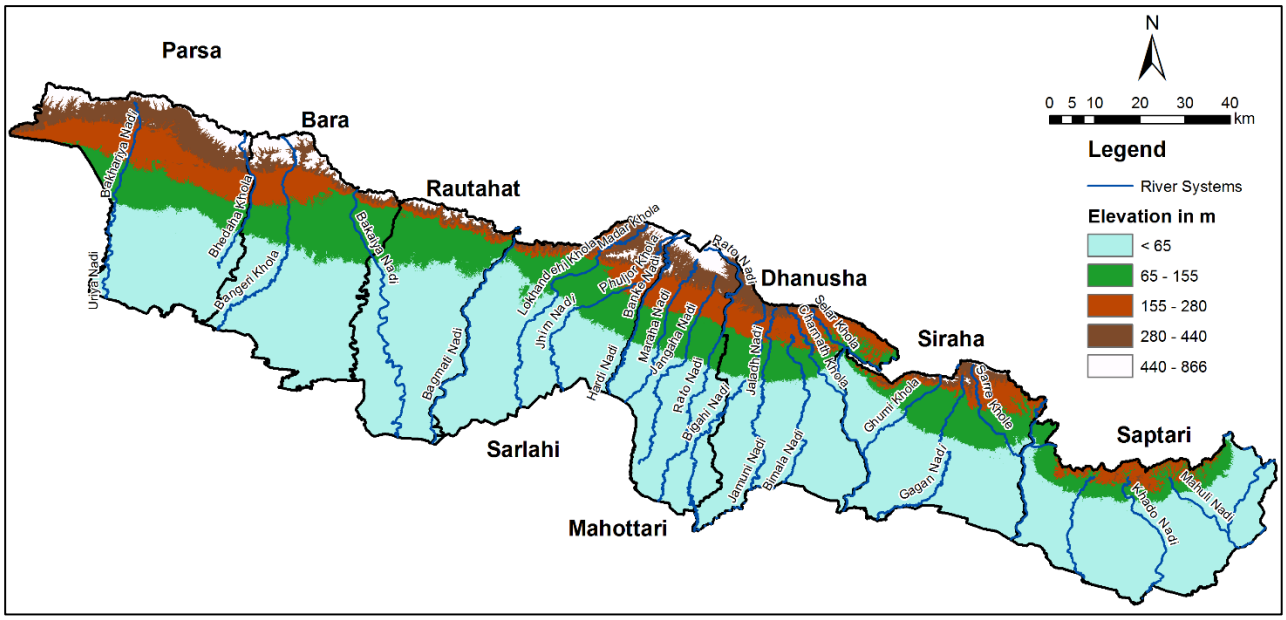


Figure 3. Digital Elevation Model of Province 2.

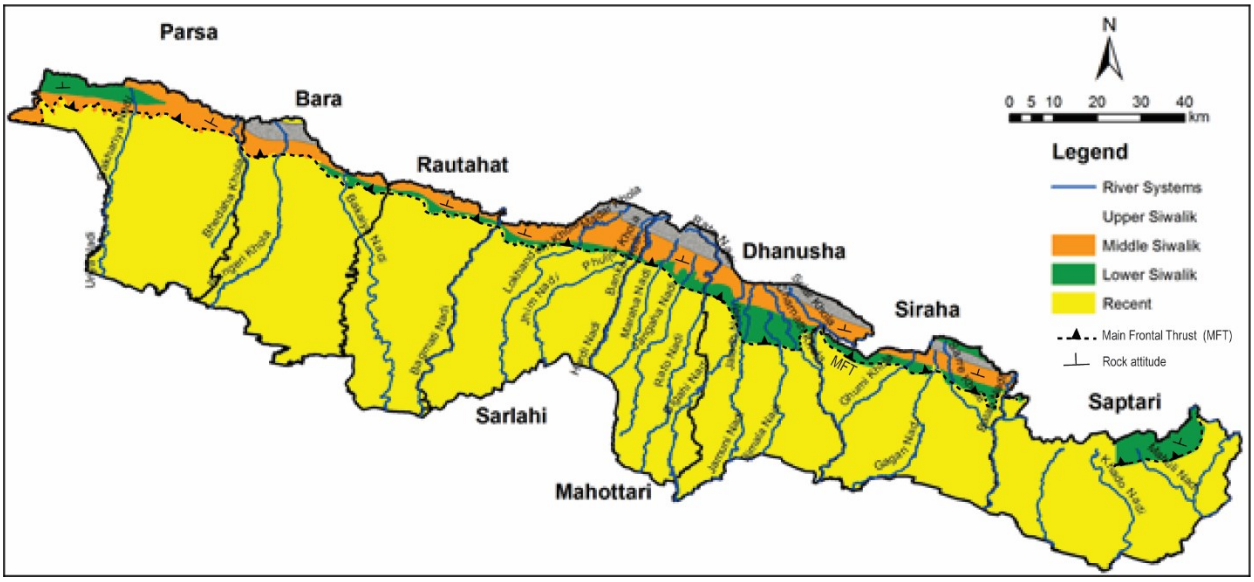


Figure 4: Generalized geological map of Province 2, Nepal (modified after DHM, 1987).

1.5.4 Land cover

The land cover of the study area consists of agriculture land, forest, grassland, shrubland, built-up area, barren land and the water bodies (Figure 5). Agriculture occupies the maximum area (63.62%) followed by forest (26.81%), barren area (5.31%), grassland (1.50%), built-up area (1.07%), water body (0.91) and shrubland (0.78%) respectively (Table 1).

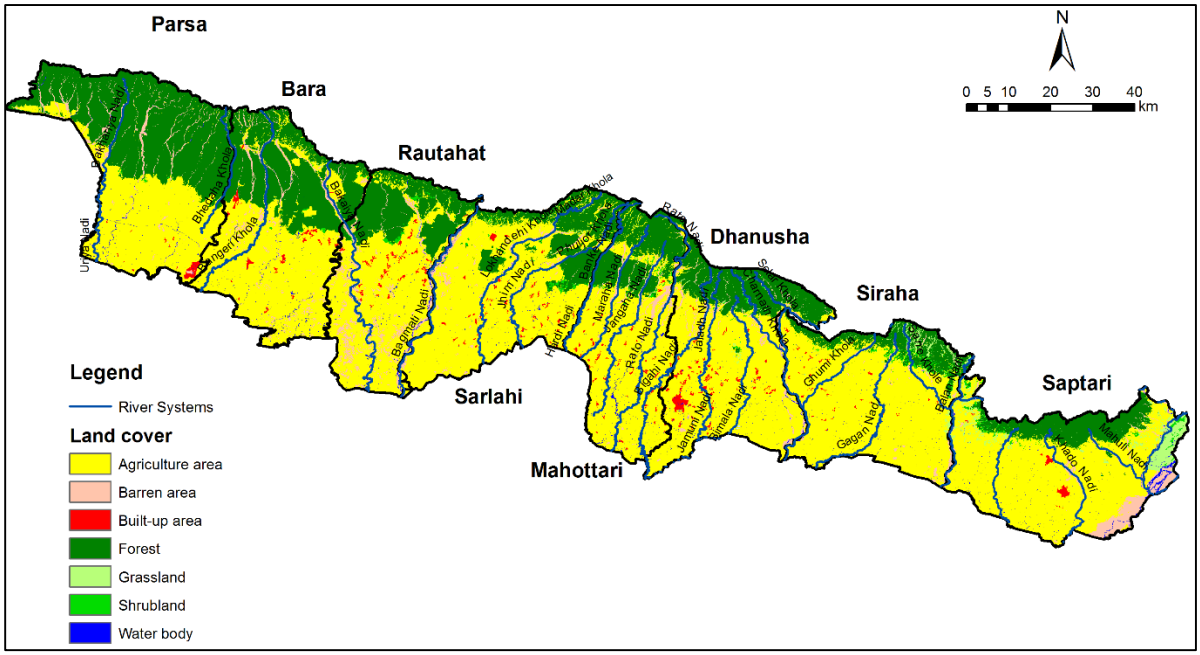


Figure 5. Land cover map of the study area in the year 2010. (Adapted from Uddin et al., 2014)

Table 1. Land cover distribution in the study area.

Land cover	Area (sq km)	% coverage
Forest	2570.14	26.81
Shrubland	74.50	0.78
Grassland	144.21	1.50
Agriculture area	6099.12	63.62
Barren area	509.26	5.31
Water body	87.29	0.91
Built-up area	102.62	1.07
Total	9587.147	100

The agriculture land is mostly located in the terai region whereas the forest mostly covers the chure and the bhawar region. The barren land and the water body mostly consists of the active corridor of the river and jointly constitutes of about 6.2% of the land cover of the study area.

1.5.5 River systems

The study area is bordered by Bakhriya River in the west and Koshi River in the east. There are 39 river systems in the study area most of which origin from the Chure region. Only Bagmati, Kamala and Bakaiya Rivers originate from the Mahabharata Range. Figure 6 shows the river systems in the study area.

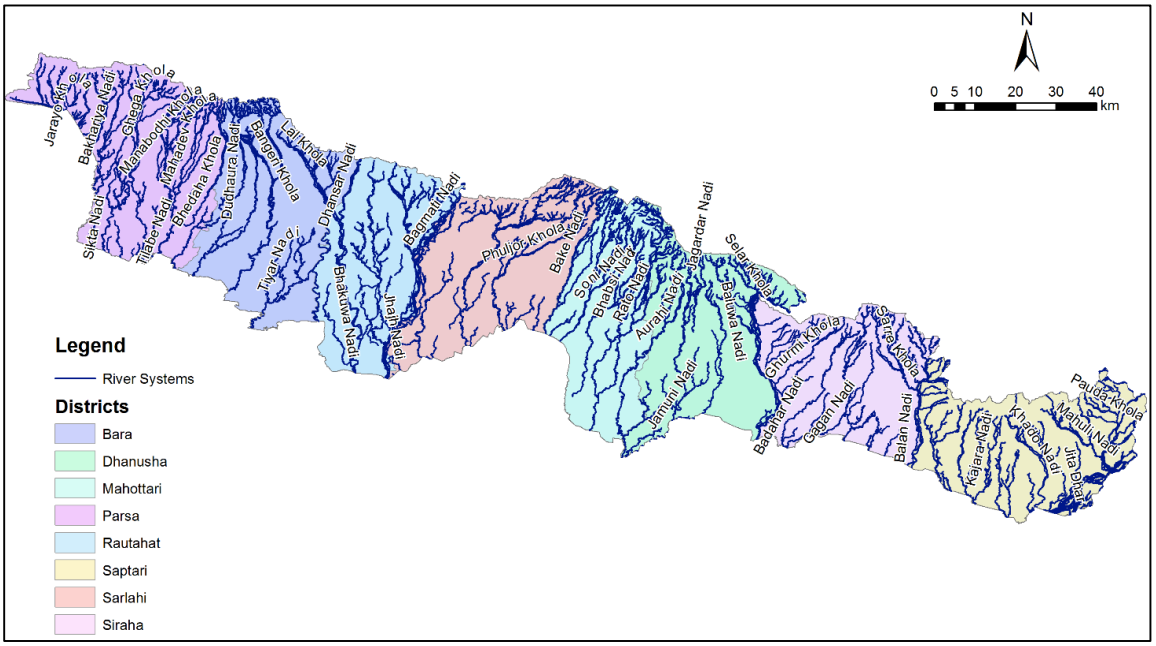


Figure 6. River systems in the study area

2 River system and hydrological study

2.1 River system

There are 39 river systems identified by PCTMCDB are presented in Table 2. Bakaiya, Bagmati and Kamala River systems, which originate from the middle mountains, are the perennial rivers. The width of Bakaiya River hence the river flow during the dry season seeps through the riverbed. So it can also be treated as the ephemeral river along with all of the remaining 36 river systems, which originate from the Chure Region, at least in the Bhawar zone. However, further downstream in the Terai zone these rivers are perennial. Figure 7 shows the major (larger) river systems.

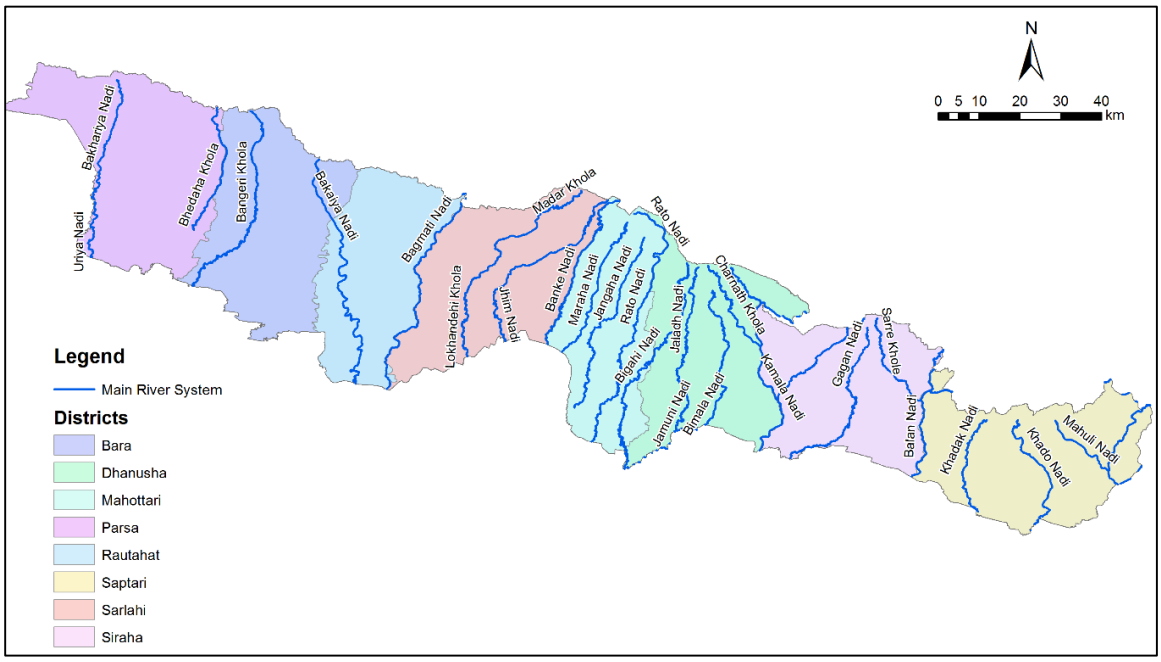


Figure 7. Major river systems in the study area

Table 2. List of river systems in the study area.

River System No.	River System	Main River	Tributary	District
16	Saptakoshi River	Koshi River First Section	Saptakoshi River	Sunsari, Saptari, Udayapur
19	Trijuga Nadi Northen Section	Trijuga River First Section	Trijuga River	Saptari, Udayapur
20	Trijuga Nadi Southern Section	Trijuga River Second Section	Trijuga River	Saptari, Udayapur
21	Pauda Khola	Puda Khola	Puda Khola	Saptari
22	Mahuli Khola	Mahuli Khola	Mahuli Khola	Saptari

River System No.	River System	Main River	Tributary	District
23	Tiljuga Khola	Tiljuga Khola	Tiljuga Khola	Saptari
24	Khado Khola	Khado Khola	Khado Khola	Saptari
25	Ghordaha River	Ghordaha River	Ghordaha River	Saptari
26	Khadak River	Khadak River	Khadak River	Saptari
27	Bihul River	Bihul River	Bihul River	Saptari
28	Balan River	Balan River	Balan River	Sunsari, Saptari, Udayapur
29	Trishula-Kataniya-Kalyandai Khola	Trishula-Kataniya-Kalyandai Khola	Trishula Khola	Siraha
30	Badhar-Gagan Khola	Badhar-Gagan Khola	Gagan Khola	Siraha
31	Ghurmi Khola	Ghurmi Khola	Ghurmi Khola	Udayapur, Siraha
32	Bataha Khola	Bataha Khola	Bataha Khola	Siraha
41	Kamala River-Charnath Khola	Charnath Khola	Charnath Khola	Dhanusha
42	Baluwa-Bilauti River	Baluwa-Bilauti River	Baluwa River	Dhanusha
43	Jaladh River	Jaladh River	Jaladh River	Dhanusha
44	Bigahi Khola	Bigahi Khola	Bigahi Khola	Dhanusha, Mahottari
45	Ratu Khola	Ratu Khola	Ratu Khola	Dhanusha, Mahottari
46	Maraha Khola	Maraha Khola	Maraha Khola	Mahottari
47	Banke-Hardi Khola	Banke-Hardi Khola	Banke-Hardi Khola	Mahottari, Sarlahi
48	Sapaha-Singhyahi-Banari Khola	Sapaha-Singhyahi-Banari Khola	Sapaha Khola	Sarlahi
49	Jhim River	Jhim River	Jhim River	Sarlahi
50	Lakhandehi Khola	Lakhandehi Khola	Lakhandehi Khola	Sarlahi
51	Bagmati River-Mansumara-Bagahi River	Bagmati River First Section	Bagmati River	Sarlahi
59	Bagmati River-Chandi Khola	Chandi Khola	Chandi Khola	Rautahat
60	Lamaha-Jhanj Khola	Lamaha-Jhanj Khola	Alajor Khola	Rautahat
63	Lal Bakaiya River	Lal Bakaiya River	Lal Bakaiya River	Rautahat, Bara
64	Kamal River-Belsot River	Kamal River-Fourth Section	Kamala River	Siraha, Dhanusha, Udayapur, Sindhuli
68	Dhansar Khola	Dhansar Khola	Dhansar Khola	Makawanpur, Rautahat, Bara
69	Tiyar - Adhuwa Khola	Tiyar - Adhuwa Khola	Tiyar Khola	Bara
70	Pasaha Khola	Pasaha Khola	Pasaha Khola	Bara
71	Dudhaura Khola	Dudhaura Khola	Dudhaura Khola	Bara
72	Sirisawa Khola	Sirisawa Khola	Sirisawa Khola	Parsa
73	Tilabe River	Tilabe River	Tilabe River	Parsa
74	Dhongahi River	Dhongahi River	Dhongahi River	Parsa
75	Bhalubahi-Bakhariya River	Bhalubahi-Bakhariya River	Bhalubahi-Bhata-Sikta River	Parsa
76	Thute-Sikharbas Khola	Thute-Sikharbas Khola	Thute Khola	Parsa

2.2 Hydrological analysis

Most of the river systems originating from Chure region of Province 2 are of ephemeral nature. Almost all of the sediment transport in such rivers occur during flood period. So, flood frequency analysis is important requirement for understanding sedimentation processes in these rivers. The river systems in the study area are ungauged (Figure 8). Hence, the flood estimation has to be based on empirical methods developed on basis of the statistical analysis by different scientific studies. Empirical methods namely WECS/DHM method and Modified Dicken's method were used in this study. These methods have been widely used in engineering analysis of flow estimation for designing drains, prefeasibility of hydropower projects, flood risk analysis. Floods of 2 years, 5 years and 10 years were estimated using the empirical methods. It shall be noted that these methods were developed based on data of different perennial rivers, with different catchment characteristics compared to Chure river systems.

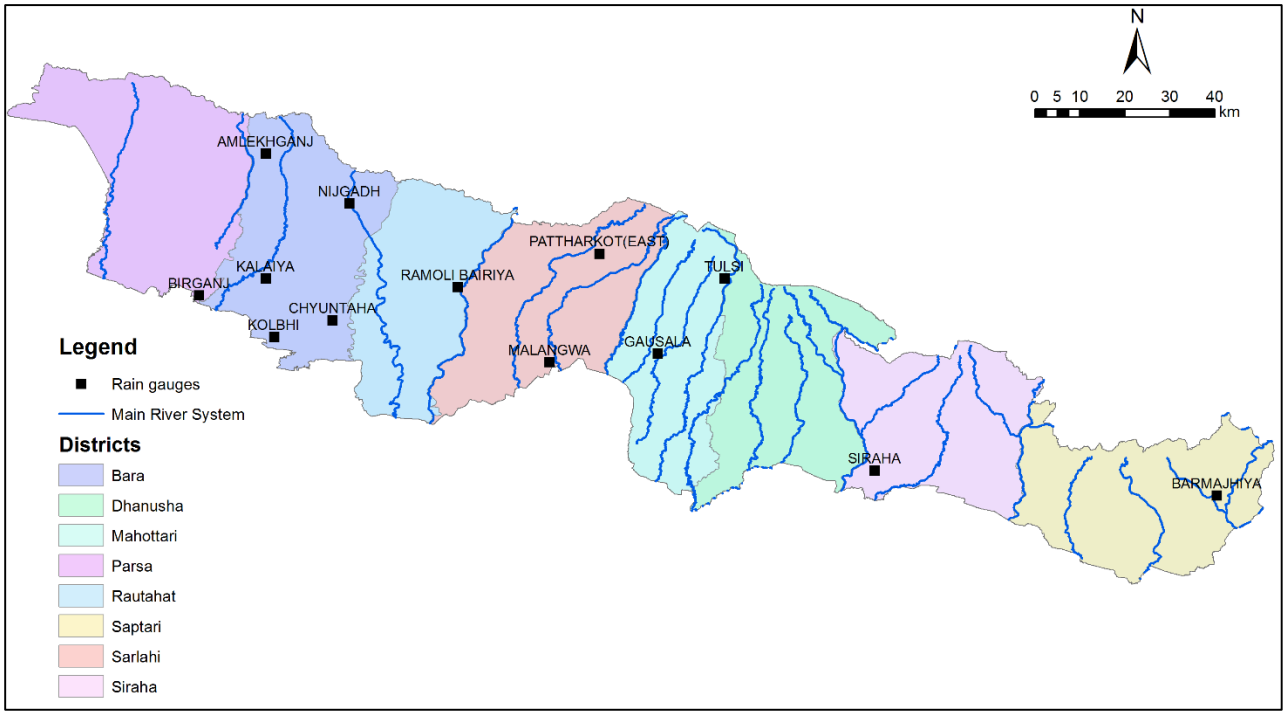


Figure 8. Existing Hydro-metrological stations in the study area. Only rain gauge stations are located, mostly in the downstream part of the catchments.

The required catchment characteristics were derived based on the DEM and other relevant data. The detailed procedure of hydrological estimation is presented in the section below.

2.2.1 Watershed Delineation

All of the empirical hydrological methods used for flood estimation first require information of the watershed area. ALOS PALSAR DEM data of 12.5 m resolution was used to derive the watersheds using ArcGIS software. The pour points were provided in the river systems as outlets of the watersheds. The points were selected such that it contributes to maximum upstream watershed and lies immediately at the exit of Chure hillslope. Thus, this estimated the discharge value which contributes to the transport of sediment yielding from the watershed. The contribution of rainfall to the peak river flood discharge in lower area below pour point is neglected compared to the upstream watershed. The steps performed in GIS for watershed computation are briefly explained below:

a) DEM filling

The DEM may contain sinks in data. The large sinks in DEM may cause the accumulated water to concentrate in the sink and not reach the stream. Thus it is necessary to fill those large holes in elevation data.

b) Flow direction

The filled DEM is used to define the flow direction for each raster cells, the direction along with the water travels, from higher to lower elevation.

c) Flow accumulation

This step accumulates the flow to lower elevation cells which receives water from higher elevation cell surrounding it. Thus, all water which falls on higher grounds are collected to lower elevation and stream like accumulation raster feature is generated.

d) Watershed generation

On the basis of flow accumulation and pour points, exact pour points are marked. Then watershed area is generated from pour point and flow direction raster processing. GIS has inbuilt tools to perform these activities

Although the process for calculating watershed area for all rivers is same, the large number of rivers means the manual processing takes considerable amount of time. To avoid this huge amount of time investment on generation of watershed map for entire Chure (Province 2), an automated watershed generation tools was developed in GIS model builder. This tool basically takes DEM map and pour points as input and perform all the repetitive task of watershed generation for each pour points in an iterative manner. Hence, the repetitive process for

generation of each watershed is avoided. This tool automatically adds area attribute value to each watershed results. The final name and results for each watershed is then imported to excel file from .xml result format. The outline of the entire automation process is shown in the Figure 9. The delineated watersheds of river systems are shown from Figure C-1 to Figure C-5, Appendix C.

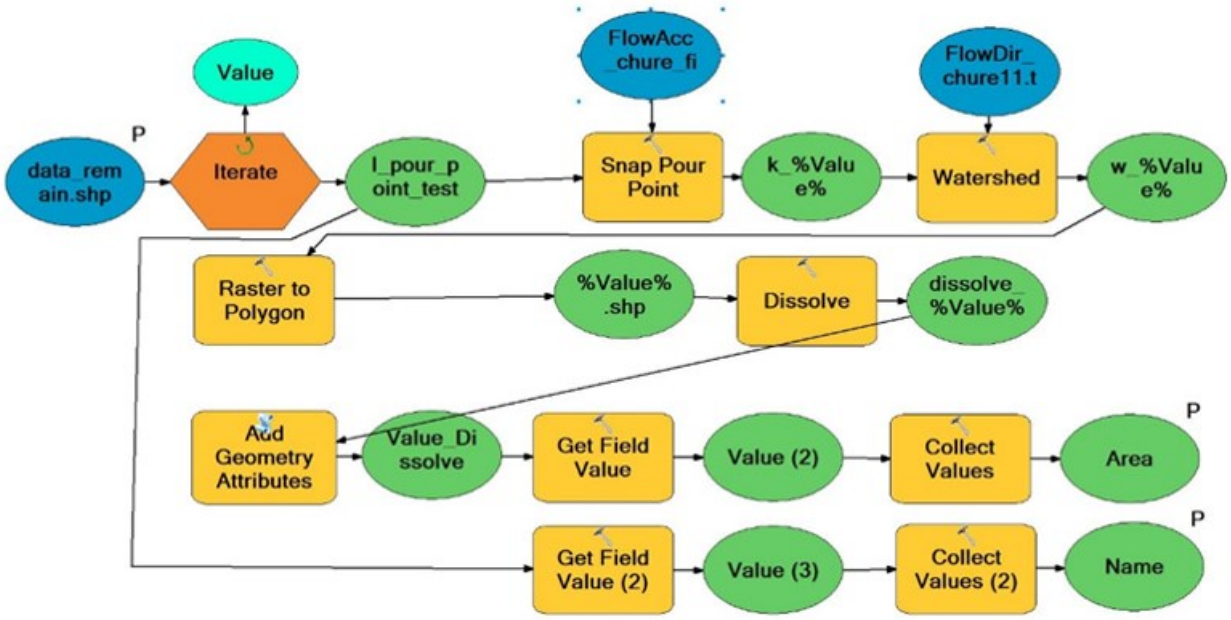


Figure 9. GIS based model used to derive watersheds.

2.2.2 Flood Estimation using empirical methods

Following methods were used to assess the flow (flood) of different frequency:

a) WECS/DHM(Hydest) Method

This method is based on hydrologic theories, empirical equations and statistics. It treats the entire country as a single hydrologic region. This method is used for predicting flows in ungauged river basins. The main input for flood forecasting in the Hydest method are area of basin below 5000m and area of basin below 3000m elevation along with monsoon wetness index. Developed exclusively for ungauged basin in Nepal, thus is applicable in determining flows with certain degree of statistical reliability. The flood estimate is defined as the function of area coefficient and empirical coefficient (Q=CA^{α}). $where\ Q = Discharge,\ A = Area,\ \alpha = Coefficient$. Value for A and Monsoon Wetness Index provided by user. Coefficient for different return period of flow are estimated based on empirical equations. The details on the equations used are given below:

Estimation for 2 years (Return Period) instantaneous flood

$$Q_2 = 2.29(A_{\leq 3000} + 1)^{0.8448} \quad (1)$$

Where,
$A_{\leq 3000}$ = area of basin below 3000 m elevation (Contributes to peak events).

Similarly, estimation for 100 years instantaneous flood is given in Equation 2 - 3.

$$Q_{100} = 20.7(A_{\leq 3000} + 1)^{0.72} \quad (2)$$

$$k = \frac{\ln(\frac{Q_{100}}{Q_2})}{2.326} \quad (3)$$

General formula for other return period is given by

$$Q_T = e^{[\ln(Q_2) + S_T k]} \quad (4)$$

Where,
S_T = values of standard normal variate for different return period T as provided in Table 3.

Table 3. Values of standard normal variate for different return periods adopted by WECS/DHM method.

Return Period (T) in years	Standard Normal Variate
2	0
5	0.842
10	1.282

Now, the flow for different return period is calculated using Equations 5 - 8.

$$Q_5 = e^{[\ln(Q_2) + 0.842k]} \quad (5)$$

$$Q_{10} = e^{[\ln(Q_2) + 1.282k]} \quad (6)$$

$$Q_{20} = e^{[\ln(Q_2) + 1.645k]} \quad (7)$$

$$Q_{50} = e^{[\ln(Q_2)+2.054k]} \quad (8)$$

These equations were coded in MATLAB and processed for all watersheds generated in previous step. Thus the values of flood for different return period of 2, 5 and 10 years were calculated. The results are presented in Table D-1, Appendix D.

b) Modified Dicken's Method

This method is based on frequency studies of Rivers by Irrigation Research Institute, Roorkee, India. This method is widely used in Nepal to estimate flood for designing drains. The T year flood discharge in cubic meter per seconds is determined as:

$$Q_T = C_T A^{0.75} \quad (9)$$

The value of C_T is based on total catchment area and perpetual snow area.

$$C_T = 2.342 \log(0.6T) \log\left(\frac{1185}{p}\right) + 4 \quad (10)$$

Where p is perpetual snow area which is defined as the ratio of snow cover basin area plus 6 to the total basin area plus snow area.

$$p = \frac{a+6}{A+a} \quad (11)$$

c) Adoption of the formative floods

Flood of magnitude higher than the 1 year return period is typically adopted as the channel forming discharges for the braided rivers. This assumption is more valid for the perennial streams. However, lack of proper research and understanding on the formative conditions of ephemeral streams, 2 years return period flood discharge is adopted as the formative discharge in this study. The formative events is expected to occur frequently. The comparison of results between WECS/DHM method and Modified Dicken's methods are presented in Table D-1, Appendix D. The modified Dicken's method flood magnitudes about 3 times higher than the WECS/DHM method. Both Modified Dicken's method and WECS/DHM methods were derived for the Perennial streams. However, the latter method was developed using the observed discharges of rivers in Nepal. So, it is expected to perform better than the Modified Dicken's method. Thus, flood

discharge of 2 years return period estimated by the WECS/DHM was adopted as the formative floods for river reaches in this study.

2.2.3 Duration of formative events for ephemeral rivers

The duration of formative events is equally important to determine the annual depositional volume at the river reaches. For ephemeral rivers the formative events occur during the rainfall. Discussion with the informants in the field also revealed that floods in such rivers are flashy in nature and subside after the rainfall events. So, daily rainfall data recorded at the rainfall stations in the study area were analyzed to determine the duration. The rainfall stations are concentrated in the Terai region and very sparse in the Bhawar region and Chure region. So, it is assumed that the rainfall in the Chure region will be similar to that observed in the Terai region.

The river systems were divided into three zones based on the network of the rain gauge stations. The first zone covers River systems west of Bagmati River. The second zone covers River systems between the Bagmati River and the Balan River and the third zone covers the River systems east of Balan River. To determine the duration, the annual maximum rainfall of each rainfall station was first determined. Then the total days with weightage by rainfall was computed. The duration was obtained dividing the total days with rainfall weightage by maximum annual rainfall. Finally the duration of all rainfall stations in each zones were averaged to obtain the representative duration of the formative event of each zone. The duration of the formative events for first, second and the third zone were computed as 13 days/ year, 17 days/ year and 12 days/ year respectively.

2.2.4 Monthly flow of perennial rivers

Bagmati River has long-term flow observed at Pandhera Dovan gauging station (Station No.589) from the year 1979. The station is located about 4.25 km upstream of the barrage in Bagmati River. The average monthly data was derived from the observed flow data from 1979 to 2006. The catchment area at the station is 2812 km^2. Kamala River does not have a gauging station. So, the observed data of Bagmati was transposed to Kamala River using Catchment Area Ratio (CAR) method. The catchment area of Kamala River at the outlet from Chure region is 1569 km^2. So, CAR of 0.55 was adopted for the transposition. The average monthly flow hydrograph of Bagmati River and Kamala River are shown in Figure 10 and Table 4.

Table 4. Average monthly flow of Bagmati and Kamala Rivers.

Months		Jan	Feb	Mar	Apr	May	Jun	Jul	Aug	Sep	Oct	Nov	Dec
Bagmati	Flow (m3/s)	20.8	16.7	14.8	15.3	33.6	127.6	458.7	431.5	271.6	109.6	42.2	26.1
Kamala		11.6	9.3	8.2	8.5	18.7	71.2	256.0	240.8	151.5	61.2	23.6	14.6

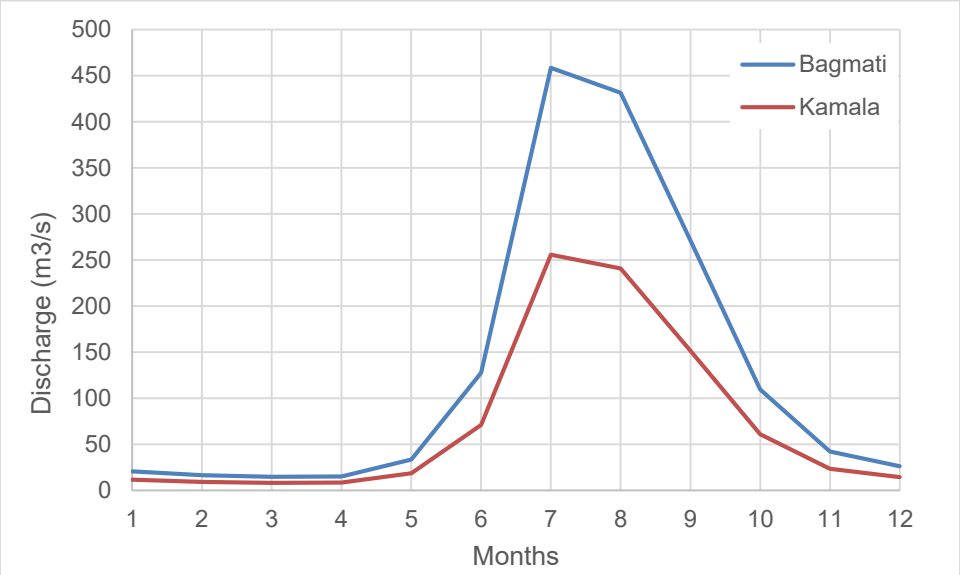


Figure 10. Average monthly flow of Bagmati and Kamala Rivers.

3 Geological study

3.1 Geology of the Himalaya

The Himalaya was formed as a result of collision of the Indian continent in the south and the Eurasian landmass in the north by closing the intervening Tethys Sea (Figure 11) about 50 million years ago. Located south of the Tibetan Plateau, the Himalayan Mountain chain stretches from the Brahmaputra River in the east to the Indus River in the northwest. The Himalaya is about 2400 km long and 200 km to 300 km wide (Ganseer, 1964) (Figure 12). The Himalaya covers an area of approximately 600,000 sq. km in south Asia. Out of the 2400 km long Himalayan chain, the Nepal Himalaya occupies the central 800 km.

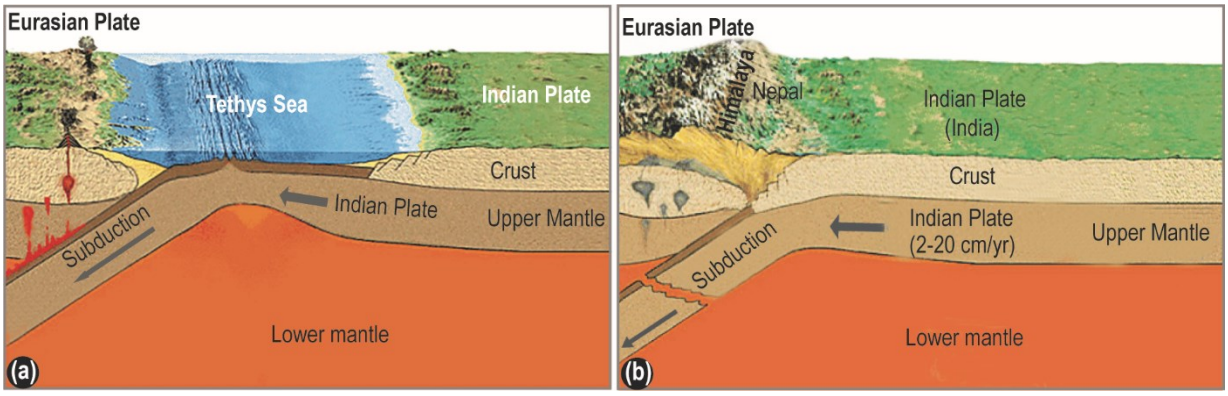


Figure 11: (a) In the process of formation of the Himalaya the Indian Plate subducts below the Eurasian Plate and the Tethys Sea between the Plates shrinks; (b) Collision of the Plates gives birth of the Himalaya in expense of the closure of the Tethys Sea.

The Himalaya is the youngest mountain range on the Earth and the mountain building process has been continuing since its birth due to the continued northward movement of the India which is 5 cm a year at present (Bilham et al., 1998). The continued convergence has made the Himalaya an active seismic zone, resulting into frequent major earthquakes all along the Himalaya in time and space, and the latest major event in the Nepal Himalaya was the 2015 Gorkha earthquake (Bilham et al., 1998). Most of the convergence is accommodated within the Himalaya by movement on various thrusts and mountain upliftment (Dhital, 2015; Upreti, 1999).

3.1.1 Tectonic division of Nepal Himalaya

Like other parts of the Himalaya, the Nepal Himalaya is divided into the following five, east-west extending major tectonic zones (Ganseer, 1964) (Figure 13). Hagen (1969) divided the Nepal Himalaya into eight longitudinal physiographic belts.

1. Terai Zone (Gangetic Plain)
2. Siwalik/Churiya Zone (Sub-Himalayan Zone)
3. Lesser Himalayan Zone
4. Higher Himalayan Zone
5. Tibetan-Tethys Himalayan Zone

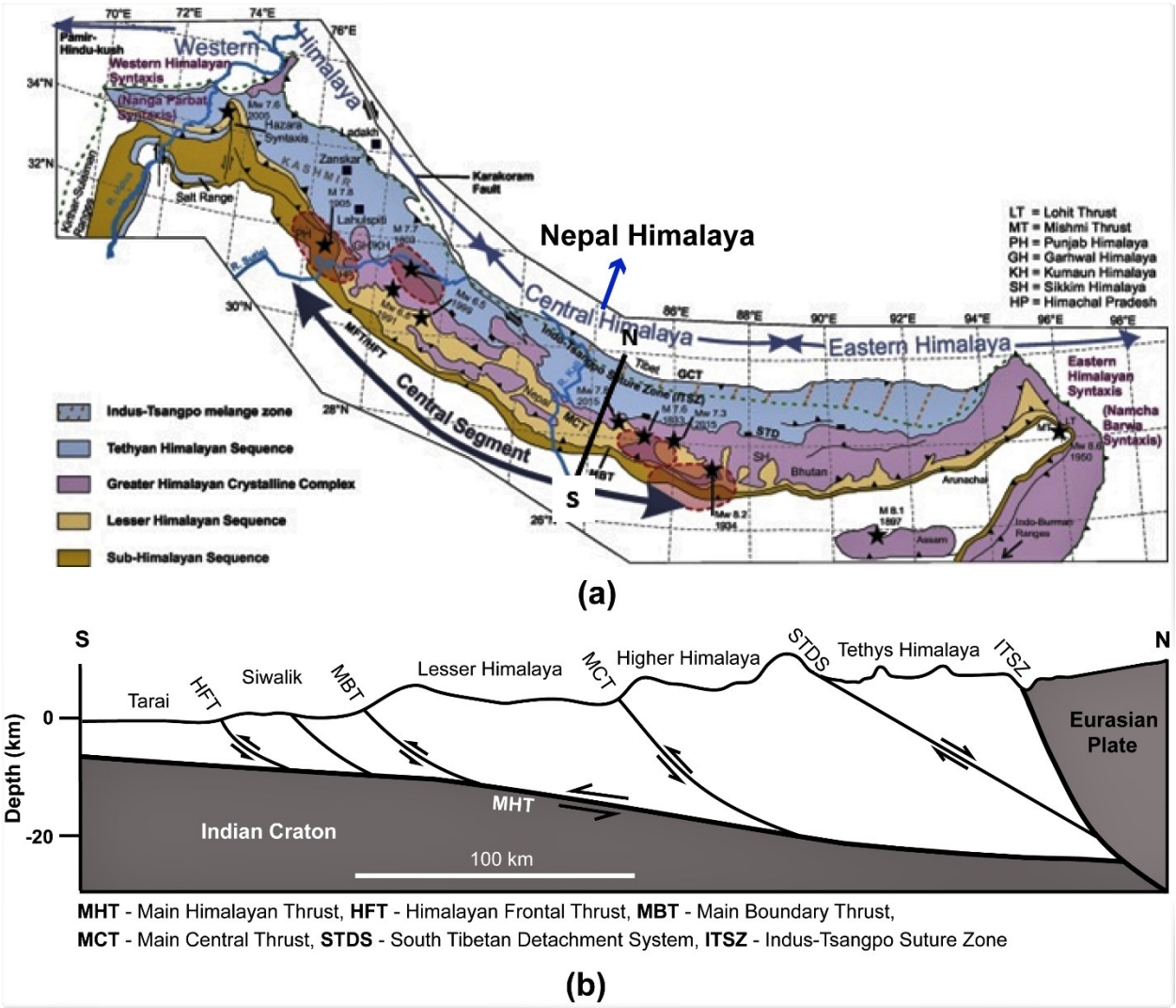


Figure 12. a) Map of the Himalaya plate boundary showing the important lithological and structural units and the limits of the western, central (Nepal), and eastern segments of the Himalaya (after Rajendran et al., 2017); b) Geological cross-section along the N-S line in Figure 2a.

Each of the above zones has different lithology, structure, and geological history, and run almost parallel to each other. Figure 12-b and Figure 13 show the tectonic division of the Nepal Himalaya.

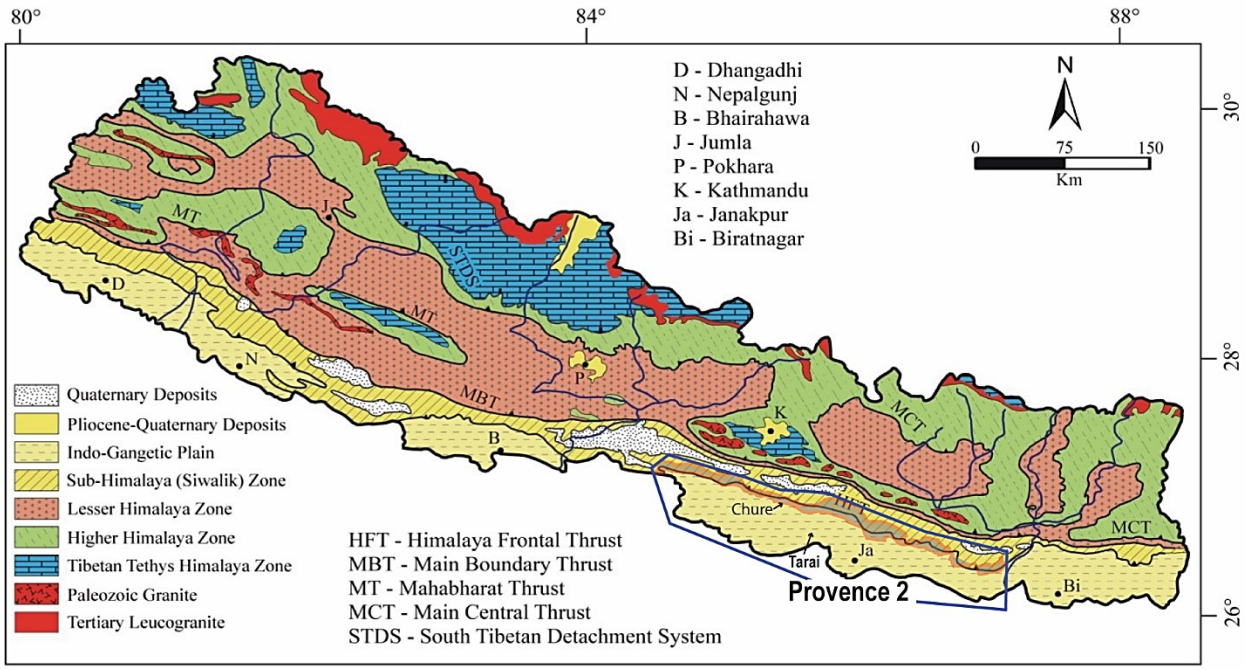


Figure 13: Geological map of Nepal with location of Province 2 (modified after Upreti,1999).

The tectonic zones are separated from each other by the thrust faults as shown in Figure 12 and Figure 13. The southernmost fault, the Main Frontal Thrust (MFT) separates the Siwalik (Sub-Himalayan) Zone from the Gangetic Plain. The Main Boundary Thrust (MBT) separates the Lesser Himalayan Zone from the Siwalik. The Main Central Thrust (MCT) separates the Higher Himalayan Zone from the Lesser Himalayan Zone. The South Tibetan Detachment System (STDS) is the boundary between the Higher Himalayan Zone and the overlying fossiliferous sequence of the Tibetan-Tethys Himalayan Zone (Figure 12-b). The Indus-Tsangpo Suture Zone (ITSZ) marks the initial collision zone between the Indian Plate and the Tibetan (Eurasian) Plate.

The present tectonic architecture of the Himalaya is dominated by three master thrusts, the Main Central Thrust (MCT), the Main Boundary Thrust (MBT) and the Main Frontal Thrust (MFT) (Figure 12-b) (Upreti, 1999). The age of initiation of these thrusts becomes younger from north to south, with the MCT as the oldest and the MFT as the youngest. All these thrusts are considered to come together at depth in a flat-lying decollement called the Main Himalayan Thrust (MHT) (Upreti, 1999). The main geological zones of the Nepal Himalaya are described below.

3.1.1.1 Terai Zone (Indo-Gangetic Plain)

The Terai zone, also known as the northern edge of the Indo-Gangetic Plain, is the southernmost and the youngest geological unit of Nepal (Figure 13). It is made from alluvium consisting of gravel (boulder, cobble, pebble, granule), sand, silt and clay of Pleistocene (2.6 million years) to Recent

age. The Terai gradually rises from about 100 m in the south to 200 m in the north, and, in average the alluvium is considered to be 1,500 m thick. The width of Terai Zone varies from 10 to 50 km and forms a nearly continuous belt from east to west. The Terai zone is bounded by the Main Frontal Thrust (MFT) in the north along the southern front of the Churia Range. The northern part of the Terai Zone represents a mountain in the making (Upreti, 1999). The Himalayan mountain front is propagating to the south through this zone.

A large number of borehole logs and geophysical investigation made during the groundwater and petroleum exploration in Terai has been instrumental in the study of the surface and subsurface geology of the Terai. In the light of the grain-size variation of the alluvium, the Terai Plain is divided into northern, middle, and southern parts.

a) Northern Terai

The northern part of the Terai is known as the Bhabhar Zone and it comprises of boulder, cobble, pebble and granule derived from the Siwalik and the Lesser Himalaya. These coarser sediments close to the mountain front form large alluvial fans. The Bhabhar Zone acts as a recharge zone for the groundwater of Terai. Most of the rivers lose their water while passing through this zone. Water tables in Bhabhar Zone show sharp fluctuations between the summer and rainy seasons. At some places the wells become completely dry in summer. Due to the very coarse nature of the sediments, low water table and quick percolation of rainwater, this zone is particularly not productive for agriculture and therefore ideal for the development of forest resources. The maximum width of the Bhabar zone is about 12 km.

b) Middle Terai

The middle Terai zone has domination of sand, sometimes pebbly, with some clay partings. Clay is mostly dark grey and intercalated with brown colored sand layers. The medium- to coarse-grained sandy layers possesses good groundwater reservoir. Because of lower elevation from the Bhabar Zone, this zone has spring line and development of marshy land with natural ponds and lakes. Immediate south of the spring lines lies many artesian layers, generally from 25 m to 200 m depth. The permeability of the Middle Terai Zone diminishes towards south and finally non permeable layers are encountered in boundary of the Southern Terai Zone. The Middle Terai zone of about 10-12 km wide.

c) Southern Terai

As the name implies, Southern Terai Zone is the southernmost part of the Terai. Sediments in this zone consist sand, silt and clay, and clay is the dominant component. Since the sediments are finer than the Middle Terai and fining southward, aquifers become poorer and the water table is generally seen below 3 m from the surface. Because of the aquifer characteristics, development of the groundwater also appears to be difficult by deep tube wells in this part of the Terai. However, in old river channels area, north-south extending better aquifers are found.

3.1.1.2 Churiya (Siwalik) Zone

Also known by the Sub-Himalaya in other parts of the Himalaya, the hills north of the Terai Plain is known as the Churiya or Siwalik Zone in Nepal. The Churiya Zone forms one of the largest foreland basin accumulations on the Earth. It consists of fluvial sediments of Neogene to Quaternary (23 to 1.6 million years) age, and it is separated from the Terai Plain by the Main Frontal Thrust (MFT) to the south and separated from the Lesser Himalaya by the Main Boundary Thrust (MBT) to the north (Figure 12-b and Figure 13). Extending all along the Himalaya, the Siwalik forms 5 to 50 km wide southernmost hill range. It has number of east-west running thrusts, and the rocks, generally, dip to the north. Siwalik Zone is also rich in both plant and animal fossils. Lesser Himalayan metasedimentary rocks have been thrust southward over the Siwalik rocks along the MBT and a large part of the Siwalik rocks must be buried beneath the cover of the overthrust Lesser Himalayan rocks to the north (Upreti, 1999). The Churia Group, itself, is thrust over the recent alluvium of the Terai Zone along the MFT.

Based on the rock types or their combinations, the Siwalik is divided into Lower, Middle and Upper Group from south to north in younging order. The Lower Siwalik is essentially composed of alternations of fine-grained sediments such as variegated mudstone, siltstone and shale with subordinate amounts of fine-grained sandstone. Like the Lower Siwalik, the Middle Siwalik has alternating beds of sandstone and mudstone but sandstone is dominant over mudstone. The sandstone has multistoried thick beds measuring several meters to tens of meters in thickness, and the mudstone is not variegated. Presence of abundant biotite and light-colored quartz and feldspars gives the Middle Siwalik sandstones salt- and- pepper appearance and are called the “salt and pepper sandstones". They are medium-to coarse-grained. The upper part of the Middle Siwalik is marked by the occurrence of pebbly sandstone beds. The Upper Siwalik, on the other hand, is characterized by the occurrence of very coarse sediments such as conglomerate and boulder conglomerates with minor intercalation of mudstone and siltstone. The mudstone beds are sometimes massive, irregularly bedded, and contain invertebrate fossils. The Siwalik Hills are

generally believed to have uplifted after 1.7 Ma, and turned out to hills around 0.7 Ma (Kizaki, 1994).

3.1.1.3 Lesser Himalaya Zone

The Lesser Himalayan Zone lies between the Siwalik Zone in the south and the Higher Himalaya in the north (Figure 12-b and Figure 13). The MBT and MCT are the tectonic boundaries that separate the Lesser Himalaya from the Siwalik and the Higher Himalaya, respectively. Physiographically, the Lesser Himalaya has a higher, Mahabharat range in the south and a subdued midland zone in the north. The Lesser Himalayan zone is uniquely characterized by the presence of autochthonous and allochthonous sequences, and are composed of sedimentary to low-grade metamorphic rocks of the Precambrian to early Paleozoic age. They mainly comprise of unfossiliferous, sedimentary and meta-sedimentary rocks such as slate, phyllite, schist, quartzite, limestone, dolomite, etc. Kunchha Phyllite of the Lesser Himalaya, which dates Precambrian, is considered as the oldest rock in the Himalaya. Unlike the above rocks, the Gondwana sediments form a unique sequence of fossiliferous fluviatile rocks of Permo-Carboniferous time in the Lesser Himalaya of Tansen unit of western Nepal (Sakai & H., 1983).

The autochthonous rocks are overriding by crystalline nappes and klippen. Eastern Nepal is characterized by the development of extensive thrust sheets (allochthonous) of high-grade metamorphic rocks (gneiss and schist) which have moved southwards. Below this sequence, due to erosion, large exposure of the low-grade metamorphic rocks (autochthonous) can be seen. In Central Nepal, a large thrust sheet called the Kathmandu Nappe (allochthonous) covers a wide area around the Kathmandu region. In addition, there are some granitic intrusions of various ages in the Lesser Himalaya (Figure 13).

3.1.1.4 Higher Himalaya Zone

The Higher Himalayan Zone mainly consists of huge pile of strongly metamorphosed crystalline rocks such as kyanite-sillimanite bearing gneisses and schists, and marbles and quartzites. The Higher Himalaya is separated from the Lesser Himalaya in the south by the MCT and the STDS separates it from the overlying highly fossiliferous Tibetan Tethys Zone in the north (Figure 12-b and Figure 13). It extends incessantly along the entire length of the country as in whole Himalaya, and its width varies from place to place. Granites are the other rock types in the upper part of this unit (Figure 13).

3.1.1.5 Tibetan-Tethys Himalayan Zone

The Tibetan-Tethys Himalayan Zone is the northernmost geological unit of Nepal (Figure 12-b and Figure 13). It is bounded by the STDS to the south and the Indus-Tsangpo Suture Zone (ITSZ) to north. The STDS is a normal fault and the ITSZ is the zone of initial collision of the Indian Plate and the Eurasian Plate. The Tibetan-Tethys Zone comprises of weakly metamorphosed to un-metamorphosed fossiliferous rock sequence such as limestone, sandstone and shale deposited on the Tethys Sea during Cambrian to middle Cretaceous period. Among the fossils, Ammonite (popularly known as Saligram) is remarkable in Mustang and Dolpa districts. In eastern Nepal, Tibetan Tethys Himalayan rocks are negligible except at the top part (Yellow band and above).

3.2 Geology of Province-2

Being located in southern part of Nepal, Province 2, geologically, belongs to the Siwalik and the Terai Plain. A general geological map and geological coverage of the Province are showed in Figure 4 and Table 5, respectively. Since an elaborated geological description of the Nepal Himalaya is already given above, the section below gives a brief outline of the Terai Plain and the Siwalik of Province 2.

Table 5: Geological coverage of Province 2, Nepal.

Geology		Area (sq m)	Area (sq km)	% coverage
Group	**Lithology**			
Upper Siwalik	Conglomerate	269,986,000	270.0	2.83
Middle Siwalik	Sandstone, mudstone	794,479,000	794.5	8.33
Lower Siwalik	Mudstone, sandstone	559,076,800	559.1	5.86
Terai Plain	Gravel, sand, silt, clay	7,911,352,020	7911.4	82.97
Total		9,534,893,820	9534.89	100

3.2.1 Terai Plain

As in other parts of Nepal, the Terai Plain forms the southernmost geological unit of Province 2. It is composed of alluvial boulder, cobble, pebble, gravel, sand, silt and clay of Pleistocene (2.6 million years) to Recent age, and it has an average thickness of 1,500 m. Consistent to the general description of the Terai Plain given above, the Terai portion of Province 2 is divided into southern, middle and northern parts based on the composition of the materials it is made from. The southern Terai is nearly flat and mostly dominated by clay. The Middle Terai has domination of sands, and

is marshy. The northern part has about 12 km wide highly permeable zone comprising boulder to pebble size fractions known as the Bhabhar Zone. About 83% area of the province is located in the Terai Plain (Figure 4 and Table 5). The widest part of the Plain is about 35 km and it lies in the Rautahat and Mahottari districts, while the narrowest part is about 10 km in the western part of Parsa district (Figure 14).

3.2.2 The Churiya

The hills north of the Terai Plain are the Siwalik (Figure 4). The Siwalik is made from the fluvial sedimentary rocks of the Tertiary Period [Neogene (23 ma- 1.6 ma)]. The Siwalik is bounded by the Main Frontal Thrust (MFT)/the Himalayan Frontal Thrust (HFT) in the south and the Main Boundary Thrust (MBT) in the north. The Siwalik rocks consist of upward-coarsening successions of fluvial mudstone, siltstone, sandstone, and conglomerate. The Siwalik in Province 2 has threefold division, such as Lower, Middle and Upper Siwalik in stratigraphic up sections. The Lower Siwalik is composed of siltstone/mudstone with minor sandstones (Figure 15). The Middle Siwalik consists of the fine- to medium-grained salt- and- pepper sandstone with interbeds of siltstone and mudstone (Figure 15), and the Upper Siwalik are composed of conglomerate with subordinate sandstone and mudstone (Figure 16). The rocks dip to the north. Other details of the Siwalik described above under geology of Nepal Himalaya apply in Province 2. Figure 14 gives a picture of the geological disposition of the Terai Plain and the Siwalik.



Figure 14: A view of part of the Terai Plain and the Siwalik as seen north from the Terai Plain. MFT=Main Himalayan Thrust.

The Siwalik zone makes a 5-15 km wide strip along east-west direction in the northern edge of the Province except the western half of the Saptari district where the Siwalik is missing (Figure 4). The Siwalik represents about 17% area of the province (Table 5). The width of the Siwalik is

minimum in Bara and Rautahat districts and the widest part lies in the Sarlahi and Dhanusa districts (Figure 4).



Figure 15: Exposures of the Lower Siwalik mudstone north of Bardibas (left), and the Middle Siwalik sandstone at the Churiya Khola section, Parsa district (right).



Figure 16: An exposure of the Upper Siwalik conglomerate beds at the Churiya Khola section, Parsa district.

3.2.3 Sediment characteristics

Out of the 32 river systems in Province 2, Bagmati and Kamala River have origin in the Lesser Himalaya and they flow to the south through the Siwalik range, carrying materials from both the Lesser Himalaya and the Siwalik. The remaining 30 river systems, on the other hand, are originated within the Siwalik of Province 2 and north of it, and have materials derived from the Siwalik Hills. Surface distribution of the river-generated materials were studied in 28 river systems for their composition and size distribution. They are illustrated on Figures C-6 to C-39, Appendix C and summarized in Table 6.

3.2.4 Material Sources

The study on riverbed materials showed that some of the rivers have sand and silt dominant while others have gravel as the main component. Some of them have white sands but distinctly black sands in others. In terms of composition, some rivers have only the clasts of the Siwalik rocks (sandstone, siltstone, mudstone) whereas clasts of the metamorphic rocks (quartzite, schist, phyllite, slate, marble, gneiss) and igneous rock (granite) of the Lesser Himalaya and the Higher Himalaya make main or subordinate composition. Shape, size, and texture (roundness, sphericity, sorting) of the clast are also not uniform even if we examine the riverbed materials along the East-West highway section. Like size and composition, volume of materials carried by similar-size rivers are also widely variable as some of the riverbeds are aggrading rapidly while others are not so much. Except the Bagmati and Kamala Rivers, rest of the other rivers in Province 2 have origin in the Siwalik and it means that material source is the Siwalik. But, the material size, composition and volume different in each riverbed is the major aspect needs to understand to make sustainable extraction and use of the materials. All the concerns raised above are largely controlled by the watershed geology as summarized below.

Conglomerate beds were typically present in the form of huge masses of cemented gravel hills of the Upper Siwalik. It mostly contained sand, silt, clay, and gravel (coarser than sand) in various proportions, with gravel more predominant in some parts. Well sorted to poorly sorted clast sizes of the conglomerate beds ranged from pebble to boulders. At many places, weathering of the conglomerate had already washed-out cementing materials making it heaps of loose or less compacted gravels, cobbles or boulders. They were highly permeable due to weak cementing materials. Mostly, these rocks were cohesionless and looked like the loose alluvial deposits. When saturated with water or undercut by rivers, the materials can easily take course with the rivers, making riverbed materials in downstream section rich in gravel. The Upper Siwalik is present almost throughout the Siwalik, but its thickness varies. In some cases, thrust and local faults repeat the conglomerate beds or lost or make thinner. These conditions therefore control the volume and composition of gravel in downstream section.

Sandstone is one of the main lithologies of the Siwalik. It occurs in the Lower, Middle and Upper Siwaliks. Sandstones were fine- to coarse- grained, massive to medium bedded, and moderately to weakly compacted. Sandstone in the Lower Siwalik is smaller in proportion and finer in grain size, and that in the Middle Siwalik is thicker and coarser. The sandstones were sometimes jointed

and fractured and were fresh to weathered. The availability of sandstone clasts in the riverbed materials is largely controlled by how much sandstones crop out in the watershed.

Mudstone occurs in the Middle Siwalik and is the main lithology of the Lower Siwalik. The Lower Siwalik mudstones were medium bedded to massive in structure. They are very weak and most vulnerable for physical weathering, and therefore the mudstones in Lower Siwalik are highly to completely weathered, which were in the form of residual soil in the surface at many places. These are less permeable but can be easily eroded by rain action due to soft nature and eroded mass are soluble with water and moved through erosional gullies. Most of the clay fraction on the riverbed materials were derived from the mudstone. Therefore, more the mudstones in the watershed, more the chances of having clay in the riverbed materials.

Table 6. River deposits (locations and material characteristics) studied in Province 2

	River Basin	Location		Elevation (m)	Description of the *River Bed (RBd)/ River Bank (RBk)/Terrace (Te) Material*
		Geographic	Geological		
1	**Churiya Khola** (Photographs and Pi diagrams are included)				
	Churiya - 1	N 27-21-20.4 E 084-59-38.4	Upper Siwalik	601± 6	RBd gravel deposits with sub angular-rounded particles of cobble, pebble and granule. Few boulders and little fines (sand, silt and clay). Compositionally- Quartzite (~78%), Phyllite (~2%), Sandstone (~20%) (Photo 1-a, Appendix-B; Figure C-35, Appendix-C).
	Churiya - 2	N 27-20-26.8 E 084-59-32.0	Upper Siwalik	509± 3	RBd gravel deposits from a point source with sub angular-rounded particles of cobble, pebble and granule. No boulders, and have more fines than in Churiya-1. Compositionally- Quartzite (~90%), Sandstone (~10%) (Photo 1-b, Appendix-B; Figure C-35, Appendix-C).
	Churiya - 3	N 27-18-56.2 E 085-00-02.0	Middle Siwalik	402± 4	RBd gravel deposits with angular-rounded particles of cobble, pebble and granule. No boulders, and have some fines. Compositionally- Sandstone (~60%), Quartzite (~40%)
	Churiya -4	N 27-17-49.3 E 084-59-45.6	Middle Siwalik	335± 3	RBk gravel deposits on the erosion section contains angular-rounded particles of cobble, pebble and granule. Few boulders and has more fines. Compositionally-Quartzite (~70%), Sandstone (~30%) (Photo 1-c, Appendix-B).
2	**Dudhoura Khola**	N 27-11-23.0 E 085-00-42.5	Recent deposits (Terai Plain)	142± 3	RBk Gravel deposits on the erosion section with sub angular-rounded particles of Quartzite (~60%), Dolomite (~20%), and Sandstone (~ 20%). Has no boulders but some fines (Photo 2-a, Appendix-B).
3	**Balganga Khola**	N 27-10-49.3 E 085-02-16.1	Recent deposits (Terai Plain)	128± 3	RBd Gravel deposits with sub angular-rounded particles of Quartzite (~90%) and Sandstone (~10%) with very little fines but no boulders (Photo 2-b, Appendix-B).

	River Basin	Location		Elevation (m)	Description of the *River Bed (RBd)/ River Bank (RBk)/Terrace (Te) Material*
		Geographic	Geological		
4	**Pasaaha Khola**	N 27-10-08.3 E 085-04-21.9	Recent deposits (Terai Plain)	122± 3	RBd deposits of gravely sand and gravely silt. The gravel fraction contains sub angular-rounded particles of Quartzite (~60%) and Sandstone (~40%), and are mostly of pebble and granule size (Photo 3-a, Appendix-B).
5	**Bakaiya Khola**				
	Bakaiya - 1	N 27-14-33.6 E 085-10-11.0	Lower Siwalik	170± 4	RBd Gravel deposits with sub angular-rounded particles. Boulder (dominant): Sandstone (~95%), Quartzite (~5%). Cobble, pebble, granule: Sandstone (~50%), Quartzite (~50%). No finer fractions (Photo 3-b, Appendix-B; Figure C-36, Appendix-C).
	Bakaiya - 2	N 27-13-31.5 E 085-10-07.6	Recent deposits (Bhabar)	157± 3	RBd Gravel deposits with sub angular-rounded particles. Boulders (~20%) are of sandstone (~100%). Cobble, pebble and granule (dominant) with Sandstone (~50%) and Quartzite (~50%). No finer fractions (Photo 4-a, Appendix-B).
	Bakaiya - 3	N 27-11-16.0 E 085-09-57.3	Recent deposits (Terai)	139± 4	RBd Gravel deposits with sub rounded-rounded particles. No boulder. Cobble, pebble and granule: Sandstone (~45%), Quartzite (~55%). Some layers of sand deposits (Photo 4-b, Appendix-B).
	Bakaiya - 4	N 27-10-54.4 E 085-10-09.2	Recent deposits (Terai)	135± 3	RBd deposits with sub rounded-rounded particles. No boulder. Cobble, pebble and granule (~70%): Sandstone (~40%), Quartzite (~60%). Sand and silt deposits (~30%) (Photo 5-a, Appendix-B).
	Bakaiya - 5	N 27-09-33.4 E 085-10-54.1	Recent deposits (Terai)	130± 3	RBd deposits with sub rounded-rounded particles. No boulder. Cobble, pebble and granule (~50%): Sandstone (~20%), Quartzite (~80%). Sand and silt deposits (~50%) (Photo 5-b, Appendix-B; Figure C-36, Appendix-C).

	River Basin	Location		Elevation (m)	Description of the *River Bed (RBd)/ River Bank (RBk)/Terrace (Te) Material*
		Geographic	Geological		
6	**Dhansar Khola** (Bakaiya Tributary)	N 27-09-09.3 E 085-14-25.0	Recent deposits (Terai)	127± 3	RBd deposits with sub rounded-rounded particles. No boulder. Cobble, pebble and granule (~50%): Sandstone (~10%), Quartzite (~90%). Sand and silt deposits (~50%) (Photo 6, Appendix-B).
7	**Bagmati River**				
	Bagmati 1	N 27-08-03.6 E 085-28-58.9	Recent deposits (Bhabar)	108± 3	RBd deposits with sub rounded-rounded particles. Few boulder. Mostly cobble, pebble and granule: Quartzite (~75%), Granite (~15%), Sandstone (~10%). Fines-insignificant (Photo 7-a, Appendix-B; Figure C-37, Appendix C).
	Bagmati 2	N 27-06-54.4 E 085-28-14.6	Recent deposits (Terai)	101± 3	RBd deposits on the eroded section with sub rounded-rounded particles. Few boulders (~5%). Mostly cobble, pebble and granule (~75%): Quartzite (~75%), Granite (~15%), Sandstone (~10%). Fines-~20%. (Photo 7-b, Appendix-B)
8	**Chaapini Khola**	N 27-05-05.1 E 085-34-30.3	Recent deposits (Bhabar)	120± 4	RBd with silts and sands. No gravel deposits (Photo 8, Appendix-B).
9	**Lakhandehi Khola**	N 27-04-29.9 E 085-34-59.0	Recent deposits (Terai)	120± 3	RBd deposits of sandy gravel and gravely sand. Gravel particles:sub rounded-rounded. Cobble, pebble and granule (~45%): Quartzite (~80%), Sandstone (~20%). Sand -~55% (Photo 9-A, Appendix-B).
10	**Phuljor Khola**	N 27-02-08.6 E 085-40-23.4	Recent deposits (Terai)	140± 3	RBk deposits of sandy gravel and gravely sand. Gravel particles:sub rounded-rounded. Cobble, pebble and granule (~55%): Quartzite (~80%), Sandstone (~20%). Sand -~45% (Photo 9-B, Appendix-B).
11	**Bankhe Khola**	N 27-00-51.7 E 085-44-30.0	Recent deposits (Terai)	161± 4	RBd deposits of sandy gravel and gravely sand. Gravel particles:sub rounded-rounded. Cobble, pebble and granule (~45%): Quartzite (~90%), Sandstone (~10%). Sand -~55% (Photo 10, Appendix-B).

	River Basin	Location		Elevation (m)	Description of the *River Bed (RBd)/ River Bank (RBk)/Terrace (Te) Material*
		Geographic	Geological		
12	**Mahara Khola**	N 27-00-12.9 E 085-47-44.0	Recent deposits (Terai)	171± 3	RBk section with layers of sandy gravel and gravely sand. Gravel particles (Cobble, pebble and granule): sub rounded-rounded with Quartzite (~80%), Sandstone (~20%) (Photo 12-a, Appendix-B).
13	**Dhungre Khola**	Photo only			RBd of sand and gravely sand. Rapid aggradation of the river bed (the E-W Highway bridge is ~ 2.5 m above the river bed!) (Photo 11-a, Appendix-B).
14	**Gadhaantaa Khola**	N 27-00-06.2 E 085-51-05.6	Recent deposits (Bhabar)	190± 4	RBd deposits of sand and sandy gravel. Gravel particles (Cobble, pebble and granule): sub rounded-rounded with Quartzite (~80%), Sandstone (~20%). Rapid aggradation of the river bed (the E-W Highway bridge is ~ 3 m above the river bed!) (Photo 12-b, Appendix-B).
15	**Jangaha Khola**	Photo Only			RBd of sand and gravely sand. Rapid aggradation of the river bed (Photo 11-b, Appendix-B).
16	**Bhapsi Khola**	N 26-59-36.3 E 085-52-57.1	Recent deposits (Bhabar)	191± 4	RBd deposits of sandy gravel. Gravel particles (Cobble, pebble and granule): sub rounded-rounded with Quartzite (~60%), Sandstone (~40%). Bridge partially collapsed in 2019 due to high flood (Photo 12-c, Appendix-B).
17	**Khuti Khola**	N 26-44-07.4 E 86-28-47.4	Recent deposits (Terai)	102± 4	RBd deposits of sand, sandy gravel, and gravely sand. Gravel particles (Cobble, pebble and granule): sub rounded-rounded with Quartzite (~70%), Sandstone (~30%). Extensive extraction of the materials (Photo 12-d, Appendix-B).
18	**Balaan Khola**				
	Balaan 1	N 26-42-36.2 E 086-30-25.5	Recent deposits (Terai)	92± 4	RBd deposits of sand, silty sand, and sandy silt. No gravel. (Photo 13, Appendix-B).

	River Basin	Location		Elevation (m)	Description of the *River Bed (RBd)/ River Bank (RBk)/Terrace (Te) Material*
		Geographic	Geological		
	Balaan 2	N 26-44-10.9 E 086-32-03.1	Recent deposits (Terai)	105± 3	RBd deposits mostly of sand with some patches of gravel deposits. Gravel particles (Cobble, pebble and granule): sub rounded-rounded with Quartzite (~80%), Sandstone (~20%) (Photo 14, Appendix-B; Figure C-38, Appendix-C).
19	**Khando River**				
	Khando - 1	N 26-37-36.4 E 086-43-34.3	Recent deposits (Terai)	96± 3	RBd entirely made from sand and silt deposits though it is not far from the Siwalik range in the north. No gravel deposits (Photo 15-a, Appendix-B).
	Khando - 2	N 26-38-13.7 E 086-43-00.9	Recent deposits (Terai)	105± 3	RBd entirely made from sand deposits though it is not far from the Siwalik range in the north. No gravel deposits but the presence of mud balls (Photo 15-b, Appendix-B).
20	**Gagan Nadi**	N 26-47-02.1 E 086-21-07.0	Recent deposits (Terai)	114± 3	RBk section shows layers of sandy gravel and gravely sand. Gravel particles (cobble, pebble and granule): sub rounded-rounded with Quartzite (~70%), Sandstone (~30%). Sand becomes dominant from little down. Material extraction ongoing from ~50 m downstream from the bridge (Photo 16-a, Appendix-B).
21	**Kamala Nadi**	N 26-52-31.9 E 086-08-35.9	Recent deposits (Terai)	87± 3	RBk section shows layers of sandy gravel, gravely sand, and sand. Sands on the river banks are clean and shiny. Gravel particles (cobble, pebble and granule): sub rounded-rounded with Quartzite (~70%), Granite (10%), Sandstone (~20%) (Photo 16-b, Appendix-B).
22	**CharNath Khola**	N 26-53-23.6 E 086-05-55.1	Lower Siwalik	101± 4	Gravely sand on the present day riverbed, and some gravel layers in the past deposits. Cobble and pebbles are of Quartzite (~85%) and sandstone (~15%), while the granules are dominated by sandstone. Rapid aggradation of riverbed (Photo 17-a, Appendix-B).

	River Basin	Location		Elevation (m)	Description of the *River Bed (RBd)/ River Bank (RBk)/Terrace (Te) Material*
		Geographic	Geological		
23	**Baaluwa Khola**	N 26-53-46.4 E 086-03-49.0	Lower Siwalik	118± 4	Gravely silty sand on the present day riverbed. The gravel is largely pebble and granule size with Quartzite (~70%) and sandstone (~30%) (Photo 17-b, Appendix-B).
24	**Jaladh Khola**	N 26-54-51.3 E 085-59-49.2	Recent deposits (Bhabar)	132± 3	Gravely sand and sandy gravel deposits. The gravel fraction contains ~50% cobble and pebble and ~50% granule. The cobble and pebble are of Quartzite (~60%) and sandstone (~40%), while the granules are of sandstone (Photo 17-c, Appendix-B).
25	**Aauraahi Khola**	N 26-55-24.4 E 085-58-52.2	Recent deposits (Bhabar)	145± 3	RBd is sandy gravel and gravely sand. The gravel fraction contains Quartzite (~70%) and sandstone (~30%). Rapid aggradation of riverbed puts the E-W highway bridge under flood risks (Photo 17-d, Appendix-B).
26	**Barahari Khola**	N 26-57-05.0 E 085-55-49.2	Recent deposits (Terai)	169± 4	RBd is sandy gravel and gravely sand. The gravel fraction contains Quartzite (~70%) and sandstone (~30%) with cobble and pebble ~40% and granule ~60%. Some aggradation of the riverbed and risks to the highway bridge (Photo 18-a, Appendix-B).
27	**Baisi Khola**	Photo only	Recent deposits (Bhabar)		Gravely sand and sandy gravel deposits. Rapid aggradation of the riverbed (Photo 18-b, Appendix-B).
28	**Ratu Khola (**riverbed extracted more extensively)				
	Ratu Khola - 1	N 26-58-59.3 E 085-54-35.2	Recent deposits (Bhabar)	206± 3	Eroded channel section shows layers of gravel and sandy gravel. Gravel particles (cobble, pebble and granule) are sub angular-rounded with Quartzite (~80%) and Sandstone and dolomite (~20%) (Photo 19-a, Appendix-B; Figure C-39, Appendix-C).
	Ratu Khola - 2	N 26-53-31.5 E 085-52-37.4	Recent deposits (Terai)	101± 3	Eroded channel section shows layers of sand, gravel, and sandy gravel. Their thicknesses are variable. Gravel particles (cobble, pebble

	River Basin	Location		Elevation (m)	Description of the *River Bed (RBd)/ River Bank (RBk)/Terrace (Te) Material*
		Geographic	Geological		
					and granule) are sub rounded-rounded with Quartzite (~90%) and Sandstone (~10%). Sand becomes dominant as we move downstream (Photo 19-b, Appendix-B).
	Ratu Khola - 3	N 26-52-57.9 E 085-52-10.6	Recent deposits (Terai)	91± 3	Eroded and excavated channel section show layers of sand, gravely sand, and gravel. The sand and gravely sand are dominant over the gravel beds. Gravel particles (cobble, pebble and granule) are sub rounded-rounded with Quartzite dominant over Sandstone.
	Ratu Khola-4	N 26-53-23.7 E 085-52-24.6	Recent deposits (Terai)	99± 4	Eroded channel section shows layers of gravel, gravely sand, sand, and silt. Gravel particles (cobble, pebble and granule) are sub rounded-rounded with Quartzite dominant over Sandstone.
	Ratu Khola-5	N 26-54-29.5 E 085-52-40.9	Recent deposits (Terai)	113± 4	Eroded channel section shows layers of sand and sandy gravel, while there are patches of gravel and gravely sands on the river bed. Gravel particles (cobble, pebble and granule) are sub rounded-rounded with Quartzite dominant over Sandstone.
	Ratu Khola-6	N 26-55-45.4 E 085-53-14.5	Recent deposits (Terai)	133± 3	Eroded channel section shows layers of gravel and sandy gravel, and similar materials are seen on the river bed. Gravel particles (cobble, pebble and granule) are sub rounded-rounded with Quartzite (~90%) and Sandstone (~10%) as the maim composition (Figure C-39, Appendix-C).
	Ratu Khola-7	N 26-57-32.1 E 085-54-08.4	Recent deposits (Terai)	169± 4	Eroded channel bank shows layers of gravely sand and sandy gravel, and excavated channel section also shows similar materials. Gravel particles (cobble, pebble and granule) are sub rounded-rounded and Quartzite is dominant over Sandstone (Photo 19-c, Appendix-B).

	River Basin	Location		Elevation (m)	Description of the *River Bed (RBd)/ River Bank (RBk)/Terrace (Te) Material*
		Geographic	Geological		
	Ratu Khola-8	N 26-58-24.7 E 085-54-28.1	Recent deposits (Terai)	189± 4	Eroded channel section shows layers of gravel and sandy gravel. Gravel particles (cobble, pebble and granule) are sub angular-rounded with Quartzite (~80%) and Sandstone (~20%).
	Ratu Khola-9	N 26-59-57.3 E 085-54-50.3	Lower Siwalik	223± 3	The river bed materials is largely a sandy gravel. The gravel particles (cobble, pebble and granule) are sub angular-rounded with Quartzite (~80%) and Sandstone (~20%) (Photo 19-d, Appendix-B).
	Ratu Khola -9’		Lower Siwalik	289± 3	The river bed materials is largely a sandy gravel. The gravel particles (cobble, pebble and granule) are sub angular-rounded with Quartzite (~90%) and Sandstone (~10%).
	Ratu Khola-10	N 27-02-30.4 E 085-54-53.9	Middle Siwalik	288± 3	The river bed materials is largely a sandy gravel. The gravel particles (cobble, pebble and granule) are sub angular-rounded with Quartzite (~90%) and Sandstone (~10%) (Figure C-39, Appendix-C)..
	Ratu Khola-11	N 27-04-17.2 E 085-56-19.6	Middle Siwalik	356± 3	The river bed materials is largely gravel deposit with particle size ranging from cobble to granule. Local people said boulders were already collected. The gravel particles (cobble, pebble and granule) are sub rounded-rounded with Quartzite (~90%) and Sandstone (~10%). No sand deposits on the river bed (Photo 19-e, Appendix-B).

4 Engineering geological study

4.1 Introduction

Engineering geology is the applied science devoted to the investigation, study and solution of engineering and environmental problems which may arise as the result of the interaction between geology and the works and activities of man as well as to the prediction and of the development of measures for prevention or remediation of geological hazards (IAEG, 1992). In general, engineering geology is concerned with the properties of soil and rocks used in engineering projects, including the quantitative assessment of their strength, permeability, and compactness. These properties help in the selection of sites for civil engineering structures. Engineering geology uses data, techniques, and principles of varied branches of geology to study the surface and subsurface materials for evaluating their origin, distribution, and effects on engineering constructions (Gangopadhyay, 2013). In recent decades, engineering geology has been widely applied in geohazard management and assessment and evaluation of construction materials in a given region.

In this section, some aspects of engineering geology associated, especially, with the landslide phenomena and landslide distribution in Province 2 are discussed. Engineering geological aspect is necessary for this study because landslides are the important geological processes that supply and control availability of riverbed materials downstream all way to the Terai Plain, besides the associated geohazards. Though engineering geology has wide scopes and applications, only landslides on the Siwalik hill slopes and river bank erosion or landslides due to toe cutting are considered here.

4.2 Landslide: Process and Types

Landslide is defined as the outward and downward movement of slope forming materials along the definite plane of failure under the influence of gravity (Adhikari & Koshimizu, 2005; Dhakal et al., 2020). The materials involved in the landslides can vary from loose soil to competent rock masses or their combination. Their movements can be very fast like avalanche, imperceptible like creeping or in between these extremities (TU-CDES, 2016). The nature of damage, destruction or disaster by landslides therefore varies according to their types, materials involved and speed of movement. Landslides are the product of a complex interplay of various triggering and conditioning in-situ factors. When combined with human interferences, they become complex and

hazardous. Most of the damage and major proportion of human and infrastructure losses in mountain and hilly areas are often associated with landslides (Subodh Dhakal, 2015).

Consistent with the landslide classification of Varnes (1978), the Siwalik has three source material types (rock, debris, earth) and four movement types (fall, topple, slide, flow) involved in landslide. The source materials consist of rocks (sandstone, mudstone, conglomerate) and sediments (alluvium, colluvium). Loosely consolidated sandstones alternating with interbedded mudstone in the Siwalik are technically rock formations, but due to the fact that they are loosely consolidated and generally heavily weathered at the surface, they are referred to as *"earth"* in Varnes's (1978) terminology and therefore considered here as earth materials in addition to the alluvium and colluvium.

Bedrock have rockfall, rock topple, rock slides movements. Rockfall is a common type of landslide on steep slopes (natural or engineered). Differential weathering in stratified sandstone and mudstone facilitate the initiation of rockfall. Rockfall debris accumulates at the slope base as talus and remove downstream by river actions in the course of time. Rockslides have occurred along single planar, circular, and compound surfaces. The brittle rocks, especially sandstone is jointed, making the slope vulnerable to rock falls and slides. Wedge sliding involves movement along the intersection of two discontinuities. Toppling occurs when an unstable rock block rotates in a vertical plane about a fixed point. Progressive failure involves gradual decrease of intact, discontinuity, and rock mass strength (either simultaneously or independently) as rock deforms. They have a wide range of volume from an individual sliding block to some large-scale landslides. The failure surfaces of planar slides are generally associated with stratigraphic contacts (e.g., bedding), which provide mechanical zones of weakness and zones of preferential groundwater flow and/or permeability contrast (Varnes, 1978).

Movements of the earth materials in the Siwalik are mainly related to falls, topples, slides and flows. As a result, four main types of landslides are recognized on the earth materials as follows:

Earth fall: Occurs in steep or overhanging slopes from the detachment of soil along a surface on which little shear displacement takes place. This typically occurs where artificial cuts have been made and along eroded or undercut riverbanks.

Earth topple: Occurs in vertical slopes with cohesive materials. Vertical joints or cracks develop behind the edge of the slope, resulting in a forward rotation of a compartment or column of soil.

Field observations typically reveal mixed features associated to both fall and topple, making it difficult to clearly distinguish between the two types.

Earth slide: Occurs in moderate slopes and often consists of shallow weathered soil sliding onto a stronger or impermeable substrate (e.g., interbedded clay layers). Rotational slides (also referred to as slumps) involve sliding of the materials along a curved surface. Their occurrence is usually limited to an initial movement that evolves into compound slides or flows.

Earth flow (or mudflow): Occurs in moderate slopes during or after heavy rain events and involves excess pore pressure or liquefaction of the sliding materials. It forms characteristic bowl- or balloon-shaped scars on the hill flanks, with the mobilized material spreading out onto the valley floor and being subsequently rapidly washed away, only leaving the main scar visible over time. Earth flows often initiate as compound slides. Small-scale surface erosion may also be reported as landslides, though they occur mostly in artificial fills.

4.3 Slope Stability Factors

Genetically formed by the very weak, fragile and youngest rocks of the Himalaya, and lying in the most dynamic area within the Himalaya, Siwalik area is exposed to various types of slope instabilities and landslide hazard (TU-CDES, 2016). Consistent to the slope stability study of (Popescu, 1994), mountain slopes in the Siwalik can be viewed as existing at various points along a stability spectrum ranging from high margins of stability with low probabilities of failure at one end, to actively failing slopes, with no margin of stability, at the other (Figure 17).

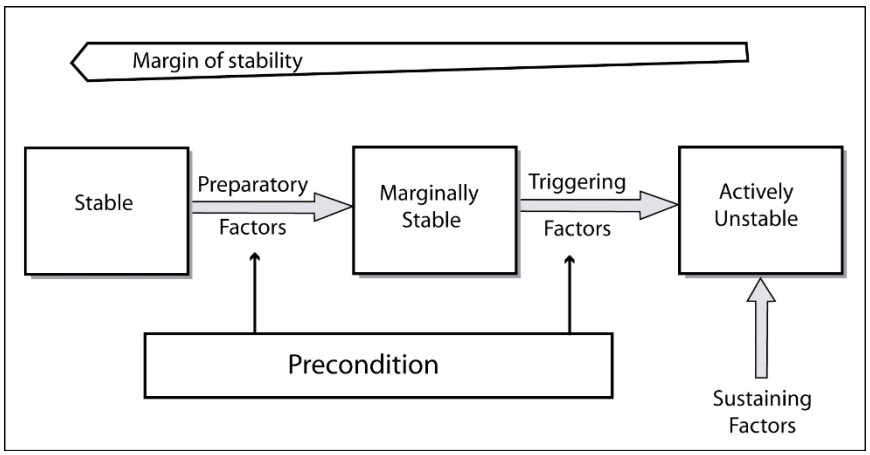


Figure 17: Slope stability states and destabilizing factors (Adopted from Popescu, 1994).

First is the ‘stable state’; defined as slopes with a margin of stability which is sufficiently high to withstand the action of all-natural dynamic destabilizing forces likely to be imposed under the current environmental/geomorphic regime. Second is the ‘marginally stable state’, represented by static slopes, not currently undergoing failure, but susceptible to failure at any time that dynamic external forces exceed a certain threshold. Third is the ‘actively unstable state’, represented by slopes with a margin of stability close to zero and which undergo continuous or intermittent movement.

Factors promoting slope instability are important to consider. The concept of three stability states offers a useful framework for understanding the causes and development of instability in the Siwalik. In this context four groups of factors promoting instability (‘destabilizing factors’) can be identified on the basis of function (Figure 17).

Pre-disposing Factors (Preconditions) are static, inherent factors which influence the margin of stability and more importantly act as catalysts to allow other dynamic destabilizing factors to operate more effectively. The thick soils both in the dip and counter dip slope and the highly fractured and jointed bedrocks that lose strength more readily than others in the presence of water have predisposed the slope to failure during rainstorms in most sites. Orientation of bed rocks in the dip slope face of the mountains has also enhanced the destabilizing effects of undercutting.

Preparatory factors are dynamic factors that decrease the margin of stability in a slope over time without actually initiating movement. Hence, facilitated by preconditions, they are responsible, for shifting a slope from a ‘stable’ to a ‘marginally stable’ state (Figure 17). Factors, such as reduction in strength by weathering, tectonic uplift, faulting, thrusting, and shearing operating since the formation of the Siwalik Hills and others effective in shorter time periods e.g., slope oversteepening by erosional activity, deforestation, and slope disturbance by human activity are the preparatory factors.

Triggering factors are those factors that initiate movement, i.e., shift the slope from a ‘marginally stable’ to an ‘actively unstable’ state (Figure 17). The most common triggering factors in the Siwalik zone are intense monsoon rainstorms, prolonged periods of sustained rainfall, seismic shaking, and slope undercutting. The triggering threshold varies with the inherent stability of the terrain and therefore the spatial differences in the value of triggering thresholds can provide a relative measure of the geographic distribution of terrain susceptibility to landslide occurrence. It is also clear that in some situations the triggering threshold for a given terrain is not a constant but varies temporally as a result of landslide occurrence. As susceptible material is successively

removed from hill slopes there is a residual strengthening of the terrain and the triggering threshold rises. This phenomenon is referred to as 'event resistance'. A similar phenomenon can be observed with debris flow occurrence. The activation of debris flows depends not only on the magnitude of the triggering event but also on the availability of transportable material. For example, if all source material is removed by a rainfall-triggered debris flow, further rainstorms of the same magnitude are unlikely to generate flows. Triggering thresholds can thus also be seen as a function of the time required to establish a critical volume of rock debris in the source area.

Sustaining factors are those that dictate the behavior of 'actively unstable' slopes, e.g. duration, rate, and form of movement. Some of these may be dynamic external factors such as rainfall, others may relate to the progressive state of landslide movement or the terrain encountered in the landslide path and other inherent material properties.

4.4 Methodology

A high resolution Google Earth Pro data was obtained for the year 2018-2019. This imagery was used to digitize the location and shape of the landslide in ArcGIS 10.5 platform. The landslides were visually identified based on the interpretation of the shape, size, texture and location. Landslides are generally identified by their color varying between light gray to light color, and based on their shape which usually is triangular, spoon like or tree like. Based on their location, landslides usually occurs near ridges, cutoff slopes of riverbanks, gully head or geological boundaries. This resulted in spatial distribution of the landslides. A field validation on the demarcated landslides were conducted during the field visit of the river systems. This approach was based on a similar study of landslides undertaken by Central Department of Environmental Science, Tribhuvan University for PCTMCDB (TU-CDES, 2016).

4.5 Landslides in Province 2

Table D-4, Appendix-D gives the details of the watershed area, landslide area, and area covered by the landslides in the entire 129 watersheds of the region. Study of Google Pro Earth Imagery 2019/20 reveals more than 40,000 landslides of various sizes in the entire watershed areas draining through Province 2, including the watersheds of Bagmati and Kamala Rivers, which have origins in the Lesser Himalaya (Figure 18). Total area covered by the landslides is about 47 km^2. Table D-4, Appendix-D shows that the Bagmati River has the largest watershed (2812 km^2) and it is followed by the Kamala River (1569 km^2). Among those having the watersheds within the Siwalik, Trijuga River (696 km^2) and Bakaiya River (317.4 km^2) are two largest watersheds (Table D-4, Appendix-D).

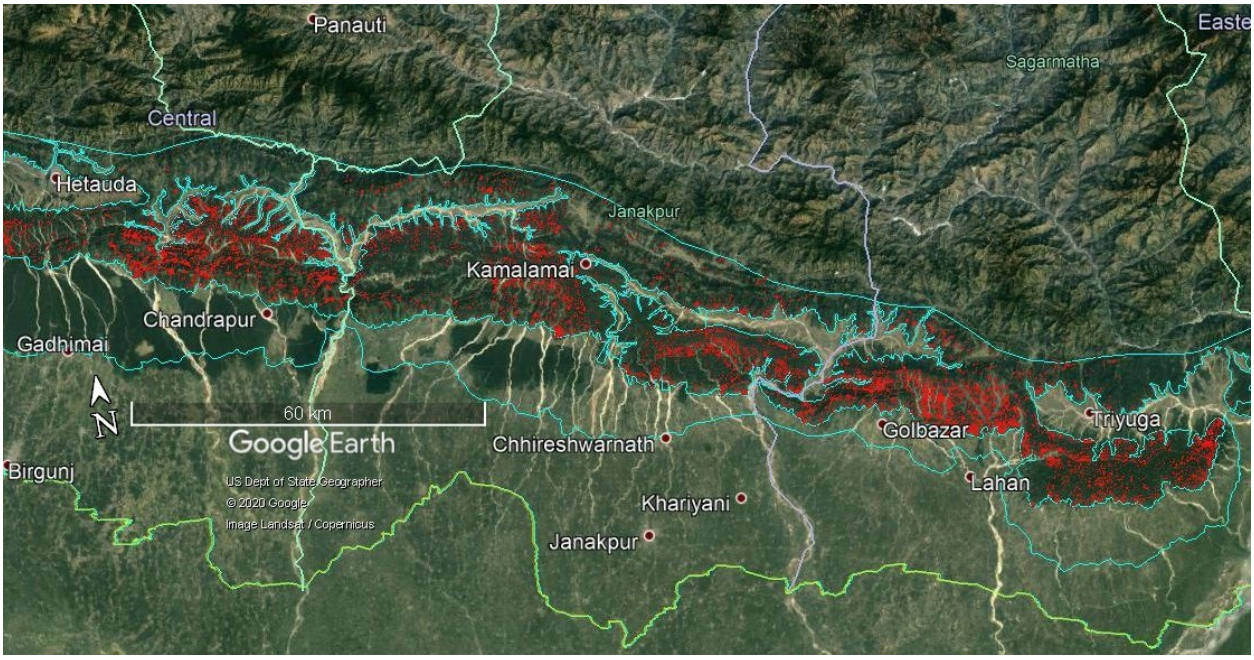


Figure 18: An overview of landslide distribution on the Google earth image in the Siwalik watersheds of the 129 river systems mentioned on Table 1. Red marks indicate landslide spots which are more than 40,000.

Among the 129 watersheds, landslide area varies from 0% to 3. 53% of the watershed (Table D-4, Appendix-D). Baluwa1, Dulan, Dumajor, Gagan2, Ghordana2, Indrabati, Jhinge, Labhitiya3, Manabodhi, Mutani, Patauna, Paurai2, Shitals, Sikta, Suklai, and Thuteup watersheds have no landslides, whereas Khuti, Bhakahariya, Betaha, Mahajan, Jhadi, Khadak1, and Lekeshwor1 are the top seven watersheds having 3.53%, 3.45%, 2.98%, 2.7%, 2.46%, 2.45%, 2.1% landslide area of the entire watersheds, respectively (Table D-4, Appendix-D). The landslides represent 47 km^2, which is about 1% area of the watershed.

There are 41,091 landslides detected based on the Google earth image (Figure 19) and their size varies from around 8 m2 to 4218 m2 with average size being 938 m2 (Table D-5, Appendix-D, and Figure 20). The distribution of different numbers of landslides for different area values are shown in (Figure 20). Landslides having large area is small in number. The landslides have occurred both in rocks and soils and are mostly fall and slide in terms of their movements. Table 7 and Figure 21 summarizes the landslides and slope relationship. Almost two-third of the 41,091 landslides mentioned above fall on 10° -15° slope range, 15.5% on 15° -20°, 6.25% on 20° -25°, 2.86% on 25° -30°, and 0.27% on 25° -30° slope. Generally, there are small number of landslides on slopes steeper than 30°.

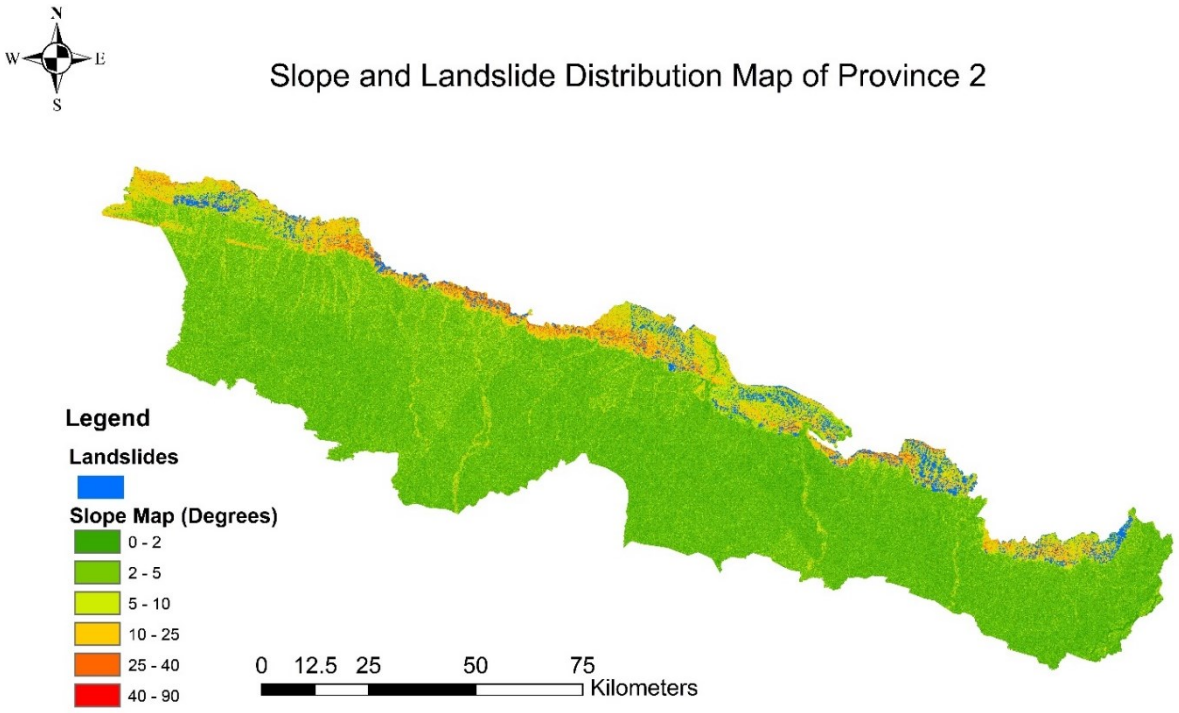


Figure 19: Slope and landslide distribution map of Province 2, Nepal.

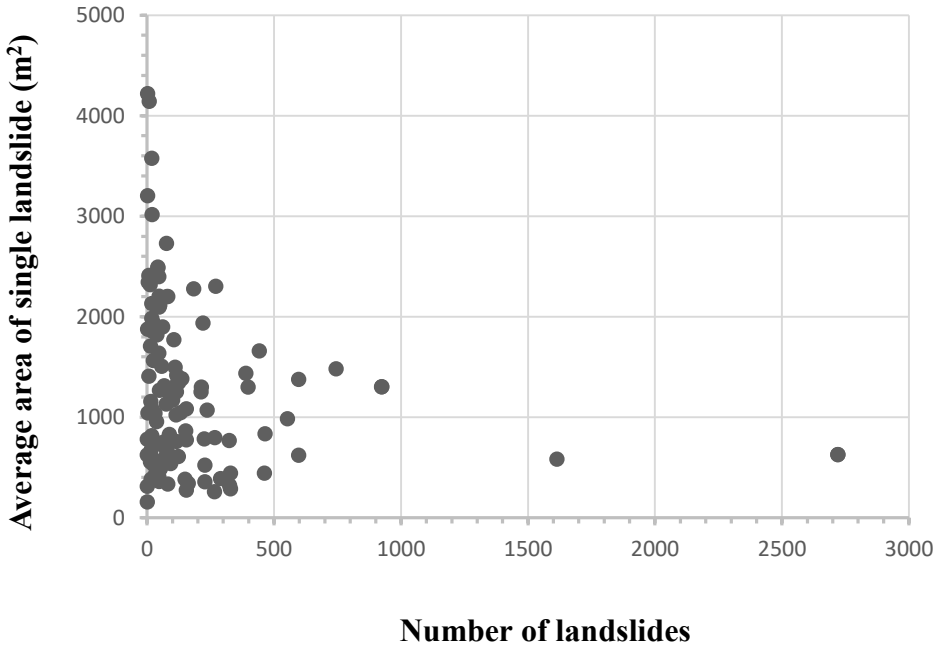


Figure 20: Distribution of landslides in different slope range of Province 2.

Table 7: Landslide distribution in different slope range in the Siwalik of Province 2

Slope range (degree)	Number of Landslide	Percentage of total landslides
5-10	1896	8.5
10-15	14574	65.3
15-20	3722	16.7
20-25	395	1.8
25-30	1588	7.1
30-35	133	0.60
Grand Total	**22308**	

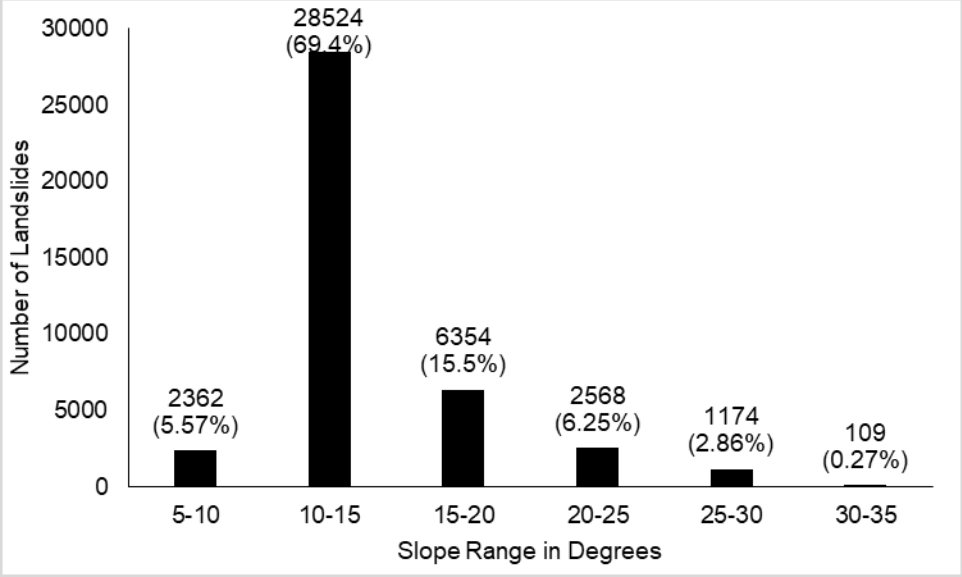


Figure 21: Distribution of landslides in different slope range in Province 2

4.5.1 Observed Representative Landslides

It is already mentioned above that landslides in Province 2 have verities of source materials and movements. Since describing each type of landslide in each watershed separately is beyond the scope of this work, photographs of the landslides taken in the field and some satellite images of

some of the representative watersheds are presented in Figure 22 - Figure 34 below to give a picture how landslides are distributed and whether they are responsible to make riverbed materials available to the extent seen at present in downstream section of rivers all way down to the southern edge of Nepal.

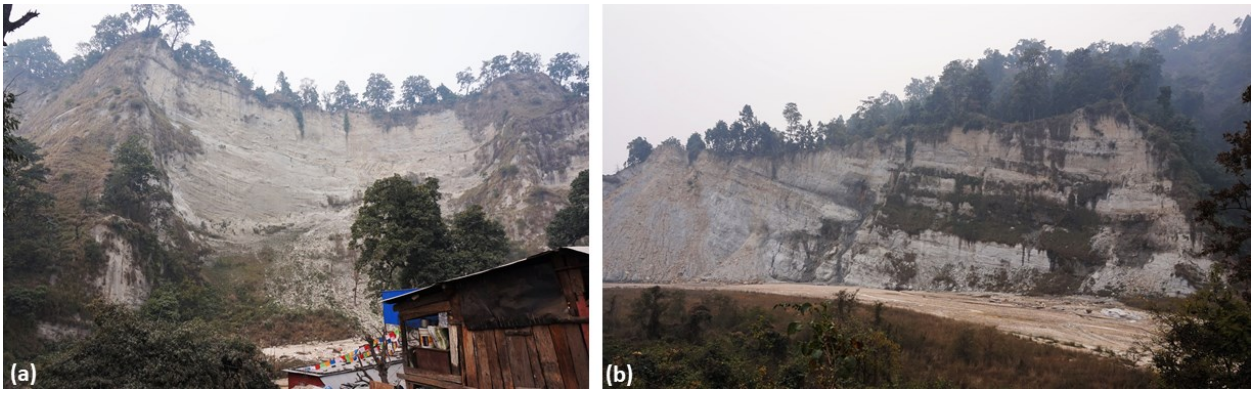


Figure 22: Photograph showing a) Rock fall on the Middle Siwalik sandstone on right bank of Churiya Khola, Bara District; b) Rock fall on the Middle Siwalik sandstone cliff on right bank of Churiya Khola adjacent to the E-W Highway, Bara District.



Figure 23: Photograph showing a plane rock failure along the bedding plane of the Middle Siwalik sandstone on right bank of Churiya Khola, Bara District (Photograph after TU-CDES, 2016). The slabby nature of the sandstone beds, its dipping parallel to the hill slope, and toe cutting by the Chriya River are the cause of the failure.



Figure 24: a) Landslide on Upper Siwalik conglomerate beds on right bank of Churiya Khola, Bara District. The conglomerate is highly-moderately weathered making it easier to develop landslide. The dry tributary stream of Churiya Khola has full of gravels generated from the landslide upstream; b) Landslide on hill face of the highly weathered Upper Siwalik conglomerate as source of river bed material in Churiya Khola valley, Bara District.



Figure 25: Google Earth images showing landslide distribution on the catchment of Bagmati River watersheds. Old landslide scars are abundant in the watershed.



Figure 26: An upstream view of Bakaiya Khola valley about 7 km north from the E-W Highway at Nijgad. Two landslides seen on the right side are caused by the Fast-track opening (at the bottom of the slides). The hills are made from the Middle Siwalik sandstone. The riverbed materials seen in the front part are of the Siwalik sandstone and Lesser Himalayan Quartzite with the large boulders mostly of sandstone. A belly bridge over the Bakaiya Khola is seen at the toe part of the landslides.



Figure 27: Photographs showing a) An example of river bank erosion and remobilization of the old river terrace materials of Bakaiya Khola as source of sediments to the downstream in addition to the materials added to the rivers by landslide from the mountain slope. The site is on the right bank of the Bakaiya Khola about 5 km north from the E-W Highway; b) River bank erosion caused by the Bakaiya Khola in the Terai Plain (when river runs high discharge during summer monsoon) south of the E-W Highway also supply sediments further downstream. The marks on the measuring stick are at 10 cm interval.



Figure 28: Photographs showing a) Landslides (white/grey marks) on the hills of Middle Siwalik sandstone on the right bank of the Bagmati River as seen north from about 1 km south from the E-W Highway at Karmaiya. The debris generated from the landslides delivers to the Bagmati River. Bagmati River and extracted riverbed materials are seen on the foreground; b) A close-up view of part of the photograph shown in (a) with the Bagmati River and Barrage on the foreground.



Figure 29: A view of Chapini Khola watershed a) With the Middle Siwalik hills and landslides (white/grey marks) on the mountain slopes. The sandstone is moderately-highly weathered. The Chapini riverbed is filled with white sands. View towards north (upstream); b) A distant view of a landslide (white/grey marks) on the Middle Siwalik sandstone further east from Chapini Khola.



Figure 30: Photograph showing a) An upstream view of Khando Khola (as observed from the E-W Highway) with the Khando Khola itself on the foreground and the Middle Siwalik hills upstream. The Middle Siwalik sandstone has landslides (white/grey marks) of various sizes and that contribute sediments to the stream.

The rocks are fresh to moderately weathered. The riverbed materials seen on the photograph is sand and silt. View towards north; b) A view of the Middle Siwalik hills in the catchment of Khando Khola further east with swamps of landslides (white/grey marks) on sandstone beds. The debris derived from the landslides ultimately discharges into the Khado Khola. View towards north from the E-W Highway.



Figure 31: Landslides and gully erosion caused huge erosion on the already weathered Lower Siwalik mudstone on the right bank of Ratu Khola north of Bardibas, Mahottari District. This process produces abundant clay to the downstream section.



Figure 32: Landslides on the cliff face of the highly weathered Lower Siwalik mudstone and the overlying Quaternary deposits (brown) on the right bank of Ratu Khola north of Bardibas, Mahottari District. The landslides are caused due to the slippery nature of the weathered mudstone, when wet, and toe cutting of the Ratu Khola.



Figure 33: Photographs showing landslides (white marks) on Middle Siwalik sandstone on left bank of the Ratu Khola north of Bardibas, Mahottari District. The rocks are moderately weathered. Landslides on the Ratu Khola produces abundant sand which is white in color.



Figure 34: Photographs showing a) A landslides (rockfall) on highly weathered sandstone and mudstone beds of the Middle Siwalik north of Lalbandi, Sarlahi District; b) Landslides on the Middle Siwalik sandstone in upstream section of Gagan Khola.

4.6 Summary and discussion

The adverse topography, dynamic geomorphology, weak geology and presence of geological structures are the contributing factors for landslide occurrence in the Nepal Himalaya (Adhikari & Koshimizu, 2005; Bhandari & Dhakal, 2019b, 2019a, 2020; Dhakal et al., 2020) and this remains valid in the Swalik zone too. Landslides and debris flows are common phenomena in the Siwalik zone, especially when summer monsoon brings abundant rains. Landslides are the result of the convergence of a series of unfavorable stability conditions, both natural and human induced. Evidence of past landslides dominates most of the watersheds as illustrated in Figure 24. Field observations suggest that alternate bed of sandstone and mudstone in the Middle Siwalik have pre-disposed the slopes to incipient instabilities; tectonic uplift, stream erosion and deforestation are the preparatory factors; monsoon rains (both concentrated and sustained) and slope undercutting are the triggers; and monsoon rains and the material availability are the sustaining

factors of the landslides. In most cases, the upper part of Province 2 (Siwalik) is prone to landslides and the lower part (Terai Plain) is vulnerable to sediment-induced disasters.

The type, size and number of landslides were highly influenced by geology. For example, gully erosion, earth slides, mudflow and debris flow are the dominant processes in the landslides of the Lower Siwalik as weathering of the mudstone and fine-grained sandstone in this part of the Siwalik makes things easier for such types of movements. Rock slides and rock falls are the common landslide types in the Middle Siwalik due to the reason that the succession of competent, massive sandstone beds alternating with incompetent mudstone layers have undergone differential weathering, and the mud, when wet, serves as lubricant for sliding the overlying materials. Similarly, being brittle, the Middle Siwalik sandstones have joints to facilitate wedge failure; and being hard, the sandstones develop steep cliffs where most of the rockfalls were seen. Granular flow, debris fall and gully erosion were dominant in the Upper Siwalik, where conglomerate is the main lithology. Vertical and overhanging slopes of conglomerates or the differently graded gravels were common features that control the landslide type in this area. Moreover, many landslides in Province 2 were complex in terms of process, type and temporal domain (TU-CDES, 2016). At many places like that shown in Figure 28-a, Figure 29-a, Figure 30-b and Figure 33-b, swarms of landslides can contribute lot of sediments to the rivers. However, the exact quantity of sediments contributed by landslides in a watershed to its rivers is unknown and is a subject of future research.

Reworking of the colluvium at the foot of the mountain slopes, landslides on the mountain slopes, and alluvium in river terraces, by rains and rivers, especially during summer time carry large volume of sediments downstream and deposit on the riverbeds within the Siwalik and Terai Plain. Landslides triggered by the toe cutting action of river also contribute sediments to the drainage. Based on the engineering geological study mentioned above, landslides and the related processes in Province 2 are known to be one of the main processes to generate and remove sediments from the Siwalik and upstream section to the Terai Plain in the south. To control the sediment load in the river systems in the Terai Plain and save infrastructures, settlements, and agricultural lands, slope stabilization in the mountains and river bank protection are inevitable. Forestation also can helps protect lands from land sliding and river bank erosion. In many places, unscientific extraction of riverbed materials has changed riverbed profile and caused slope instability. Such human activities also need to be done properly.

5 Geophysical study

5.1 Background

The study Electrical Resistivity Tomography (2D-ERT) is used for the subsurface geological exploration in the river bed and banks. For carrying out 2D-ERT, electrical current of very low frequency is passed through the geological subsurface. The response of current on geological formations such as clay, silt, sand, gravel, boulders, and bedrock are different. By virtue of different capacity of different material on electrical conductivity, it is possible to separate different materials from each other.

The area is located in the river channel of the Bagmati River, Balan River, Bakaiya River, Khado River and Ratu River of Province no. 2. An electrical resistivity tomogram (ERT) survey was conducted to investigate subsurface geology based on the electrical properties of earth materials. During the process of data acquisition, an apparent resistivity was obtained by measuring potential difference. The obtained apparent resistivity from the fieldwork were later converted to true resistivity using the software RES2DIN Ver.4.8.3. The software gives the image of the profile and from which true resistivity of the geological conditions were evaluated. The interface between unconsolidated materials and consolidated materials such as bed rocks, residual soil, colluvium, weathered rock from fresh rock, water table etc. were explored using ERT profile. The summary on the location and length of surveyed ERT profiles along different river cross-sections are listed in the Table 8.

Table 8: Summary of ERT profiles (The coordinate system used is WGS84, UTM, N45)

River	Transect	ERT Profile	Length	Start Coordinate		End Coordinate	
				X Coordinate	Y Coordinate	X Coordinate	Y Coordinate
Bakaiya	Bakaiya L2	Bakaiya-L2-ERT-1	177	318400	3010340	318239	3010410
		Bakaiya-L2-ERT-2	177	318239	3010410	318075	3010480
	Bakaiya R3	Bakaiya-R3-ERT-1	177	321192	3003540	321038	3003470
		Bakaiya-R3-ERT-2	177	321037	3003460	320905	3003350
	Bakaiya R4	Bakaiya-R4-ERT-1	267	323994	2991710	323731	2991660
		Bakaiya-R4-ERT-2	177	323562	2991620	323495	2991580
Bagmati	Bagmati R1	Bagmati-R1-ERT-1	177	348823	3000380	348659	3000450
		Bagmati-R1-ERT-2	87	348521	3000500	348445	3000540
	Bagmati L2	Bagmati-L2-ERT-1	177	343904	2992510	343743	2992580

River	Transect	ERT Profile	Length	Start Coordinate		End Coordinate	
				X Coordinate	Y Coordinate	X Coordinate	Y Coordinate
		Bagmati-L2-ERT-2	177	343695	2992610	343532	2992670
		Bagmati-L2-ERT-3	87	343372	2992750	343288	2992780
	Bagmati R3	Bagmati-R3-ERT-1	177	340776	2984290	340612	2964350
		Bagmati-R3-ERT-2	177	340517	2984390	340353	2984450
		Bagmati-R3-ERT-3	177	340278	2984480	340122	2984550
Ratu	Ratu R1	Ratu-R1-ERT-1	177	395513	2993860	395342	2993900
	Ratu R3	Ratu-R3-ERT-1	267	391663	2983370	391411	2983450
	Ratu R5	Ratu-R5-ERT-2	267	387792	2974330	388046	2974250
Balan	Balan R1	Balan-R1-ERT-1	177	455093	2957370	455021	2957520
		Balan-R1-ERT-2	177	455021	2957520	454940	2957680
		Balan-R1-ERT-3	177	454916	2957710	454827	2957870
	Balan L3	Balan-L3-ERT-1	177	451490	2944710	451320	2944760
		Balan-L3-ERT-2	177	451251	2944790	451085	2944840
		Balan-L3-ERT-3	177	450986	2944880	450818	2944930
Khado	Khado R1	Khado-R1-ERT-1	177	472910	2945550	472735	2945550
	Khado R3	Khado-R3-ERT-1	267	478984	2936190	478727	2936130
		Khado-R3-ERT-2	177	478727	2936130	478551	2936100

5.2 Methodology

5.2.1 Electrical Resistivity Tomography

The resistivity method is one of the oldest geophysical techniques, it is based on passing artificial electrical current in the earth through the ground via a pair of electrodes and a resulting potential difference is measured between a second pair of potential electrodes. This method has been used for many decades in hydrogeological, mining, geotechnical, archaeological, environmental and engineering investigation.

From two electrodes (A and B) the current is flowing in the subsurface earth and the current lines will take semi-circle shapes, while the equipotential lines are perpendicular on it, as shown in Figure 35, so that any changes in the conductivities of the subsurface material led to change the current flow lines, as result that equipotential lines will be disturbed, because

they flow vertically on the current lines. Thus, the measurement values will change on the ground surface. However, the potential difference (ΔV) at any point which is caused by two current electrodes (A and B) measured between the potential electrodes (M and N) is given by Equation **12**.

$$\Delta V = V_M - V_N = \rho I/2\pi\ (1/AM - 1/BM - 1/AN + 1/BN) \quad \textbf{12}$$

Where,

V_M = potential at M due to A and B.

V_N = potential at N due to A and B.

I = Electrical current.

ρ = Resistivity.

AM, BM, AN, BN = Distances between the electrodes.

From Equation 12,

$$\rho = \frac{2\pi}{\left(\frac{1}{AM} - \frac{1}{BM} - \frac{1}{AN} + \frac{1}{BN}\right)}\ \Delta V/I \quad \textbf{13}$$

Equation 13 is a fundamental equation in the direct current (dc) method of electrical prospecting.

The factor $\left\{\frac{2\pi}{\left(\frac{1}{AM} - \frac{1}{BM} - \frac{1}{AN} + \frac{1}{BN}\right)}\right\}$ is called the geometric factor of the electrode arrangement and generally is designated by the letter (K).

Therefore,

$$\rho = K\ \Delta V/I \quad \textbf{14}$$

If the measurement of (ρ) is made over semi-infinite space of homogeneous and isotropic material, then this value is called resistivity (ρ) of the material. However, if the medium is inhomogeneous and/or an-isotropic then the resistivity computed from equation (2) is called an apparent resistivity (ρ_a). Then the general equation is provides in Equation **15**.

$$\rho_a = K\ R \quad \textbf{15}$$

Where,

R = Resistance of material = $\Delta V / I$

The value of the apparent resistivity is a function of several variables such as, porosity, permeability, water saturation, the concentration of dissolved solids in the pore water, isotropic properties and other characteristics of the subsurface materials, (Keller & Frischknecht, 1966; Zhody et al., 1974).

The electric current flows into the earth by two electrodes depending on two main types of conduction. The first is electronic conduction; the current flows by free electrons, such as in metals. The second is electrolytic conduction where the current flows by the movement of ions in groundwater, (Zhody et al., 1974). In the areas where the water table lies near the earth's surface, the electrolytic conduction is probably the more common mechanism. In areas where the water table is deep, the electronic conduction will depend on the conductive minerals present, (Zhody et al., 1974).

The relation between geology and resistivity depends on the physical and chemical properties of rocks and soils. Therefore, the rocks and soils have a large range of resistivity, (Keller & Frischknecht, 1966). Hard rocks are poor conductors of electricity, but geological processes like weathering, dissolution, hydrothermal alteration, faulting and shearing can alter rock to increase the porosity and permeability of rock and hence decreases resistivity. By comparison, compaction of sedimentary rock and metamorphism of all types may result in lower porosities and permeability. Resistivity is, therefore, a widely varying parameter, which changes not only from lithology to lithology, but also within a particular formation of same lithology Figure 36.

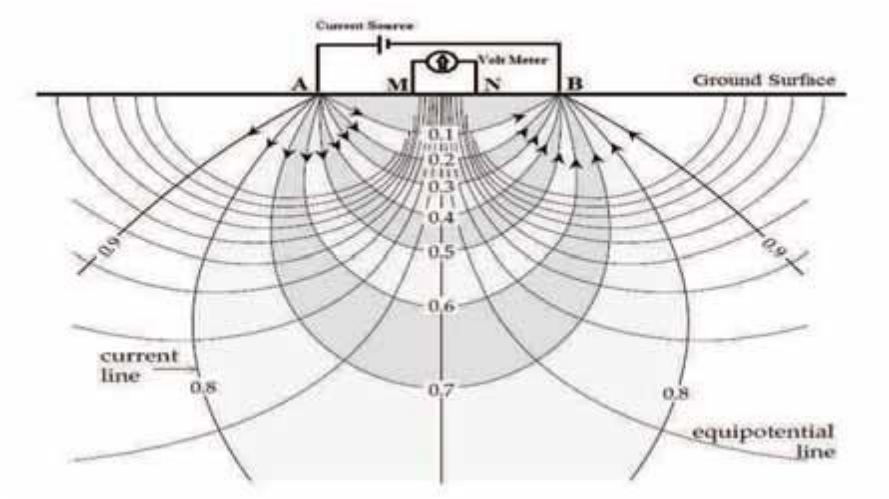


Figure 35: Schematic illustrating basic concept of electrical resistivity measurement, (Lowrie & Fichtner, 2020)

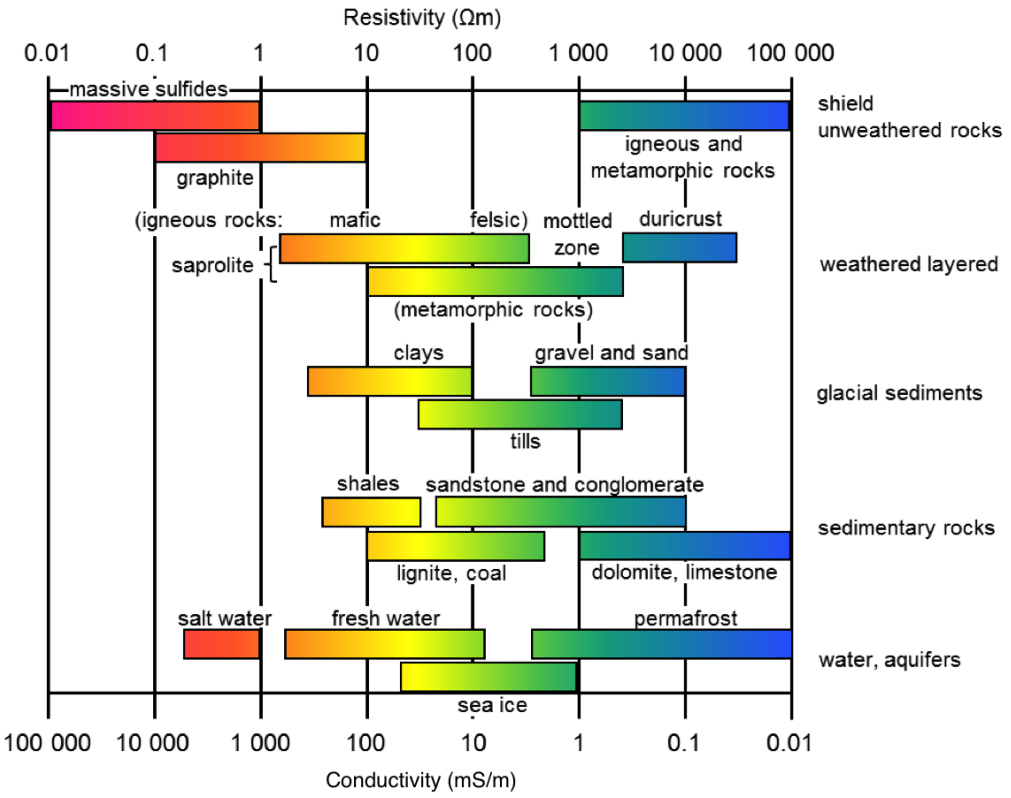


Figure 36: Conductivities and resistivity of common rocks, soils and ores.

Common trade-offs between array types include signal-to-noise ratio, sensitivity variation with depth and sensitivity to horizontal or vertical structures (Telford et al., 1990).

5.2.1.1 Common four electrode configuration

The configuration of the electrodes, which describes the ordering of the four electrodes and their respective distances, can be chosen arbitrarily. There are some specific configurations, which are commonly used. These configurations are therefore well known and established. Using these has the advantage of comparability between different measurements. Furthermore, these configurations simplify the calculation of the apparent resistivity, because the distance between the electrodes follows defined schemes.

The most common electrode configurations are namely

- the Dipole-Dipole,
- the Wenner
- the Schlumberger and
- the Wenner-Schlumberger configuration

The Wenner configuration, a common array with the four electrodes evenly spaced along the ground surface with the two current electrodes located at the ends is used. This array is known as a Wenner array (Figure 37).

This array is relatively less sensitive to vertical changes in the subsurface resistivity below the centre point of the array, and it is good in resolving horizontal changes in earth layers, especially near the earth surface. Among the common arrays, the Wenner array has the strongest signals strength, so this can be an important factor if the survey is carried in areas with high background noise, (Loke, 2012; Zhody et al., 1974). It is the most commonly used in resistivity method.

For a Wenner array, the apparent resistivity ρ_a can be calculated from a measurement of change in electrical potential $\Delta V_{MN}$with a known current *I* and electrode spacing *a* by the Equation **16**.

$$\rho_{aWenner}=2\pi aI\Delta V_{MN} \quad \textbf{16}$$

The Schlumberger configuration is similar to the Wenner configuration, but it has less restriction to the electrode spacing. Both electrode pairs are required to have a common midpoint, but there is no relation between the offset of the current electrodes and the potential electrodes.

Usually, the current electrode distance is kept much larger than the potential electrode distance. It is a method for investigating resistivity variations in depth. This array is high sensitive to vertical changes in the subsurface resistivity below the centre point of the array, and relatively less sensitive to horizontal changes in earth layers.

The Dipole-Dipole array is the most widely used in 2D imaging technique. The arrangement of the electrodes of this array is shown in Figure 37 (c). The spacing between the current electrode pair which is the same as the distance between the potential electrode pair, which controls the depth of investigation (Keller & Frischknecht, 1966).

This array is very sensitive to horizontal changes in resistivity, but relatively insensitive to vertical changes, which means it is good in mapping vertical structures, such as faults, but relatively poor in mapping horizontal structures such as sedimentary layers (Loke, 2012).

The Wenner-Schlumberger array is one of the important arrays used in 2D imaging technique. It is a combination of the Wenner and Schlumberger arrays (Pazdirek & Blaha, 1996). The advantage of this array is that it can be used with the electrodes system arranged with a constant spacing, hence it is easier than schlumberger array. The purpose of using this array is that they are moderately sensitive to both horizontal and vertical structures (Loke, 2012).

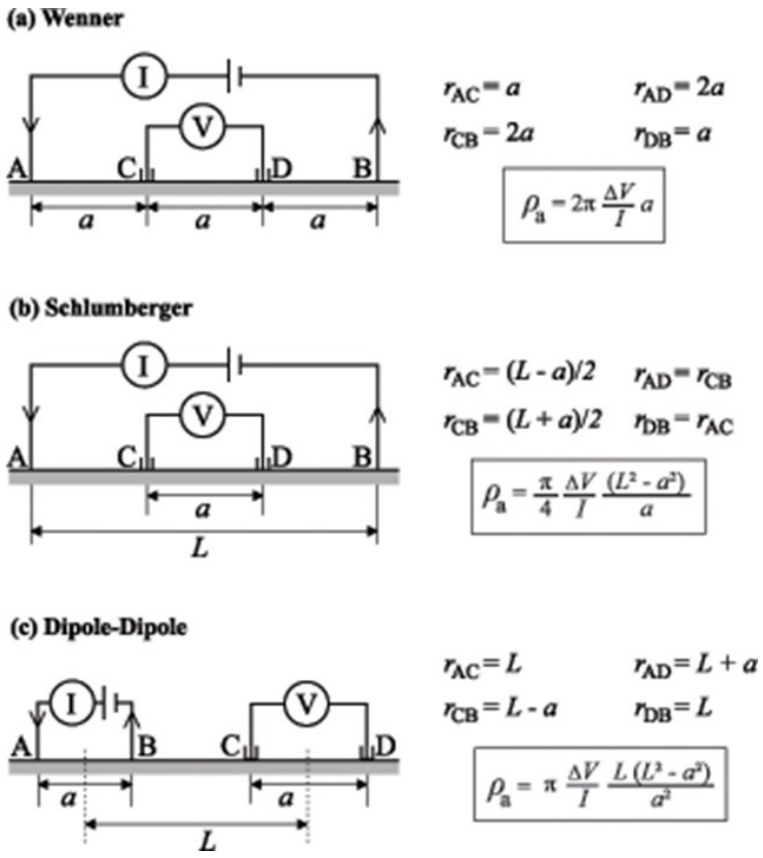


Figure 37: The different four-electrode configurations. a) Wenner, b) Schlumberger and c) Dipole-Dipole.

Apparent resistivity measurements allow for the estimation of the resistivity structure of the subsurface. Profiling techniques involve traversing an array with fixed electrode separation across a subsurface to detect lateral variations in resistivity at a consistent depth of investigation. Mathematical inversion of the data is performed to obtain possible models of the subsurface resistivity structure that are consistent with the measured data (Loke, 2012). Inversion is an iterative process in which a model is obtained by iteratively attempting to fit the acquired data (Sasaki, 1992). Inversion parameters such as number of model blocks, model block size and inversion smoothness will influence the resulting inversion and must be chosen to best suit the survey type.

With electrical resistivity surveys, compromise must be made when selecting the minimum electrode separation to use for a study. Increasing electrode separation improves sensitivity at greater depths at the cost of resolution (Loke, 2012). Surveys with smaller electrode separations also require an increased number of electrodes to cover a transect of comparable length to larger electrode separations, often resulting in performing roll-along style surveys which are more time intensive.



Figure 38: Image showing the field setup of the ERT equipment at the surveyed river section.

In our study, sixty electrodes were grounded with electrode spacing of 3 m. Roll along method is used to cover the required length of the ERT profile. All electrodes were connected via multi core cable and the cable is connected to the ERT machine. The machine decides which four of sixty electrodes to use while taking data and regulate the switching of the electrodes. The process of taking data is automatic after giving instruction to the machine (Figure 38).

5.2.1.2 Resistivity vs particle size, moisture content and density

According to previous researches, the ease of current to propagate within each geomaterial can be influenced by grain size fraction as fine particle will allowed current to easily propagate thus producing low resistivity value while coarse grain fraction will produce high resistivity value due to the difficulty of current propagation. According to Telford et al. 1979, current may propagate in geomaterials based on electrolysis conduction where the propagation is by ionic conduction from amount and conductivity of dissolved minerals present. In mineral composition of soil, Clayey SILT has a higher composition of fine soil with particular reference to clay minerals such as kaolinite, illite, montmorillonite and vermiculite which allowed the ease of the current propagation in the soil tested thus producing low resistivity value compared to the Silty SAND which has low composition of clay with high composition of coarse soil. Furthermore as reported by Abidin et al. (2012), resistivity data exhibits a low value for a fine

soil such as clayey and silty while the coarser soil such as sand and gravel will produce a higher resistivity value.

The past findings which indicated the moisture content value will increase with the decreasing of soil resistivity value (Siddiqui & Osman, 2012; Tezel & Ozcep, 2003) which can be represented using general relationship of ERV ∞ 1/w. If the water was added continuously from dry soil until it reach saturated and oversaturated condition, the ease of current propagation in soil will be increased, thus producing a high to low resistivity value. As reported by Rinaldi & Cuestas (2002), ions in pore fluid finds hard to propagate in the low moisture content soil thus producing a low soil conductivity which will cause an increasing of resistivity value. The ability of CLAY/SILT to absorbed more water due to its high quantity has greatly influenced to dropped the Electrical Resistivity value compared to the SAND which has less fine soil due to less fine soil with high coarse soil). Hence, the Electrical Resistivity value of CLAY/SILT can be obtained lower than SAND due to its higher water absorbance ability which related to the composition of the soil particle.

According to Solberg et al. 2011, air filled void possess a higher resistivity value compared with the water filled void. CLAY/SILT composed of higher fine grain particles was able to absorb more water compared to the SAND. Hence, this phenomenon was possibly has affected the relationship between Electrical Resistivity value and densities. Commonly, it was expected that the Electrical Resistivity value was supposedly to be high due to the higher soil densities. However, in CLAY/SILT, this hypothesis was unsuccessfully due to the presence of more water within the fine soils. Hence in CLAY/SILT case, higher density was associated with a higher moisture content thus producing a low Electrical Resistivity value which can be represent by Electrical Resistivity value ∞ 1/ρ. In other words, the higher moisture content causes easily a flow of current within the soil which finally produced a lower Electrical Resistivity value. However, the value for soil density of Clay/Silt was lower than SAND due to its higher quantity of fine soil. A higher Electrical Resistivity value will be produced due to the higher value of soil densities which associated by higher quantity of granular soil with particular reference to gravel particles demonstrated by SAND. As reported by Sudha et al. (2009) the bulk resistivity of soil will increase with the grain size increment since it offers more resistance to the ionic current flow. Moreover, higher granular soil will produce lower moisture content which also contributes to the increasing of Electrical Resistivity value. Hence, general relationship between Electrical Resistivity value and soil densities of Gravel or SAND can be found as ERV ∞ ρ.

5.3 Geology of the study area

The study was conducted in the Chure, Bhawar and Terai region of Province-2 of Nepal. The geology of the study area is described in Section 3.2.

5.4 2D Electrical Resistivity Tomography Survey

5.4.1 Introduction

High-resolution electrical resistivity tomography (ERT) surveys were performed at the five sites as shown in Figure 3:1. The data was collected in the field using a GD-10 Series Geo-electrical System. GD-10 Advanced 2D Multi-electrode Res Imaging System is the 2D Electric Resistivity Investigation system with functions of SP survey, 1D Resistivity/IP sounding survey and 2D Resistivity Imaging Survey. The mainframe including GD-10 mainframe and CS-60 multi-electrode switching box, which support max 60 pcs electrodes.

The quality of data acquired in the field not only depends on quality of the equipment and accessories but also depends on the topography, geological setup and density of the measurement. Highly heterogeneous conditions are created by surface topography and geological variation. Planning of the fieldwork and layout of profiles is usually based on topographical map.

At the start of each survey, the electrodes were inserted into the ground to a depth of approximately half of their length (i.e., to a depth of 0.15 metres). When inserting the electrodes into the ground, care was taken to ensure good contact was established between the electrodes and the soil. Ensuring proper contact is especially important during drier conditions when holes formed by the electrodes may not have naturally healed between acquisition days. Grounding check was performed prior to any data acquisition to ensure the system was properly connected and to monitor the level of contact resistance in the survey setup.

5.4.2 Management and Inversion of ERT data

Following the data acquisition, resistivity data were downloaded from the field system to a desktop computer using the software program Geomative studio. Inversion of the data was performed using the software package RES2DINV version 4.08 (Geotomo Software). The program generates a two-dimensional model of subsurface resistivity by minimizing the root-mean-square (RMS) difference between the predicted apparent electrical resistivity from an inversion model and the values measured in the field. The software inverts the field data and calculates the appropriate model in term of resistivity and provides output in the form of resistivity contours. This inversion data is used to draw up the lithological and geological information. The basic principle behind the relation between resistivity data and

lithology/geology are already dealt with in above sections. The inversion results showing resistivity model with interpretative cross sections of all ERT profiles are presented. Geological/ lithological information is extracted from the ERT result (resistivity contour value) & are marked in the respective ERT sections. The resistivity value adopted for the interpretation of ERT tomogram is shown in Table 9.

Table 9: Resistivity value with respective lithology

SN	Resistivity (Ohm-m)	Lithology
1	>700 or >3000	Gravel (pebble to boulder) with sand i.e. coarse sediment dominant
2	>100 to <3000	Sand with gravel deposit (fine sediment dominant soil)
3	100 to 800	Sand deposit
4	<50 or <200	Silty/clay with sand
5	>50 to 300	Sand with layers of silt/clay

The ERT investigation was carried out using the Wenner array method only. In five rivers the study was conducted. The results are presented in the following section.

5.4.3 ERT Profiles

5.4.3.1 Bakaiya River

ERT investigation was conducted in three different transects namely Bakaiya L2, Bakaiya R3, and Bakaiya R4. Different ERT profiles were prepared to cover the maximum stretch of the river cross-section.

Bakaiya L2

Two ERT profiles were performed in the Bakaiya L2 transect namely Bakaiya-L2-ERT-1 and Bakaiya-L2-ERT-2 which are shown in Figure 39. Both of the ERT profile has an electrode spacing of 3 m and have an individual length of 177 m and is presented in Figure 40.

The interpreted ERT tomogram is shown in. Four different types of soils are categorized according to the zone of resistivity. The very high resistivity zone (> 700 Ohm-m) is interpreted as a gravel with sand (coarse sediment dominant). The high resistivity zone (400 to 700 Ohm-m) is inferred as the sand with gravel (fine sediment dominant). The moderate resistivity zone (250 to 400 Ohm-m) is considered to be the sand deposit and the last low resistivity zone (< 250 Ohm-m) is sand with layers of silt/clay.

The gravel with sand which is present at the top has thicknesses of 3 m to 11 m along the river cross-section. The proportion of coarse sediment decreases as the depth increases evidenced by the decrease of resistivity value. The high resistivity and moderate resistivity zone are present below this very high resistivity zone and pockets of very low resistivity are present in the shallow depths. The ERT-1 consists of a high resistivity zone in greater proportion whereas the ERT-2 consists moderate resistivity zone. The resistivity value of ERT-1 and ERT-2 of this transect suggests that the soils are in wet to saturate condition. The photographs of ERT survey at Bakaiya L2 is shown in Photo 20, Appendix-B.

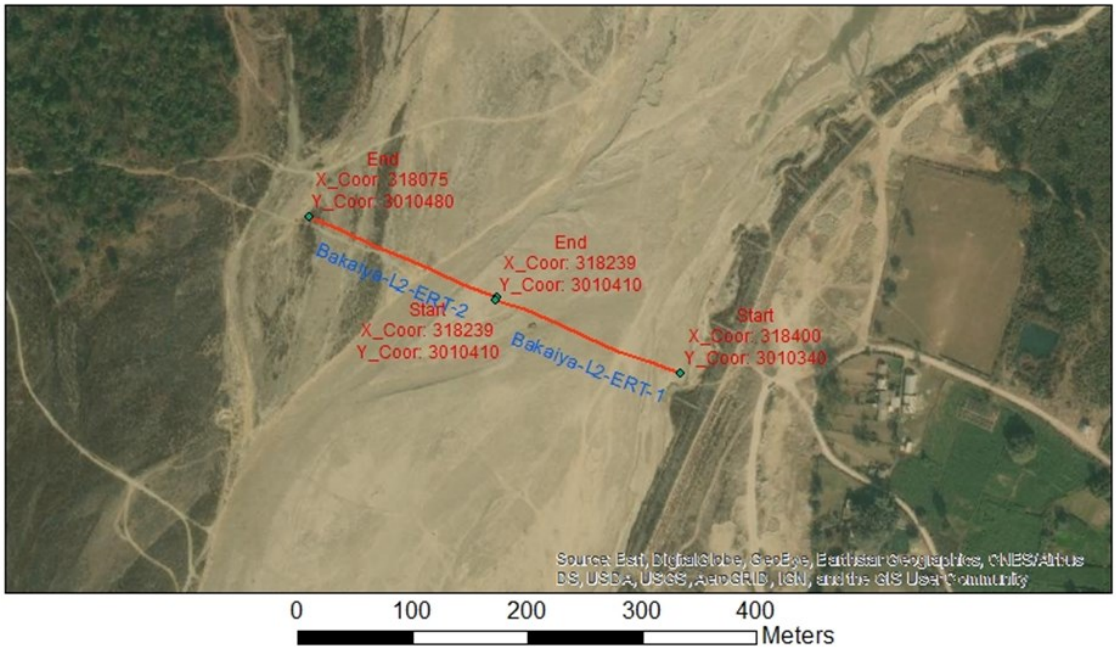


Figure 39: ERT profile alignment at the Bakaiya L2 transect.

Bakaiya R3

Two ERT profiles were performed in the Bakaiya R3 transect namely Bakaiya-R3-ERT-1 and Bakaiya-R3-ERT-2 (Shown in Figure C-40, Appendix C). Both of the ERT profile has an electrode spacing of 3 m and have an individual length of 177 m and is presented in Figure C-52, Appendix-C. The interpreted ERT tomogram is shown in Figure C-53, Appendix-C. Four different types of soils are categorized according to the zone of resistivity. The very high resistivity zone (> 1200 Ohm-m) is interpreted as the gravel with sand (coarse sediment dominant). The high resistivity zone (300 to 1200 Ohm-m) is interpreted as the sand with gravel (fine sediment dominant). The moderate resistivity zone (80 to 300 Ohm-m) is considered to be sand with layers of silt/clay and the last low resistivity zone (< 80 Ohm-m) is silt/clay with sand.

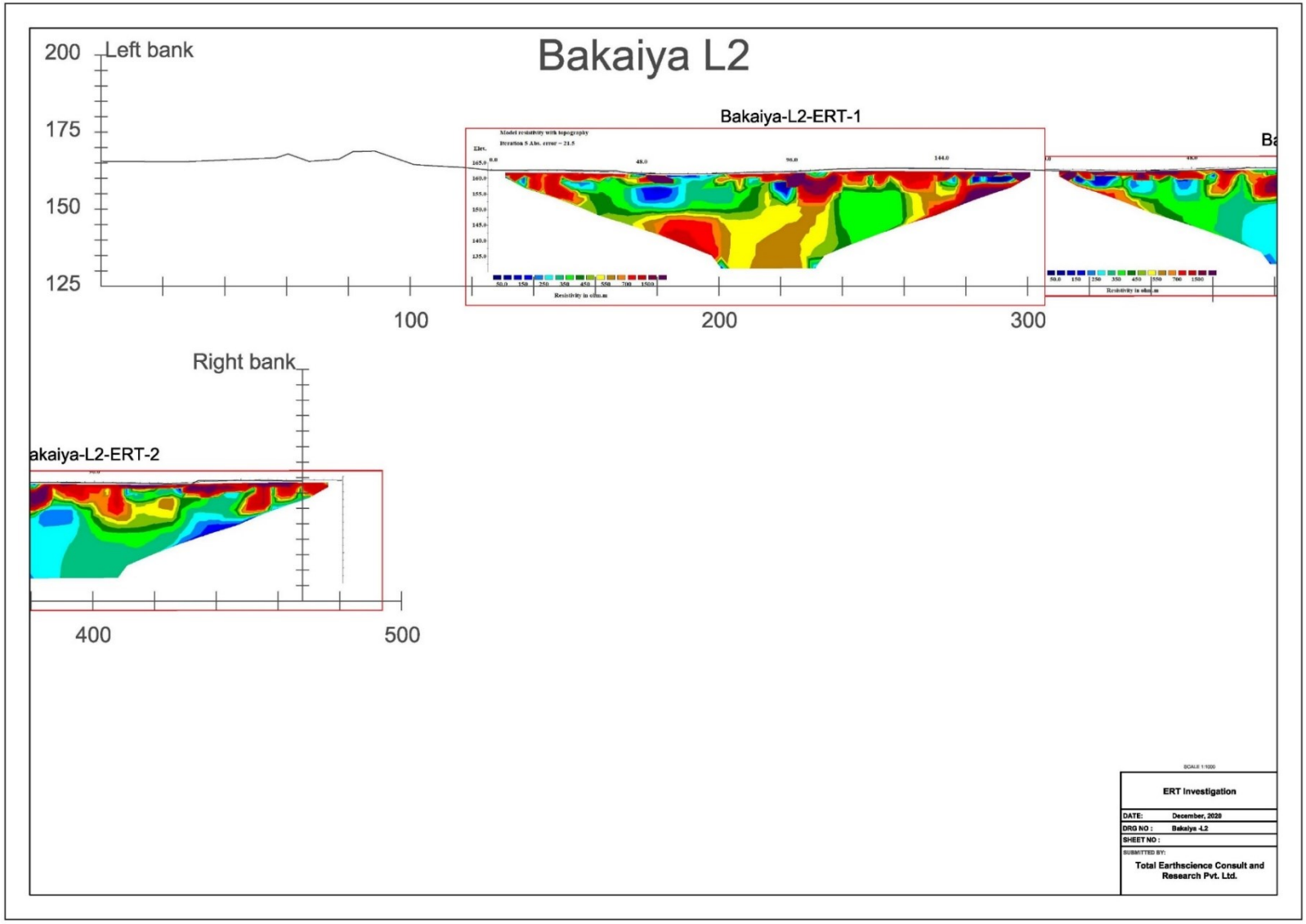


Figure 40: ERT tomogram of Bakaiya-L2-ERT-1 and Bakaiya-L2-ERT-2 presented in the river cross-section profile.

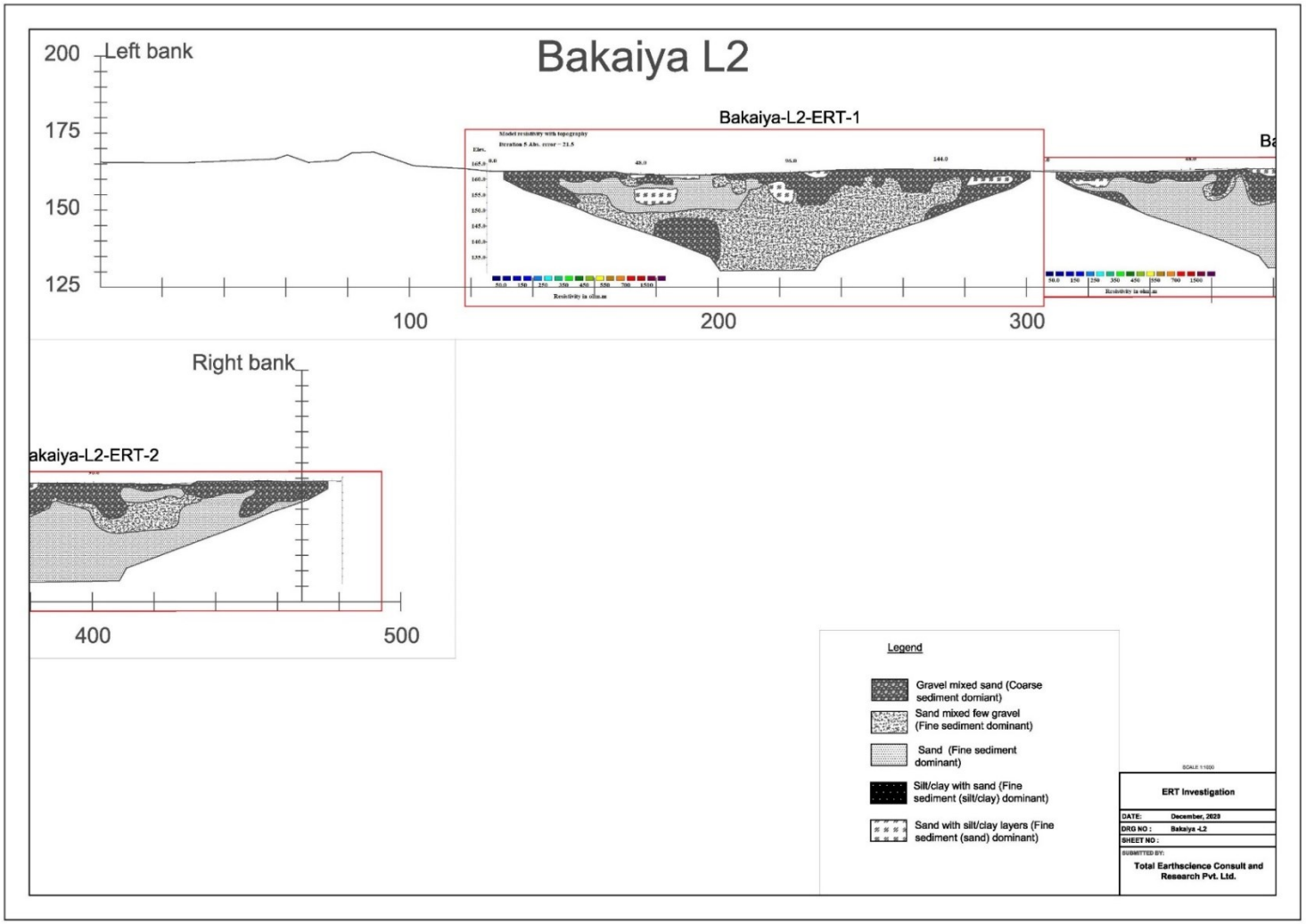


Figure 41: Interpretated ERT tomogram of Bakaiya-L2-ERT-1 and Bakaiya-L2-ERT-2 presented in the river cross-section profile.

From Figure C-53, Appendix-C, it can be observed that the resistivity value decreases as the depth increases which indicates the increase of water content and fine sediment. The gravel with sand, which is present on the top, has a thickness of 2 m to 14 m along the river cross-section. The high resistivity zone is present below having a thickness of < 1 m to > 11 m. Pockets of very low resistivity are present in both of the ERT tomograms. The photographs of ERT survey at Bakaiya R3 is shown in Photo 21, Appendix-B

Bakaiya R4

Two ERT profiles were performed in the Bakaiya R4 transect namely Bakaiya-R4-ERT-1 and Bakaiya-R4-ERT-2 (Shown in Figure C-41, Appendix-C). Both of the ERT profiles have an electrode spacing of 3 m. Bakaiya-R4-ERT-1 has a length of 267 m and the other Bakaiya-R4-ERT-2 has a length of 177 m and is presented in Figure C-54, Appendix-C.

The interpreted ERT tomogram is shown in Figure C-55, Appendix-C. Three different types of soils are categorized according to the zone of resistivity. The high resistivity zone (> 100 Ohm-m) is interpreted as sand with gravel (fine sediment i.e. sand dominant). The moderate resistivity zone (50 to 100 Ohm-m) is interpreted as the sand with layers of silt/clay (sand dominant). The low resistivity zone (< 50 Ohm-m) is considered to be silt/clay with sand (silt/clay dominant).

The resistivity value decreases as the depth increases, which indicates the increase in water content and decrease of grain size (i.e. increase of fines) (Figure C-55, Appendix-C). The top of the river cross-section consists of all three types of soil, however, it is dominated by sandy soil. The sand dominated soil (including sand with gravel and sand with layers of silt/clay) is inferred at the depth of 8 m to 20 m along the stretch of the river cross-section. Pockets of silt/clay with sand are to be found in the shallow depth i.e. within the sand dominant deposits. Below the sand dominant layer, there is a low resistivity zone i.e. silt/clay with sand.

The resistivity value on the ERT tomogram is comparatively low, which indicates the soil is in a saturated condition. The photographs of ERT survey at Bakaiya R4 is shown in Photo 22, Appendix-C.

5.4.3.2 Bagmati River

In survey in the Bagmati river was carried out at three different transects. The name of the transects are Bagmati R1, Bagmati L2, and Bagmati R3.

Bagmati R1

Two ERT profiles were performed in the Bagmati R1 transect namely Bagmati-R1-ERT-1 which is 177 m long and Bagmati-R1-ERT-2 which is 87 m long. They are shown in Figure C-42, Appendix-C. Both ERT profile has an electrode spacing of 3 m.

The interpreted ERT tomogram is shown in Figure C-57, Appendix-C. Three different types of soils are categorized according to the zone of resistivity. The high resistivity zone (> 3000 Ohm-m) is interpreted as gravel with sand (coarse sediment dominant). The moderate resistivity zone (800 to 3000 Ohm-m) is interpreted as the sand with gravel (fine sediment i.e., sand dominant). The low resistivity zone (< 800 to 300 Ohm-m) is considered to be sand dominant soil.

Figure C-56, Appendix-C illustrates that there is a drastic change in resistivity value i.e from > 3000 Ohm-m to <400 Ohm-m as the depth increases, indicating the increase of water content and fines in the soil.

The top of the river cross-section consists of damp to wet gravel dominant deposit to the depth of < 2 m to 9 m. Due to gravel dominant soil, it shows the high resistivity values. Beneath this gravel dominant layers, sand dominant layer is present up to the investigated depth. Sand with gravel (sand dominated) have a thickness of < 1 m to > 7 m. Beneath this sand with gravel layer, it is covered by sand soil. The resistivity value of the ERT tomogram is comparatively low, which indicates the soil is in wet to saturated condition. The photographs of ERT survey at Bagmati R1 is shown in Photo-23, Appendix-B.

Bagmati L2

Three ERT profiles were surveyed in the Bagmati L2 transect namely Bagmati-L2-ERT-1 Bagmati-L2-ERT-2, and Bagmati-L3-ERT-3. They are shown in Figure C-43, Appendix-C. All three of the ERT profiles have an electrode spacing of 3 m. Bagmati-L2-ERT-1 and Bagmati-L2-ERT-2 have a length of 177 m and Bagmati-L2-ERT-3 has a length of 87 m. The ERT tomograms are presented in Figure C-58, Appendix-C.

The interpreted ERT tomogram is shown in Figure C-59, Appendix-C. Three different types of soils are categorized according to the zone of resistivity. The high resistivity zone (> 500 Ohm-m) is interpreted as sand with gravel (sand sediment dominant). The moderate resistivity zone (300 to 500 Ohm-m) is interpreted as the sand (fine sediment i.e. sand dominant). The low resistivity zone (< 300 Ohm-m) is considered to be sand with silt/clay layers.

The top of the river cross-section consists of sand with gravel soil with a thickness of about 2 m to more than 9 m. The thickness of this sand with gravel is thin at the left bank and thick at the

right bank, as the coverage of the high resistivity zone is high near the right bank. It seems that the proportion of the gravel in the sand dominant soil is increasing from left bank to right bank. The sand with thin layers of silt/clay layer is thinly present in Bagmati-L2-ERT-1 and Bagmati-L2-ERT-3 (i.e. near the Left and Right bank of the Bagmati River) however, the Bagmati-L2-ERT-3 (i.e. about the center of the river cross-section) consists thick layer. The coverage of sandy soil is higher near the left bank and moderate in the center and near the right bank. The resistivity values are comparatively low, which indicate the soil is in wet to saturated condition. The photographs of ERT survey at Bagmati L2 is shown in Photo 24, Appendix-B.

Bagmati R3

Three ERT profiles were surveyed in the Bagmati R3 transect namely Bagmati-R3-ERT-1 Bagmati-R3-ERT-2, and Bagmati-R3-ERT-3. They are shown in Figure C-44, Appendix-C. All three of the ERT profile has an electrode spacing of 3 m and have a length of 177 m (Figure C-60, Appendix-C).

The interpreted ERT tomogram is shown in Figure C-61, Appendix-C. Three different types of soils are categorized according to the zone of resistivity. The high resistivity zone (> 450 Ohm-m) is interpreted as sand with gravel (sand sediment dominant). The moderate resistivity zone (200 to 450 Ohm-m) is interpreted as the sand (fine sediment i.e. sand dominant). The low resistivity zone (< 200 Ohm-m) is considered to be sand with layers of silt/clay soil. The resistivity value of the ERT tomogram is comparatively low which indicates the soil is in wet to saturated condition.

Figure C-60, Appendix-C shows that the low resistivity zone that covers the area of the tomogram. The upper part consists of pockets of sand with gravel layers and sand soil. The thickness of the sand soil ranges from 2 m to 11 m. The sand with silt/clay soil covers most of the river cross-section. This transect consists of fine sediments. The photographs of ERT survey at Bagmati R3 is shown in Photo 25, Appendix-B.

5.4.3.3 Ratu River

There are three investigated transects in the Ratu River. The transect are namely Ratu R1, Ratu R3, and Ratu R5.

Ratu R1

Only one ERT profile is conducted along the river cross-section named as Ratu-R1-ERT-1 (Shown in Figure C-45, Appendix-C and Figure C-62, Appendix-C). The length of the profile is 177 m and has an electrode spacing of 3 m.

The interpreted ERT tomogram is shown in Figure C-63, Appendix-C. Four different types of soils are categorized according to the zone of resistivity. The very high resistivity zone (> 2400 Ohm-m) is interpreted as gravel with sand (coarse sediment i.e. gravel dominant). The high resistivity zone (800 to 2400 Ohm-m) is interpreted as the sand (fine sediment i.e. sand dominant). The moderate resistivity zone (200 to 800 Ohm-m) is inferred to be sand soil. The low resistivity zone (< 200 Ohm-m) is considered to be a sand with layers of silt/clay.

The upper part of the river cross-section consists of gravel with sand which has a thickness of about 2 m to 6 m. The sand with gravel is present at the mid part of the ERT profile and has a thickness of 1 m to 8 m. The thick sand soil deposit is observed near the left and right banks. The middle part of the profile consists of thin sand deposits underlain by gravel layer. The last layer observed in the mid part of the ERT profile is sand with layers of silt/clay and has a thickness of more than 20 m. The pocket of sand with layers of silt/clay is observed near the right bank.

The top layer of the profile consists of materials with very high resistivity indicating low water content and large grain size. As the depth increases the resistivity gradually decreases illustrating an increase of water content and decreasing grain size. The gravel with sand is dry to damp in condition. The sand layer and the sediments beneath it are wet to saturate in condition. The photographs of ERT survey at Ratu R1 is shown in Photo 26, Appendix-B.

Ratu R3

One ERT profile is conducted along the river cross-section of length 267 m with electrode spacing of 3 m (Figure C-46, Appendix-C and Figure C-64, Appendix-C). The ERT profile is named as Ratu-R3-ERT-1.

The interpreted ERT tomogram is shown in Figure C-65, Appendix-C. Four different types of soils are categorized according to the value of resistivity. The very high resistivity zone (> 2400 Ohm-m) is interpreted as gravel with sand (coarse sediment i.e. gravel dominant). The high resistivity zone (800 to 2400 Ohm-m) is inferred as sand deposit with gravel (fine sediment i.e. sand dominant). The moderate resistivity zone (200 to 800 Ohm-m) is considered as sand deposits (Figure C-64, Appendix-C). The low resistivity zone (< 200 Ohm-m) is interpretated as sand with layers of silt/clay soil.

The upper part of the river cross-section consists high resistivity zone i.e. gravel with sand, which has a thickness of about 1 m to 8 m. Beneath this zone, it comprises sand-dominated soil. Sand with gravel soil is present just underneath the gravel with sand soil having various ranges of

thickness from about 1 m to more than 19 m. The moderate resistivity zone, which represents sand deposit is found beneath the sand-gravel layer. The low resistivity zone (i.e. sand with layers of silt/clay) is present at the bottom of the profile (about 17 m depth below the surface).

The upper layer consists of very high resistivity indicates low water content and larger grain size materials. As the depth increases the resistivity gradually decreases, which indicates increase in water content but decreased grain size. The gravel with sand is dry to damp condition. The sand deposits and the soil beneath it are wet to saturate in condition. The photographs of ERT survey at Ratu R3 is shown in Photo 27, Appendix-B.

Ratu R5

A single ERT survey of 267 m long with electrode spacing of 3 m was carried out in the transect Ratu R5 (Figure C-47, Appendix-C and Figure C-66, Appendix-C). The profile is named as Ratu-R5-ERT-1.

The interpreted ERT tomogram is shown in Figure C-67, Appendix-C. Three different types of soils are inferred according to the zone of resistivity. The high resistivity zone (> 1000 Ohm-m) is interpreted as gravel with sand (coarse sediment i.e. gravel dominant). The moderate resistivity zone (320 to 1000 Ohm-m) is interpreted as the sand with gravel (sand dominant). The low resistivity zone (<320 Ohm-m) is considered to be sand soil.

The thin layer gravel with sand layer is present near the right bank and as it reaches the mid part it disappears and sand dominant layer appears. Pockets of gravel with sand are present at the shallow depth around the mid part and have a thickness of about 10 m (Figure C-67, Appendix-C). Sand soil is present at the top with a thickness of 3 m to 7 m and also present at the depth of 19 m to 22 m. Sand with gravel soil is sandwiched by the topsoil (gravel with sand and sand soil) and the sand deposit (at the bottom). The resistivity values of the soils indicate the soil is wet to saturated. The photographs of ERT survey at Ratu R5 is shown in Photo 28, Appendix-B.

5.4.3.4 Balan River

ERT investigation was conducted in two transects namely Balan R1 and Balan L3.

Balan R1

Three ERT profiles of the individual length of 177 m namely Balan-R1-ERT-1, Balan-R1-ERT-2, and Balan-R1-ERT-3 were carried out in 3 m electrode spacing (Figure C-48, Appendix-C and Figure C-68, Appendix-C).

The interpreted ERT tomogram is shown in Figure C-69, Appendix-C. Three different types of soils are categorized according to the zone of resistivity. The high resistivity zone (> 160 Ohm-m) is interpreted as sand with gravel (sand dominant). The moderate resistivity zone (80 to 160 Ohm-m) is interpreted as the sand. The low resistivity zone (<80 Ohm-m) is considered to be sand with layers of silt/clay soil.

The Balan R1 transect is dominated by sand deposits. From Figure C-69, Appendix-C, it can be observed that the left bank side consists of sand deposits at the depth of 14 m to 18 m and is followed by sand deposits with a layer of silt/clay. Near the mid part of the cross-section, the increase of resistivity is observed indicating the increase of the proportion of gravel in the sandy soil. And as it comes closer to the right bank, the proportion of gravel decreases as indicated by decreasing of resistivity values. Sand with layers of silt/clay soil increases from left bank side to right bank side. The resistivity values of the soils indicate the soil is wet to saturate in condition. The photographs of ERT survey at Balan R1 is shown in Photo 29, Appendix-B.

Balan L3

Three ERT profiles of 177 m long namely Balan-L3-ERT-1, Balan-L3-ERT-2, and Balan-L3-ERT-3 were carried out in 3 m electrode spacing (Figure C-49, Appendix-C and Figure C-70, Appendix-C).

The interpreted ERT tomogram is shown in Figure C-71, Appendix-C. Two different types of soils are identified according to the zone of resistivity. The high resistivity zone (> 56 Ohm-m) is interpreted as sand deposit. And the low resistivity zone (<56 Ohm-m) is considered to be silt/clay with sand soil.

The topmost soil comprises of sand soil whose thickness is maximum at the mid part of the river cross-section up to 15 m and minimum at the banks about 1 m. Beneath sand deposit, it consists of silt/clay with sand. The resistivity values of the soils indicate the soil is saturated in condition. The photographs of ERT survey at Balan L3 is shown in Photo 30, Appendix E-20.

5.4.3.5 Khado River

ERT investigations were carried out in two transects in the Khado River. They are Khado R1 and Khado R3.

Khado R1

Single ERT profile of individual length of 177 m namely Khado-R1-ERT-1 was carried out with 3 m electrode spacing (Shown in Figure C-50, Appendix-C and Figure C-72, Appendix-C).

The interpreted ERT tomogram is shown in Figure C-73, Appendix-C. Three different types of soils are found according to the zone of resistivity. The high resistivity zone (> 100 Ohm-m) is interpreted as sand deposit. The moderate resistivity zone (56 to 100 Ohm-m) is inferred as sand with layers of silt/clay. The low resistivity zone (<56 Ohm-m) is considered to be silt/clay with sand soil.

Thin sand soil of thickness 1 to 2 m is present at the topsoil near the left and right bank of the river, and middle part of the river cross-section. A thick layer of sand with silt/clay is present near the left and right banks. The mid-part is covered by the silt/clay with sand. The resistivity values of the soils indicate the soil is in saturated condition. The photographs of ERT survey at Khado R1 is shown in Photo 31, Appendix-B.

Khado R3

Two ERT profiles, one with a length of 267 m (Khado-R3-ERT-1) and the other with a length of 177 m (Khado-R3-ERT-2) were carried out in 3 m electrode spacing (Shown in Figure C-51, Appendix-C and Figure C-74, Appendix-C).

The interpreted ERT tomogram is shown in Figure C-75, Appendix-C. Three different types of soils are categorized according to the zone of resistivity. The high resistivity zone (> 100 Ohm-m) is interpreted as sand soil. The moderate resistivity zone (56 to 100 Ohm-m) is interpreted as sand with layers of silt/clay. The low resistivity zone (<56 Ohm-m) is considered to be silt/clay with sand soil.

Topsoil consists of sand, which has a thickness of 2 m to 7 m and it is damp to wet in condition. Beneath the sand soil layer, there is a low resistivity zone (i.e. silt/clay with sand), which is followed by sand with silt/clay. The low resistivity zone has a thickness of 14 m to 19 m. Near the right bank, sand deposit is again present beneath the sand with layers of silt/clay soil. It seems the thickness of silt/clay with sand deposit and sand with layers of silt/clay is decreasing on the right bank side. The resistivity values of the soils indicate the soil is in saturated condition. The photographs of ERT survey at Khado R3 is shown in Photo 32, Appendix-B.

5.4.4 Summary of the ERT surveys

The summary of ERT survey carried out in Province 2 are presented in Table 10.

Table 10: ERT survey summary table

River	Transect	ERT Profile and Location (X, Y)	Results and Remarks
Bakaiya	Bakaiya L2	Bakaiya-L2-ERT-1 Start (318400, 3010340) End (3010340, 318239)	• Gravel with sand thickness of 3m-11m from top. • The proportion of coarse sediment decreases as the depth increases.
		Bakaiya-L2-ERT-2 Start (318239, 3010410) End (318075, 3010480)	
	Bakaiya R3	Bakaiya-R3-ERT-1 Start (321192, 3003540) End (321038, 3003470)	• Gravel with sand thickness of 2m-14m depth from the top • Increase of fine sediment with depth, mostly in saturated condition
		Bakaiya-R3-ERT-2 Start (321037, 3003460) End(320905, 3003350)	
	Bakaiya R4	Bakaiya-R4-ERT-1 Start (323994, 2991710) End (323731, 2991660)	• Sand dominated with pockets of clay and silt with varying depth of 8m-20m from the top • Pockets of silt/clay within shallow zones
		Bakaiya-R4-ERT-2 Start (323562, 2991620) End (323495, 2991580)	
Bagmati	Bagmati R1	Bagmati-R1-ERT-1 Start (348823, 3000380) End (348659, 3000450)	• Damp to wet gravel dominated deposit between 2m-9m from the top • 1m-7m gravel mixed sand deposit below gravel dominated layer • Saturated sand below the mixed layer
		Bagmati-R1-ERT-2 Start (348521, 3000500) End (348445, 3000540)	
	Bagmati L2	Bagmati-L2-ERT-1 Start (343904, 2992510) End (343743, 2992580)	• Sand dominated gravel mixed layer with 2m-9m depth from top, the depth is lower at left bank than right • Proportion of gravel in sand increasing from left bank to right bank • Central portion of cross section consist of thick sand deposit below the top sand-gravel mix layer
		Bagmati-L2-ERT-2 Start (343695, 2992610) End (343532, 2992670)	
		Bagmati-L2-ERT-3 Start (343372, 29927500 End (343288, 29927800	
	Bagmati R3	Bagmati-R3-ERT-1 Start (340776, 2984290) End (340612, 2964350)	• Sand with sparse gravel on the top • The bottom sand layer is about 2m-11m thick • Mostly fine sediment along this cross-section
		Bagmati-R3-ERT-2 Start (340517, 2984390) End (340353, 2984450)	
		Bagmati-R3-ERT-3 Start (340278, 2984480) End (340122, 2984550)	
Ratu	Ratu R1	Ratu-R1-ERT-1 Start (395513, 2993860) End (395342, 2993900)	• Top layer has gravel dominance with sand of thickness between 2m-6m • Sand dominated gravel mixed layer below has thickness of 1m-8m • Sand dominated lower layer with pockets of

River	Transect	ERT Profile and Location (X, Y)	Results and Remarks
			silt/clay
	Ratu R3	Ratu-R3-ERT-1 Start (391663, 2983370) End (391411, 2983450)	• Gravel dominated top layer with sand mix, thickness ranging from 1m-8m, mostly dry • Below above zone lies sand dominated zone of 1m-19m, with damp to saturated condition as the depth increases
	Ratu R5	Ratu-R5-ERT-2 Start (387792, 2974330) End (388046, 2974250)	• Thin top layer of gravel on right bank with sandy layer on central zone • The thickness of sand at top is about 3m-7m • Below this zone consist of gravel mixed sand • The lowermost layer is sand dominated about the depth of 19m-22m
Balan	Balan R1	Balan-R1-ERT-1 Start (455093, 2957370) End (455021, 2957520)	• Left bank has sand deposit in top with 14m-18m • The central part consists of gravel dominated top layer with sand mixed • Right bank has sand dominated deposits
		Balan-R1-ERT-2 Start (455021, 2957520) End (454940, 2957680)	
		Balan-R1-ERT-3 Start (454916, 2957710) End (454827, 2957870)	
	Balan L3	Balan-L3-ERT-1 Start (451490, 2944710) End (451320, 2944760)	• Sand dominated top layer with less thickness about 1m in the banks and 15m at center • The lower layer consists of silt/clay deposits
		Balan-L3-ERT-2 Start (451251, 29447900) End (451085, 29448400)	
		Balan-L3-ERT-3 Start (450986, 29448800 End (450818, 2944930)	
Khado	Khado R1	Khado-R1-ERT-1 Start (472910, 2945550) End (472735, 2945550)	• Thin sand layer of 1m-2m in the top • Below this layer consists of silt and clay deposits
	Khado R3	Khado-R3-ERT-1 Start (478984, 2936190) End (478727, 29361300	• Top layer consists of sand with 2m-7m depth • The lower deposits are clay/silt dominated
		Khado-R3-ERT-2 Start (478727, 29361300 End (478551, 2936100)	

6 Sediment yield from catchment

Sediment yield from a catchment is a complex process. It is combined result of the rainfall induced surface erosion and mass wasting phenomena along the hill slopes. There are different relationships to estimate the sediment yield from the catchment based on surface erosion but Revised Universal Soil Loss Equation (RUSLE) (Rennard, 1997) is widely used. It should be noted that this method was originally developed to estimate sediment loss from the farm lands. The practically applicable model which can estimate the sediment yield from the mass wasting phenomena is so far not available.

For the present study, sediment yield is proposed to be calculated using Revised Universal Soil Loss Equation is given by Equation 17.

$$A = R * K * LS * C * P \quad \textbf{17}$$

Where,

A = annual sediment yield (t/ha/yr)

R = rainfall erosivity factor (MJ mm ha^{-1} h^{-1} yr^{-1})

K = soil erodibility factor (t h MJ^{-1} mm^{-1})

L = length of the slope factor (-)

S = steepness of the slope factor (-)

C = cover and management practice factor (-)

P = conservation practice factor (-)

6.1 Rainfall Erosivity

The R-factor is a climatic parameter that takes into account the rainfall-runoff erosive capacity. Rainfall data from meteorological station within and in the vicinity of basin were used to calculate the rainfall erosivity R-factor by using the relation presented in Equation 18 (Ettazarini & Jakani, 2017):

$$R = \sum_{i=1}^{12} 1.735 * 10^{(1.5*\log_{10}\left(\frac{P_i^2}{P}\right)-0.08188)} \quad \textbf{18}$$

Where,

R = rainfall erosivity factor (MJ mm ha^{-1} h^{-1} yr^{-1})

P_i = monthly rainfall (mm)

P = annual rainfall (mm).

Due to the unavailability of original literature for citation, the R-factor has been calculated using two more relations. The first relation is presented in Equation 19 and 20 (K. G. Renard & Freimund, 1994)

$$R = 0.04830P^{1.610} \text{ for P } < 850 \text{ mm} \quad \textbf{19}$$

$$R = 587.8 - 1.219P + 0.004105P^2 \text{ for P} > 850 \text{ mm} \quad 20$$

Where,

R = rainfall erosivity factor (MJ mm ha^{-1} h^{-1} yr^{-1})

P = annual rainfall (mm)

And the second relation is presented in Equation 21 and 22 (K. G. Renard & Freimund, 1994)

$$R = 0.07397P^{1.847} \quad \textbf{for F <55 mm} \quad 21$$

$$R = 95.77 - 6.081F + 0.4770F^2 \text{ for F} > 55 \text{ mm} \quad 22$$

Where,

R = rainfall erosivity factor (MJ mm ha^{-1} h^{-1} yr^{-1})

F = modified Fournier's index computed by Arnoulds (K. G. Renard & Freimund, 1994) which is given by Equation 23.

$$F = \sum_{i=1}^{12} \frac{P_i^2}{P} \quad \textbf{23}$$

Where,

P_i = mean monthly rainfall (mm)

P = annual rainfall (mm)

The spatially distributed R-factor was computed using Inverse Distance Weighted interpolation method.

6.2 Soil Erodibility Factor

Soil erodibility factor is the readiness with which the soil gets eroded due to its intrinsic properties during rainfall. The relationship for K factor is given in Equation 24.

$$100K = 2.1\ \mathrm{M}1.14\ (10-4)\ (12-\mathrm{a})\ + 3.5(\mathrm{b}-2)\ + 2.5(\mathrm{c}-3) \quad \textbf{24}$$

Where,

M = the particle size parameter [(% silt +% very fine sand) (100-% clay)]

a = organic matter content (%)

b = soil structure code (-)

c = the soil permeability class (-)

The K-factor expressed in U.S. unit (t.acre.h/100 acre.ft.tonf.in) is multiplied by 0.1317 for conversion into the international unit (t ha h $ha^{-1}MJ^{-1}mm^{-1}$).(Foster et al., 1981)

In SOTER database of Nepal, there is zero percentage coverage of % very fine sand data. Similarly, the soil structure code and soil permeability class data are also missing, Therefore, in our present study, a substitution of the above relationship given by Williams (Neitsch et al., 2002) is used to calculate the soil erodability factor because of unavailability of all soil parameters. The relationship reduces the number of soil parameters to four and is given Equation 25 - 29.

$$K = f_{csand} * f_{cl-si} * f_{org} * f_{hisand} \quad \textbf{25}$$

$$f_{csand} = (0.2 + 0.3 * \exp\left[-0.256 * m_s * \left(1 - \frac{m_s}{100}\right)\right]) \quad 26$$

$$f_{cl-si} = (\frac{m_{silt}}{m_c + m_{silt}})^{0.3} \quad 27$$

$$f_{org} = (1 - \frac{0.0256 * orgC}{orgC + \exp[3.72 - 2.95 * orgC]}) \quad 28$$

$$f_{hisand} = (1 - \frac{0.7 * \left(1 - \frac{m_s}{100}\right)}{\left(1 - \frac{m_s}{100}\right) + \exp\left[-5.51 + 22.9 * \left(1 - \frac{m_s}{100}\right)\right]}) \quad 29$$

Where,

m_s = percent sand content (%)

m_{silt} = percent silt content (%)

m_c = percent clay content (%)

orgC = percent organic carbon content (%)

6.3 Slope Length Factor (L-Factor)

Wischmeier and Smith (1978) considered the L-factor as a function of slope length as shown in Equation 30.

$$L = (\frac{\lambda}{22.13})^m \quad 30$$

Where,

λ = slope length which is taken as 30 m or 42.426 m (Yoshino & Ishioka, 2005)

m = slope exponent that varies between 0.2 and 0.5 for slope values between 0 and 5% and then remains invariant for slopes greater than 5% classified as: S < 1%, m = 0.2; 1% ≤ S ≤ 3%, m = 0.3; 3% < S≤ 5%, m = 0.4; and S > 5%, m = 0.5 (Wischmeier et al., 1978)

6.4 Slope angle Factor (S-Factor)

Equations 31 and 32 are used to calculate the S-factor as proposed by McCool et al. (1987). The revised S-factor takes in account the conditions of slope gradient less and upper than 9 %.(K. Renard et al., 1997).

$$S = 10.8 * \sin\theta + 0.03 \text{ for slopes } < 9\ \% \quad (31)$$

$$S = 16.8 * \sin\theta - 0.5 \text{ for slopes } \geq 9\ \% \quad (32)$$

The effect of slope length L and slope angle S are presented together as topographic which is given by

LS=L*S

6.5 Cover and Management Practice Factor (C-Factor)

The cover and management practice factor is the expected ratio of soil loss from a cropped land under specific conditions to soil loss from clean tilled fallow on identical soil and slope under the same rainfall conditions. Crop management factor assigned for different land use patterns is given in Table 11.

Table 11 Cover And Management Factor For Different Land Use(A. Pandey et al., 2015)

S.N.	Land Use/Land Cover	C Factor
1	Forest	0.004
2	Shrub land	0.008
3	Grassland	0.008
4	Agriculture area	0.28
5	Barren land	0.13
6	Water body	0
7	Snow/Glacier	0
8	Built up area	0

6.6 Conservation Practice Factor (P)

The P-factor is defined as the ratio of soil loss with a specific support practice to the corresponding loss with up-and-down-slope culture. In the study area, values for the P-factor were assigned to 0.28 for the area under cultivation, 1 for all the other areas except Snow/glacier and built up area for which the P-factor are assigned 0 value (A. Pandey et al., 2015).

6.7 Results

The annual sediment yield estimated by RUSLE method for the Rivers of the Study area is presented in Table 12. The rivers with larger watershed area resulted in the high sediment yield. Similarly the spatial distribution of the sediment yield in the study area is shown in Figure 42. It can be observed that the Upper and the Middle Siwalik area produces high sediment.

Table 12: Sediment yield from Rivers of Chure region of Province 2

Watershed Name	Area in Sq. Meters	Area in Hectares	Yield (tonnes/ha/year)	Yield ($\times 10^6$ tonnes/year)
Alajor	8620540.00	862.05	925978.30	798.24
Amuwa	24048454.15	2404.85	1350414.46	3247.54
Atarauli	4719369.54	471.94	263590.87	124.40
Aurahi	22084534.16	2208.45	742259.85	1639.25
Badahari	12109516.16	1210.95	762127.01	922.90
Bagar	8698055.00	869.81	990717.97	861.73
Bagmati	2812455305.48	281245.53	491399791.55	138203995.09
Bahbsi	13629655.73	1362.97	975206.00	1329.17
Bakaiya	317360879.24	31736.09	53331940.44	1692547.15
Bakhariya	38591202.78	3859.12	1735954.06	6699.26
Balan1	55537159.98	5553.72	1489631.93	8272.99
Balan2	278390728.48	27839.07	7932134.42	220823.27
Baluwa	11425934.96	1142.59	189042.78	216.00
Baluwa1	1343438.23	134.34	57404.77	7.71
Banara	2684638.80	268.46	146046.31	39.21
Bangeri	56307850.90	5630.79	6619195.39	37271.27
Bankecheck	28854662.76	2885.47	2465055.05	7112.83
Basai	4106721.79	410.67	181340.51	74.47
Bataha	1850949282.17	185094.93	206109574.98	38149836.99
Baune	11964711.67	1196.47	735694.12	880.24
Bayarghari	10001383.50	1000.14	591991.77	592.07
Bedaha	39643950.67	3964.40	4996285.67	19807.25
Betaha	17089376.12	1708.94	334863.26	572.26
Bhalu	6043707.49	604.37	233136.54	140.90
Bhaluwahi	114816054.64	11481.61	5699795.74	65442.81
Bhamara	14092598.32	1409.26	1463622.51	2062.62
Bighai	75967732.27	7596.77	5823206.46	44237.58
Birdhana	289777469.23	28977.75	8512748.72	246680.28
Chadi	38642230.97	3864.22	4096041.16	15828.02
Chameniya	6915677.43	691.57	143617.74	99.32
Chapani	2679293.37	267.93	428648.45	114.85
Chapindar	6131362.04	613.14	140353.15	86.06
Charnath	51035551.89	5103.56	1334294.98	6809.65
Dalame	1002992.41	100.30	28053.91	2.81
Damara	3149129.83	314.91	106144.60	33.43

Watershed Name	Area in Sq. Meters	Area in Hectares	Yield (tonnes/ha/year)	Yield ($\times 10^6$ tonnes/year)
Dandunge	17239957.03	1724.00	2271419.52	3915.92
Dayani	21677639.44	2167.76	1232699.02	2672.20
Devdhar	3481176.86	348.12	94356.68	32.85
Dhansar	53534830.80	5353.48	7123725.04	38136.74
Dhansar2	85379979.68	8538.00	8963009.90	76526.16
Dheduwa	14565160.95	1456.52	944156.70	1375.18
Dhungre	8915576.88	891.56	483473.08	431.04
Dudhaila	55000431.41	5500.04	1922872.16	10575.88
Dudhaura	16072103.95	1607.21	3317523.15	5331.96
Dudhaura2	64760670.33	6476.07	7673317.44	49692.92
Dulan	10412027.85	1041.20	120173.04	125.12
Dumarjor	833562.02	83.36	114888.17	9.58
Dumre	5102651.94	510.27	270951.28	138.26
Gadhanta	7299728.91	729.97	249693.83	182.27
Gagan	14715076.04	1471.51	464872.29	684.06
Gangajali	5073897.16	507.39	124320.32	63.08
Garti	22106497.69	2210.65	1336638.77	2954.84
Ghordana2	42674274.72	4267.43	2798454.12	11942.20
Ghurmi	23922778.71	2392.28	1021381.58	2443.43
Godar	1111106.63	111.11	99787.06	11.09
Gurmi2	1873443192.39	187344.32	207199873.25	38817719.20
Hardiya2	129410284.67	12941.03	10033747.03	129847.01
Hariunn1	4740448.81	474.04	424842.71	201.39
Hariunn2	15176445.78	1517.64	1459590.84	2215.14
Indrabati	1306777.79	130.68	39659.59	5.18
Jagardhar	12652029.94	1265.20	360477.28	456.08
Jaladh	16319571.48	1631.96	567484.45	926.11
Jamuniya	83641004.41	8364.10	5726513.96	47897.14
Janagaha	19030520.29	1903.05	939445.12	1787.81
Jarayo	21213730.06	2121.37	825636.85	1751.48
Jhadi	3525001.00	352.50	39258.63	13.84
Jhijhari	31314000.09	3131.40	918560.60	2876.38
Jhinge	3004424.09	300.44	54177.03	16.28
Kalinjor	28404715.12	2840.47	2249172.88	6388.71
Kamala	1569661560.18	156966.16	188120583.43	29528564.85
Khada2	15715746.44	1571.57	297606.75	467.71
Khadak	25640749.34	2564.07	632693.54	1622.27
Khadak1	3625342.94	362.53	84790.52	30.74
Khado1	29831615.25	2983.16	621475.49	1853.96
Khado2	13792242.40	1379.22	994396.21	1371.50
Khutti	35870976.85	3587.10	1045245.73	3749.40
Khutti1	1351270.35	135.13	39331.35	5.31
Khutti2	3392989.27	339.30	87468.54	29.68
Koriya	67147456.81	6714.75	1071116.54	7192.28
Kothighumne	21632962.86	2163.30	2830443.60	6123.09
Labhitiya3	6075012.00	607.50	279337.55	169.70
Lakeshwor1	4015253.53	401.53	150047.86	60.25

Watershed Name	Area in Sq. Meters	Area in Hectares	Yield (tonnes/ha/year)	Yield ($\times 10^6$ tonnes/year)
Lakeshwor2	19007486.87	1900.75	932763.77	1772.95
Lal	51196257.14	5119.63	7139182.42	36549.94
Lalbhitiya2	8745038.47	874.50	299009.54	261.48
Lokhandehi1	23616382.60	2361.64	1691705.58	3995.20
Madar	5558955.21	555.90	482471.31	268.20
Madyan	5170921.26	517.09	117627.67	60.82
Mahadev	29386189.34	2938.62	1542237.36	4532.05
Mahajan	6808226.53	680.82	324886.56	221.19
Mahajan1	2792653.84	279.27	166111.64	46.39
Mahara	17835712.62	1783.57	1200428.82	2141.05
Mahuli1	48244367.06	4824.44	940117.61	4535.54
Mainawati	20495461.51	2049.55	1520164.89	3115.65
Majhum	66086591.80	6608.66	3218401.40	21269.32
Maleth	2474749.04	247.47	33264.36	8.23
Manabodhi	18361212.45	1836.12	169144.33	310.57
Mathe	3597200.60	359.72	208077.28	74.85
Megha	20612396.78	2061.24	495551.25	1021.45
Moraha	6602364.43	660.24	327128.26	215.98
Mutani	11989888.29	1198.99	768040.29	920.87
Narayan	15838433.80	1583.84	651661.11	1032.13
Odar1	23255554.28	2325.56	1100558.53	2559.41
Pasaha	91087637.61	9108.76	7908249.10	72034.37
Patauna	399464.79	39.95	52384.45	2.09
Pauda	12520261.89	1252.03	301745.70	377.79
Paurai1	11580280.50	1158.03	571936.87	662.32
Paurai2	3183300.81	318.33	209571.02	66.71
Phuljhor	51215585.27	5121.56	4510630.12	23101.46
Rato1	12396781.29	1239.68	683813.96	847.71
Rato2	37458135.92	3745.81	2471948.01	9259.46
Rato3	70166120.68	7016.61	4878379.96	34229.70
Sarre	25748182.03	2574.82	1108338.28	2853.77
Shakti	27882447.87	2788.24	4428777.25	12348.52
Shitals	19497375.85	1949.74	314266.68	612.74
Sikta	57354441.00	5735.44	5229515.50	29993.59
Sisabari	38761838.33	3876.18	1250048.70	4845.42
Sukhajhor	13186723.04	1318.67	1311690.52	1729.69
Suklai	1342822.99	134.28	25669.72	3.45
Sundari	16030460.88	1603.05	233825.62	374.83
Sunjhari	14442498.93	1444.25	910725.19	1315.31
Thulohard	5721192.63	572.12	478898.55	273.99
Thute1	19939173.24	1993.92	1245375.57	2483.18
Thute2	5147852.63	514.79	174488.81	89.82
Thuteup	13340558.72	1334.06	266568.12	355.62
Trijuga	695933512.52	69593.35	40185762.28	2796661.87
Uriya	93940913.55	9394.09	5058713.04	47522.01

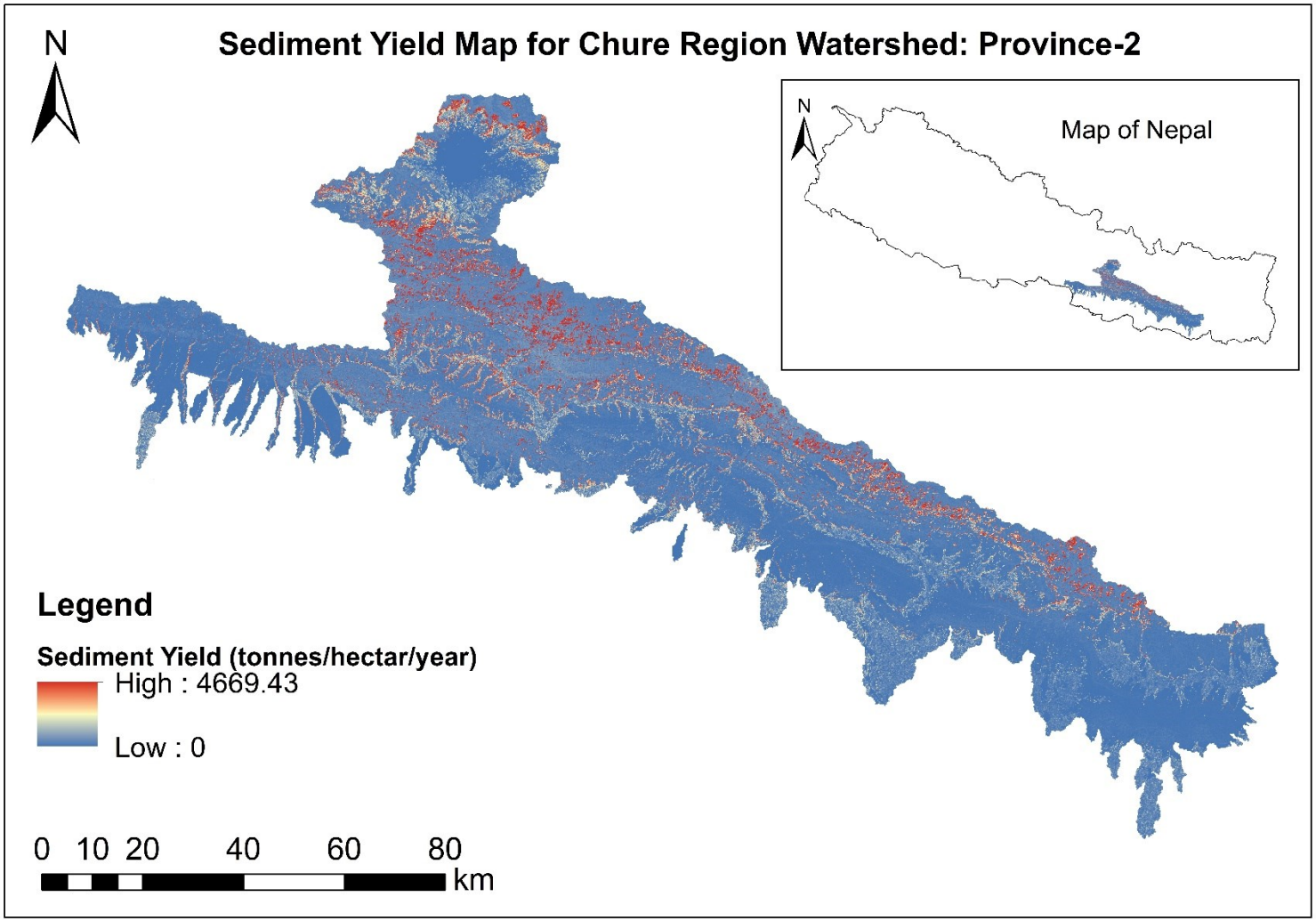


Figure 42 Spatial distribution of annual sediment yield (tonnes/hectare/year) in river systems of draining through Province 2 of Nepal

7 Topographic analysis

7.1 River cross-section survey

The river cross-section surveys were carried out to compute the hydraulics and sediment transport characteristics of the river reaches. In Bhawar and Terai region of Province 2, the rivers are very wide and braided. Cross-section survey of all rivers would require enormous financial resources as well as time. So, the river cross-section surveys were carried out only in a selected river systems namely Bakaiya, Bagmati, Ratu, Balan and Khado river systems. These river systems were carefully sampled for obtaining the spatial coverage of the study area as well as the types of river. The topographic features of the measured cross-sections will be derived and transposed to the other river systems of the study area.

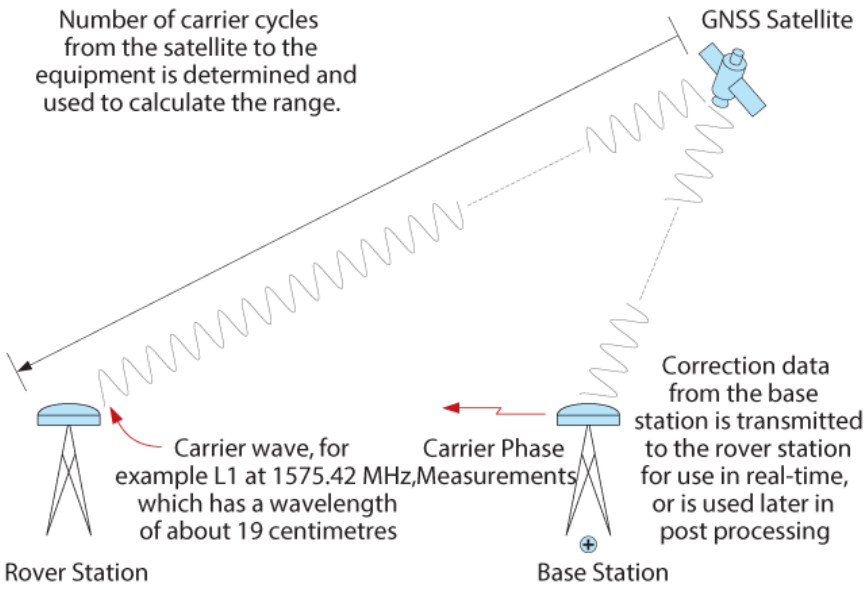


Figure 43 Schematic diagram of functioning of GNSS based Real Time Kinematic survey technique

The river reaches are very long. So, the survey cross-sections had to be spaced at longer intervals. The cross-section surveys were carried out using Differential GPS (DGPS) Real Time Kinematic (RTK) survey technique(Figure 43). A Differential Global Positioning System (DGPS) is an enhancement to the Global Positioning System (GPS) which provides improved location accuracy to about 1–3 cm in case of the best implementations. Each DGPS uses a network of fixed ground-based reference stations to broadcast the difference between the positions indicated

by the GPS satellite system and known fixed positions. GNSS-based Real Time Kinematic (RTK) survey technique were employed to capture the river cross-section data in both sides of the river. GNSS reading frequencies are set by distance moved rather than by time interval. This method will provide us accuracy of the position in less than 5 cm horizontally and vertically.

7.1.1 Methodology

Following methodology was used for the data collection of different river cross-sections at different intervals.

7.1.1.1 Desk Study and Field Planning/Mobilization

At the preliminary stage, desk study of study area was carried out based on the secondary data such topographic maps, river maps Google Earth etc. This study will also act as guide for field planning and mobilization as well as logistics requirements. After preliminary study of the available documents and proper planning, mobilization of crew to the project area and data collection is done.

7.1.1.2 Base Station Setup

Base is one of the receivers that act as a reference station in Real Time Kinematics (RTK) or Post Processing Kinematics (PPK) scenarios. It is a static unit with the determined coordinates that sends corrections to the moving unit or rover. If the base is set over the known point, it provides absolute accuracy. There is different method to fix the base station such as; Manual Coordinate Method, Averaging Method and others. In Manual Coordinate Method, the known coordinate of station is manually input and the collection of other points data is done by connecting rover to the reference where as in averaging method, we let the receiver to collect positional data for certain time period and conclude with an average coordinate for our further applications. In field, to find the coordinate of base we adopted Averaging Method to capture the reference location data and other cross-sectional data are captured by RTK methods.

Base station was established in each location of the river sections. These base stations were established with metal pole buried in the ground in the area above the high flood level so these points can be used for future monitoring propose as shown in the picture below. A view of established base points is shown in Figure 44. Whereas the location details of the Base stations established at each cross-sections are provided in Table 13.



Figure 44 View of Established base points in Bagmati River, Balan River and Bakaiya River

Table 13 Details of the base points established at the surveyed cross-sections

S.N	UTM 45		WGS84		Elevation		River	Remarks
	Easting	Northing	Latitude	Longitude	Orth. Height	Ellip. Height		
1	318626.4	3014442	27^{0}14'27.133"	85^{0}10'5.450"	135.383	196.571	Bakaiya	Right Bank
2	318442.4	3010334	27^{0}12'13.596"	85^{0}10'0.948"	109.226	171.069	Bakaiya	Left Bank
3	320906.3	3003365	27^{0}08'28.378"	85^{0}11'34.114"	71.244	133.943	Bakaiya	Right Bank
4	323503.9	2991579	27^{0}02'06.701"	85^{0}13'14.493"	38.223	102.081	Bakaiya	Right Bank
5	348352.6	3000561	27^{0}07'09.127"	85^{0}28'12.075"	66.925	128.449	Bagmati	Right Bank
6	343903.2	2992514	27^{0}02'45.900"	85^{0}25'34.173"	39.959	102.756	Bagmati	Left Bank
7	340237.2	2984480	26^{0}58'23.347"	85^{0}23'24.871"	24.424	88.244	Bagmati	Right Bank
8	335931.9	2972750	26^{0}52'00.441"	85^{0}20'54.309"	15.889	80.891	Bagmati	Right Bank
9	395339.5	2993899	27^{0}03'48.322"	85^{0}56'40.411"	299.7	357.993	Ratu	Right Bank
10	391827.9	2987629	27^{0}00'23.619"	85^{0}54'34.911"	189.639	249.437	Ratu	Right Bank
11	391407.3	2983463	26^{0}58'8.110"	85^{0}54'20.965"	143.77	204.288	Ratu	Right Bank
12	389663.1	2979894	26^{0}56'11.632"	85^{0}53'18.844"	99.451	160.641	Ratu	Right Bank
13	387793	2974331	26^{0}53'10.296"	85^{0}52'12.837"	50.902	112.953	Ratu	Right Bank
14	454832.6	2957868	26^{0}44'28.842"	86^{0}32'44.847"	66.515	125.91	Balan	Right Bank
15	450634	2952176	26^{0}41'23.330"	86^{0}30'13.656"	46.837	107.219	Balan	Right Bank

S.N	UTM 45		WGS84		Elevation		River	Remarks
	Easting	Northing	Latitude	Longitude	Orth. Height	Ellip. Height		
16	451510.2	2944710	26^{0}37'20.759"	86^{0}30'46.391"	35.162	96.292	Balan	Left Bank
17	472734.1	2945542	26^{0}37'49.873"	86^{0}43'33.867"	56.066	116.073	Khado	Right Bank
18	474459.8	2941495	26^{0}35'38.432"	86^{0}44'36.573"	44.528	104.913	Khado	Right Bank
19	478802.4	2936154	26^{0}32'45.085"	86^{0}47'13.905"	24.142	84.864	Khado	Right Bank
20	478655.8	2933681	26^{0}31'24.682"	86^{0}47'8.755"	19.519	80.452	Khado	Right Bank
21	478655.8	2933681	26^{0}31'24.682"	86^{0}47'8.755"	19.519	80.452	Khado	Right Bank
22	477294.2	2930499	26^{0}29'41.187"	86^{0}46'19.759"	15.759	76.986	Khado	Right Bank

7.1.1.3 RTK Point Pickup

After the base station was setup, the connection between the station and the rover were done by radio antenna. To connect base station and rover, frequency and air data rate in both base receiver and rover were checked and matched. Then the collection of the river cross-section data was started. In RTK, correction of positional data recorded by rover with respect to base station is made within seconds by receiver itself. Mostly preferably the data were collected in a fixed status so that the millimeter precision is achieved. In places where the obstacles to the receiver such as trees, buildings etc. were observed, float status data was also captured within centimeter level precision. The data recording time was set to 30 seconds and 60 seconds for fix status and float status data respectively (Figure 45).



Figure 45 View of data collection along river cross-sections of Balan River, Bakaiya River and Ratu River (left to right)

7.1.2 River Cross-sections

The examples of river cross-sections measured from the field in Bakaiya River, Bagmati River, Ratu River, Balan River and Khado River are shown in Figure 46, Figure 47, Figure 48, Figure 49 and Figure 50 respectively. The data of all river-cross-sections measured from the field are tabulated from Table D-6 to Table D-27 in Appendix-D.

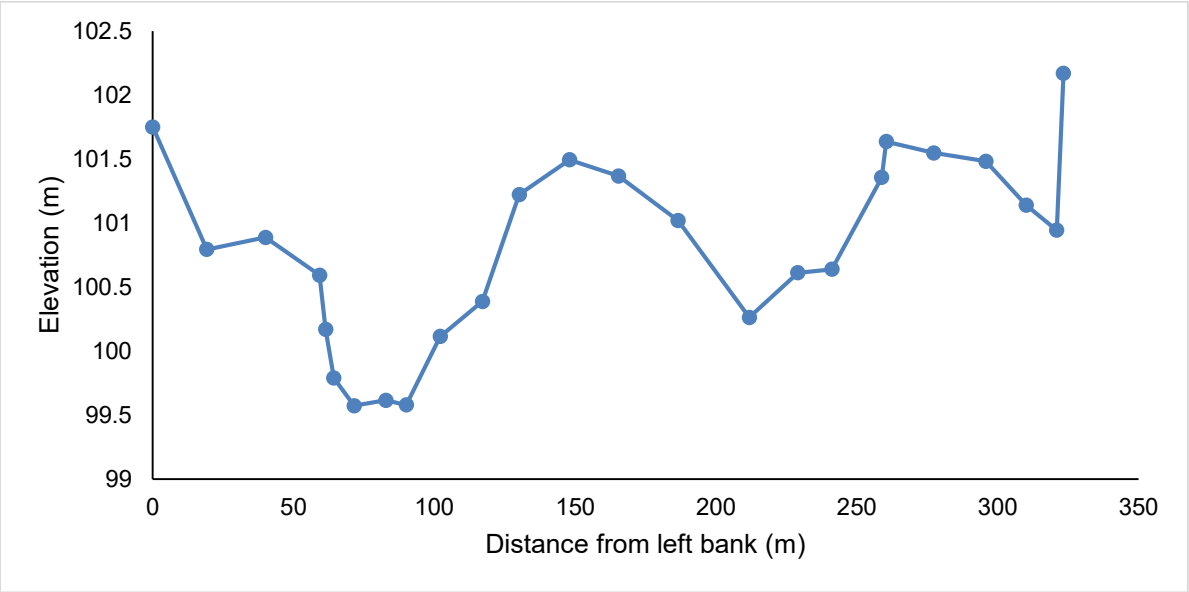


Figure 46:Cross-section of the Bakaiya River at section R2 (X= 318,525.02, Y= 3,010,336.81)

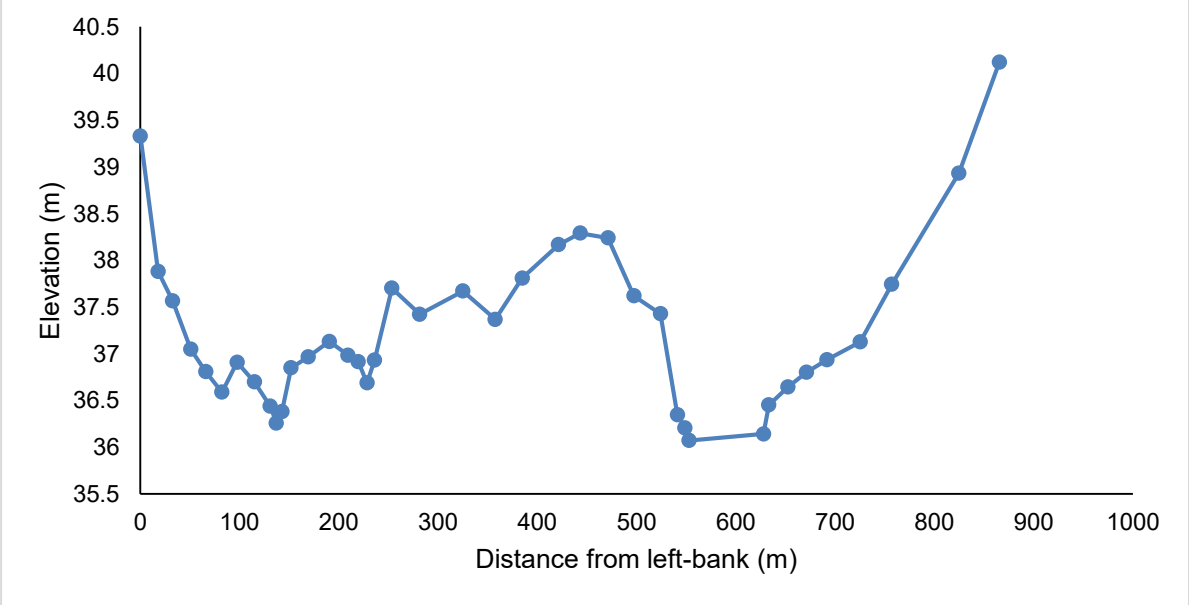


Figure 47: Cross-section of the Bagmati River at section R2 (X=343,920.71, Y=2,992,497.89)

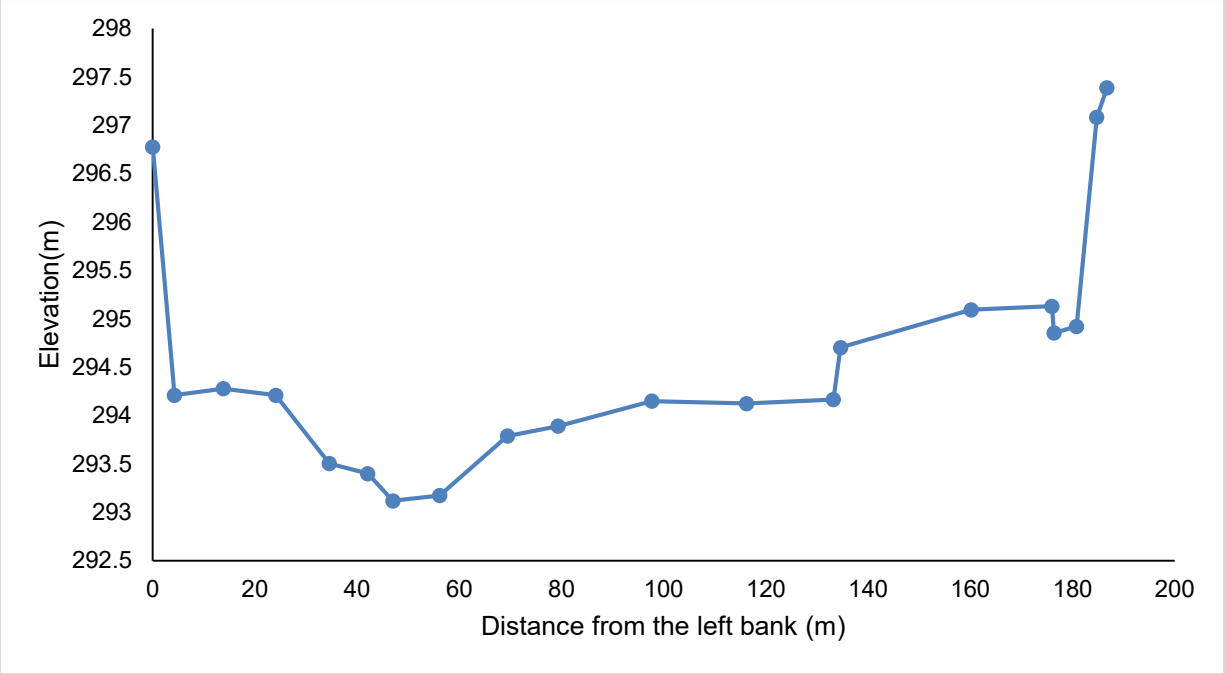


Figure 48: Cross-section of the Ratu River at section R1 (X= 395,527.22, Y= 2,993,859.33)

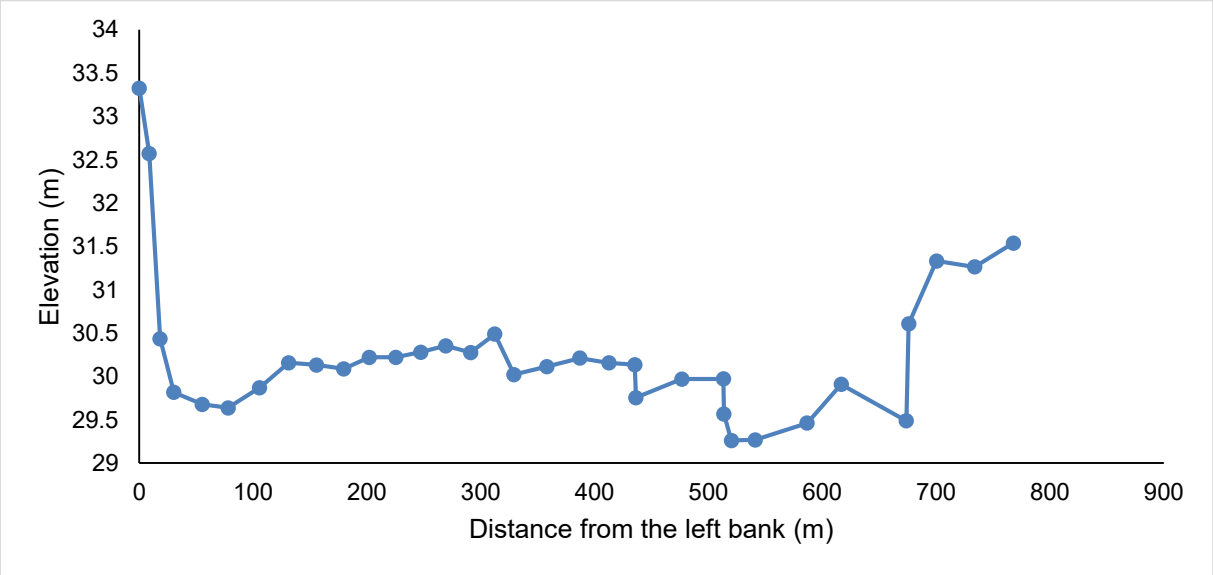


Figure 49:Cross-section of the Balan River at section R2 (X= 451,511.63, Y= 2,944,696.66)

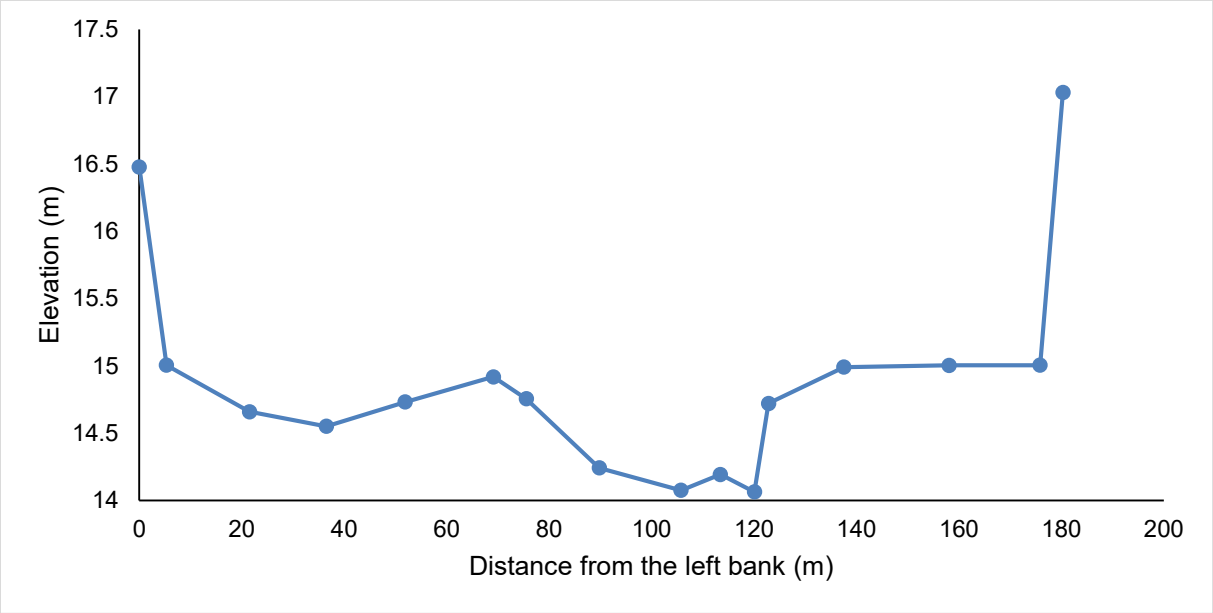


Figure 50: Cross-section of the Khado River at section R4 (X= 478,829.28, Y= 2,933,630.33)

7.2 Longitudinal profile analysis

A digital elevation map (DEM) of the whole study area including the headwaters of the watersheds were accessed from the online repository. DEM defines the topography of the study area and contains the elevation information of the location. For this study purpose the freely available ALOS-PALSAR DEM data with spatial resolution of 12.5m×12.5m was accessed from the online repository of Alaska Satellite Facility (https://asf.alaska.edu/data-sets/sar-data-sets/alos-palsar/). This DEM was further processed in the GIS application to fill the voids in data. The filled DEM was then used to generate the streamlines and watersheds of the whole study area. Each of the rivers were then extracted from the analysis. Chainage points in difference of 12.5 m were marked on each river from upstream to downstream section. The elevation values at these points were then extracted from the DEM map elevation. Thus X, Y and Z information along the river line was computed. This information was then used to plot the longitudinal profile of the rivers starting from the headwaters Figure 51.

The size of the sediment varies along the longitudinal profile of river and slope of the river reaches. Besides, the velocity of the water in the river reaches are dependent on the slope of the river reach. Thus, the longitudinal profile of the river is used for both hydraulic and sediment transport computations in later stage. A typical longitudinal profile of the Bagmati, Bakaiya and Ratu rivers generated from DEM are shown in Figure 51, Figure 52 and Figure 53 . The validation of elevation points obtained from the DEM and field survey is done for Ratu and Bakaiya river. The observed

values are in close match with the profile as shown in the profile drawing. The relative differences of elevation for DEM and survey data are same whereas the absolute values are also within 10% error margin. Profiles show steep river in upstream area and flatter in lower reaches, a typical characteristic of the river flowing from north to south in Nepal.

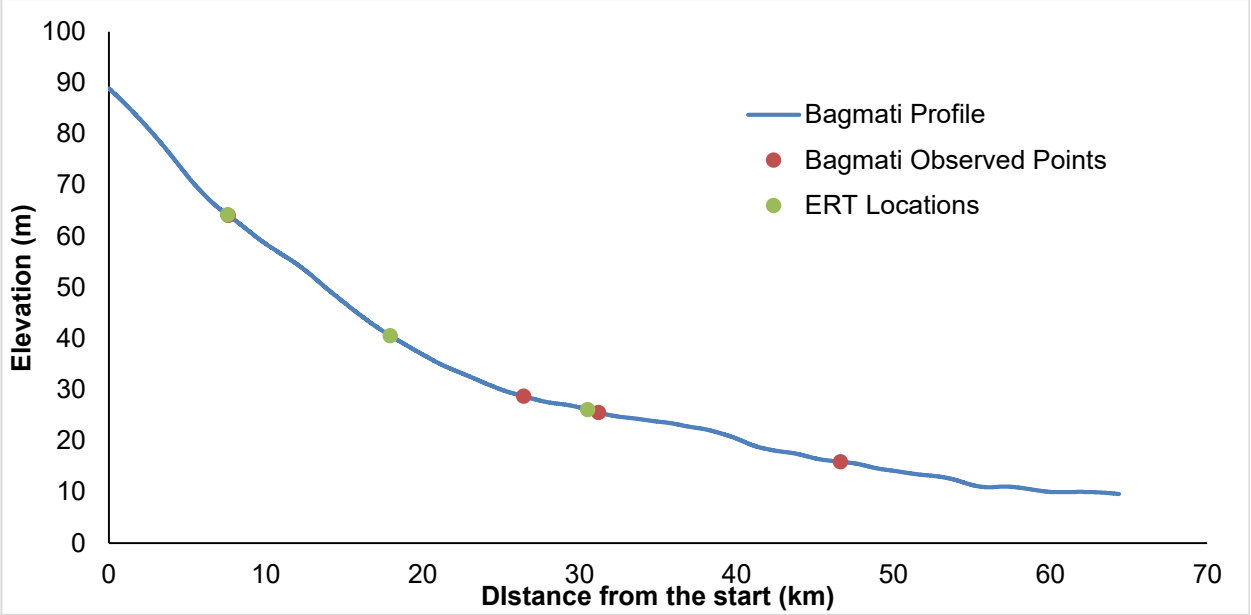


Figure 51: Longitudinal profile of the Bagmati River with location of field observation points and ERT data collection points

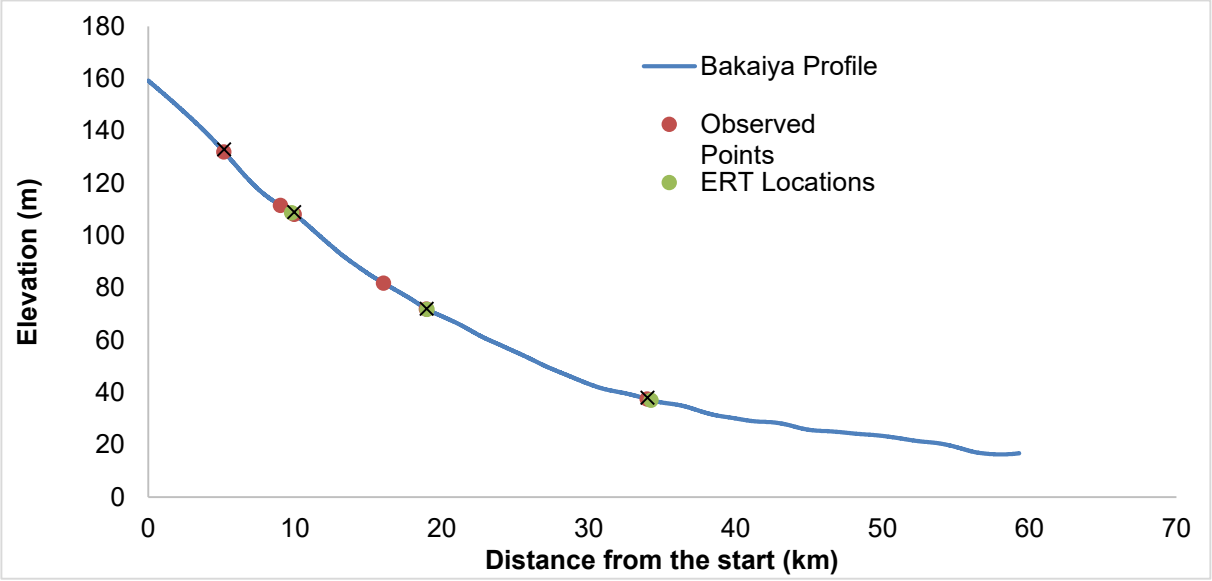


Figure 52: Longitudinal profile of the Bakaiya River with location of field observation points and ERT data collection points

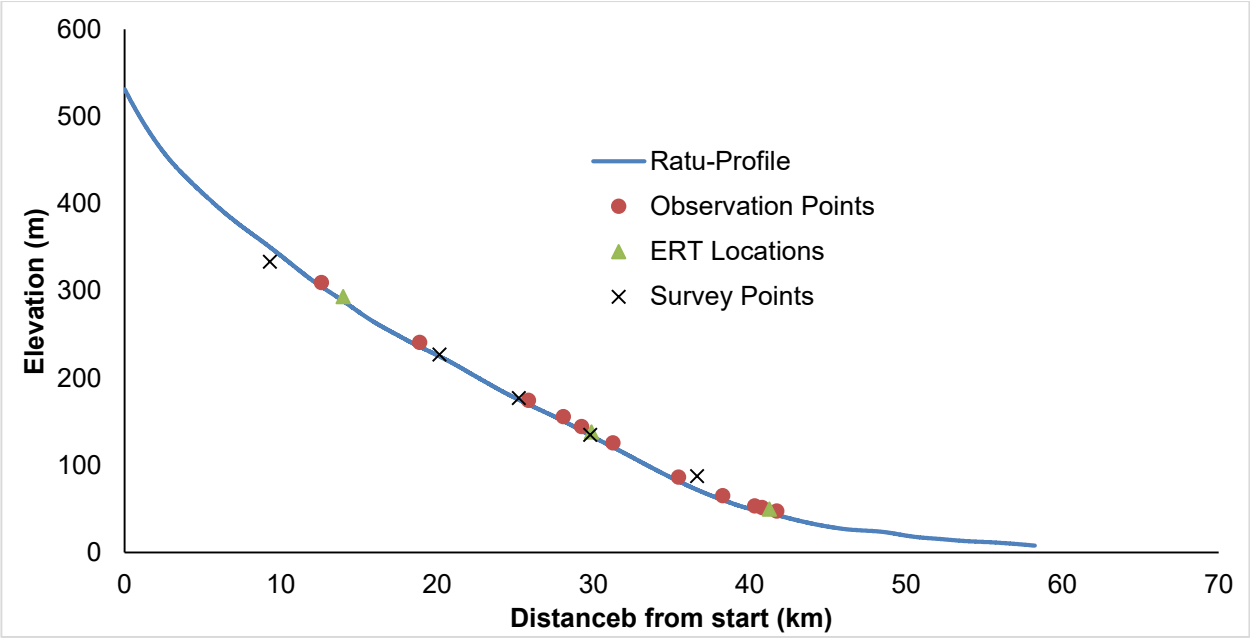


Figure 53:Longitudinal profile of the Ratu River with location of field observation points and ERT data collection points

The longitudinal profile of all rivers analyzed in this study are provided in Appendix-A.

8 Estimation of annual harvestable amount of sediment

8.1 Methods

A river system can be broadly classed into three zones namely: the production zone, the transport zone and the deposition zone (Shown in Figure 54). Sediment is dominantly produced in the headwaters, the upper portion of the river catchment where the slope is steep. In this study, Chure region is the sediment production zone. River channels in this zone have steep channel slope and have high sediment transport capacity, often exceeding the supply of the sediment. The middle part is a transport reach where a balance between the transport capacity and sediment supply rate is observed. In this study, the lower part of the Chure region are the transport zone. The lower most part is a deposition reach where the slope is mild and the sediment transport capacity is significantly reduced. As a result, major deposition of sediment occurs here. The Bhawar and the Terai areas are considered as the deposition zones in this study.

In Chure region, sediment generation from the watershed is a complex process and requires a detailed study involving rigorous data collection, at a catchment and watershed scale. Such approach is very resource intensive and could not be carried out in this study. The results of the engineering geological study and the sediment yield study provide only the qualitative understanding of the sediment production. The sediment yield models only include the sediment production by sheet erosion, which only reflects the production of the fine materials. Such models do not include the mass wasting phenomena, which is the major source of the coarse material production. So, the transport and the deposition zones of a river system are only considered in this study.

The sediments which are generated from upper reaches are regulated by the transport zones and then conveyed to the deposition zones. Theoretically, deposition zones are sediment laden zones from where the sediment extraction is possible without much altering the equilibrium state of the rivers. This is not possible in the transport zone where the supply and transport are in balance, nor in the generation zone where the channels are in a supply limited state. Thus, this study focuses on identification of the deposition zones and quantify the amount of harvestable sediment volume from those deposition zones.

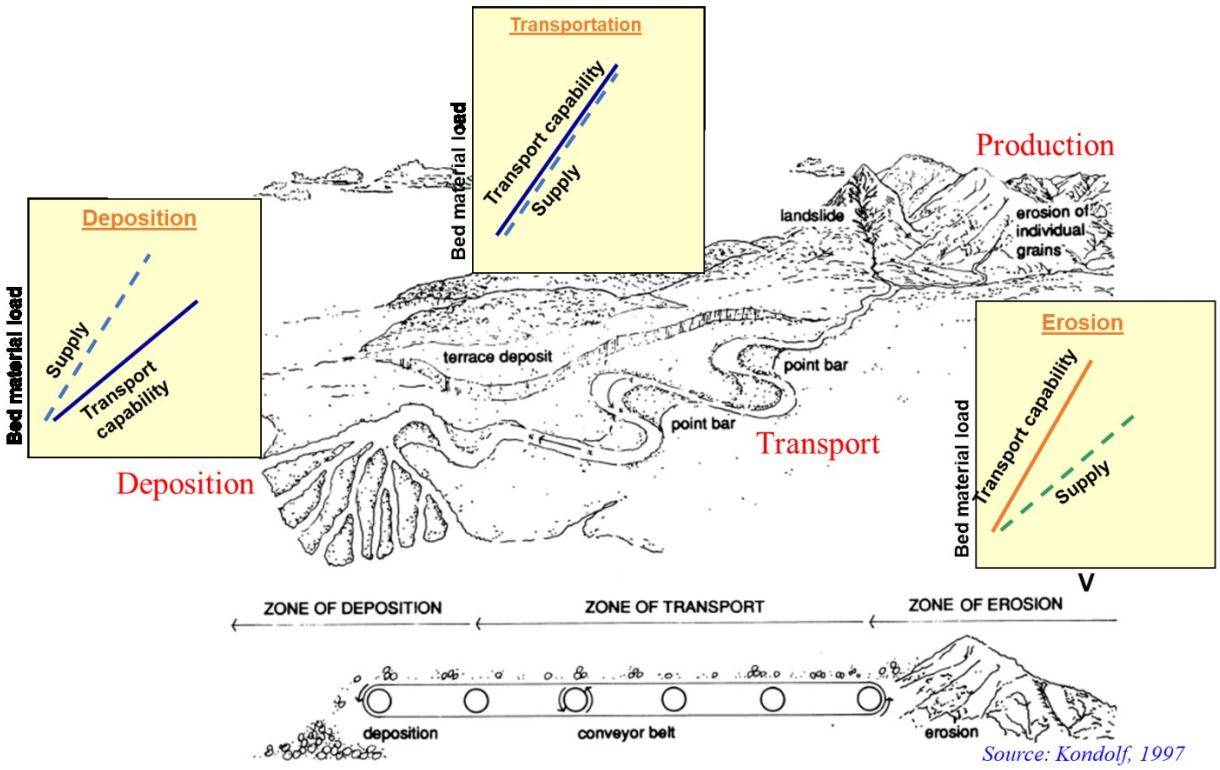


Figure 54: Sediment dynamics of a typical river system (Source: Kondolf, 1997)

8.2 Estimation of the hydraulic parameters of river reaches

Most of the river system in the Chure shows a braiding characteristic while flowing down from the hills towards the plains. This braiding creates a complex river system with spatial and temporal variability of discharge. Therefore, with this complicated system, arises a mammoth challenge and difficulty in predicting the sediment transport in the Chure river systems. The common practice of standard transport formulas using cross-sectional averaged data of river reach are unreliable. Recent progress in studies of reach-scale averaged bed elevation distribution for closely relating complex braided system into a single thread river has shown to be more efficient than earlier cross-sectional average practices. Thus, cross-sectional field data on reaches can be transformed to reach-scale geometric parameter derived on basis of the curve representing the cumulative distribution of the bed elevation. The new geometry based on the defined curve can then be used as a representative river section for the hydraulic computations. The details on the method can be referred to the Redolfi et al. (2016). A high-resolution topographic survey data on the river systems of Nepal is not available at present. So, representative river system of the area were selected for the field data collection. The acquired river cross-section data were analyzed.

The results were then transposed to other rivers in the study area based on the geomorphology of the river reaches and hydrological data.

For the area of interest, a cross sectional survey along the longitudinal profile of the river selected as representative river namely: Bakaiya, Balan, Bagmati, Khado and Ratu river were carried out. A cumulative distribution of width with increase of depth for each cross-section were computed. The distribution curve was the fitted with power law to derive the exponent coefficient values. The exponent coefficient of the fitted curve was then used for determining the representative new geometrical section for hydraulic and sediment flux computations. In Figure 55 α represents the value of exponent of the fitted curve for cumulative width and depth of river cross-section. The range of the expected value of α for different types of river cross-section are also shown in the figure (left). Finally, a representative cross section based on value of α is defined (right). This representative section is used for further computations.

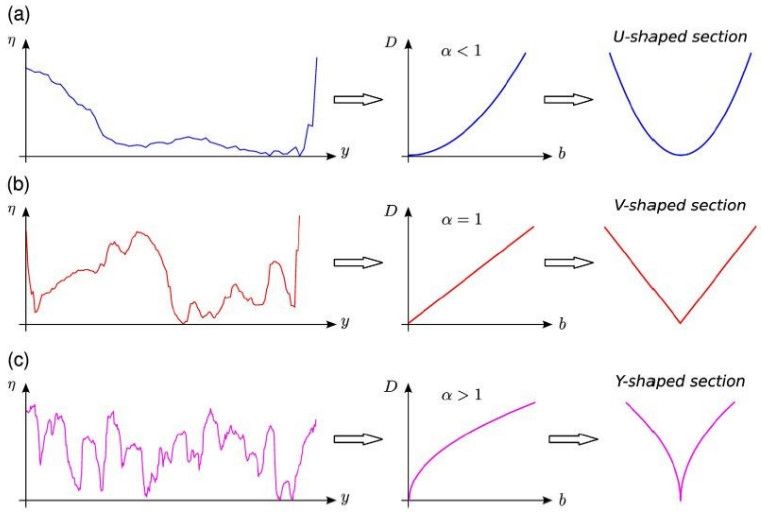


Figure 55: Representative cross-section of river based on their cross-sectional characteristics defined by the cumulative width and depth information

For other river system in the study area where detailed survey was not carried out, an approximate width of the river was computed from the latest geo-referenced aerial imagery database of Google earth. An example of cumulative width vs depth two cross section taken at the Balan and Khado River is shown in (Figure 56 and Figure 57). From the curve the values of α and K were extracted. The cumulative width vs depth of all cross-sections surveyed from the field are presented from Figure C-76 to Figure C-78, Appendix C.

The curve can be represented in the form shown in Equation 33.

$$W = KD^{\alpha} \quad (33)$$

Where,

W = width distribution of the river (m)

D = depth of the cross-section that passes discharge (m)

K = scale coefficient

α = exponent/coefficient of fitted curve

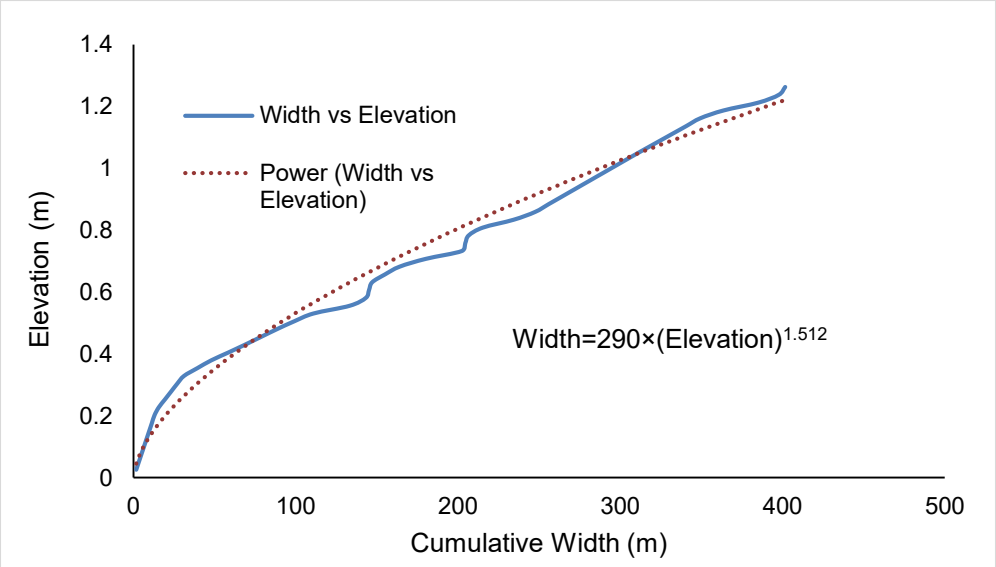


Figure 56: Y-Shaped distribution of cumulative river width vs water elevation calculated from field cross-section survey data of the Balan River at R1

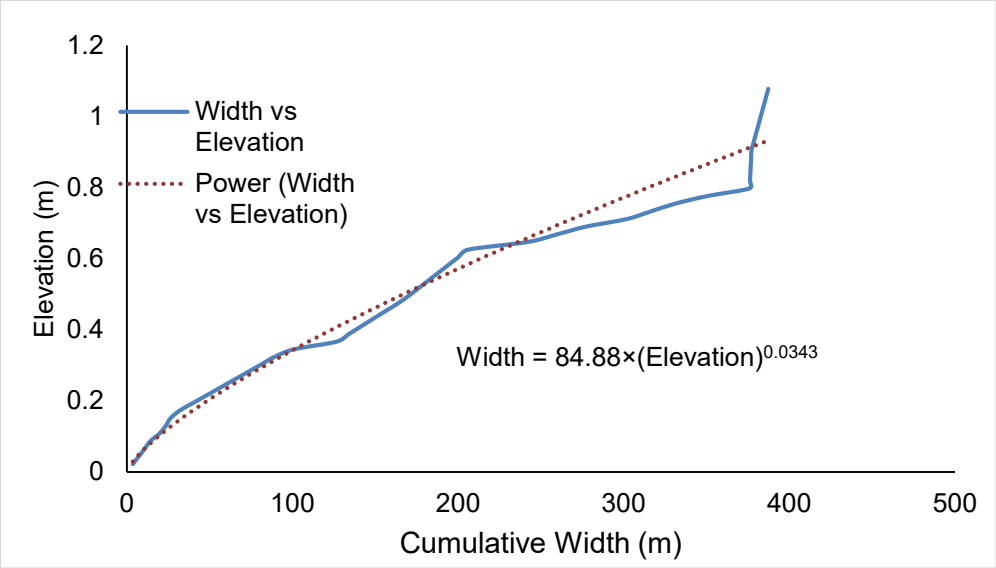


Figure 57: U-Shaped distribution of cumulative river width vs water elevation calculated from field cross-section survey data of the Khado River at R6

Thus, knowing width distribution and D we can find K and α. The main challenge is to survey along large number of river section. This is resources and time intensive, a limitation under current study time frame and budget, thus statistical regression analysis we adopted to estimate the relationship between the river width (W), K, α and maximum water depth (D) for the rivers where other intensive field measurements were not taken. At first, a relationship between the river width (W) and K was derived based on power regression (Shown in Figure 58 and Equation 34).

$$\boldsymbol{K = 1.366W^{0.834}} \qquad \textbf{34}$$

In second step, a regression equation between the "Stream Power" and alpha (α) was calculated using the Equation 35 shown in Figure 59.

$$\boldsymbol{Stream\ Power\ (P) = \gamma QS} \qquad \textbf{35}$$

Where,

γ = unit weight of water (kg/ms^2)

Q = discharge (m3/s)

S = slope of the river (-)

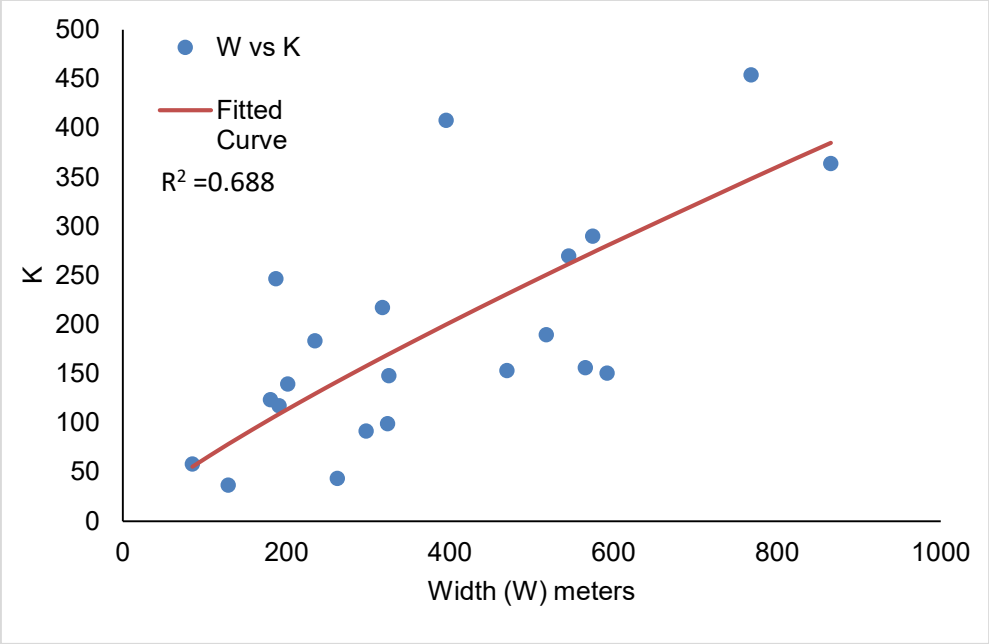


Figure 58: W vs K graph plotted for the results obtained from field survey

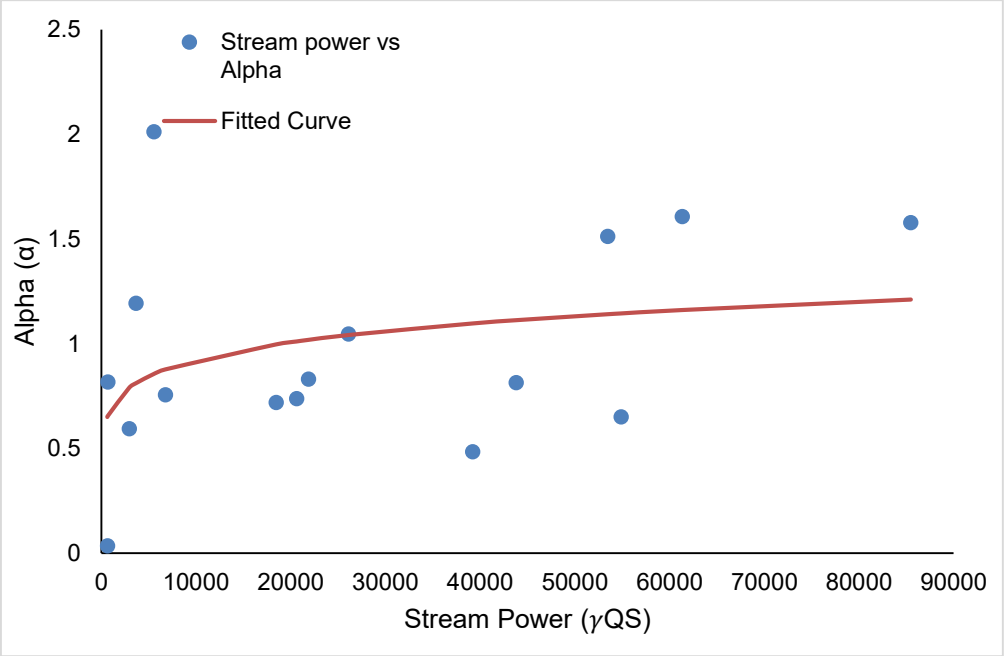


Figure 59:Stream power (P) vs alpha (α) graph plotted for the results obtained from field survey

$$\alpha = 0.286\ P^{0.1271}$$

36

Thus, from known Q and W in the reach the values of K and α were calculated. These values can be substituted in the Equation 33 to obtain the value of depth (D). The obtained D is maximum depth of the given section. This depth may not be fully attained for 2 years return period discharge passing through it. Since, our interest is to calculate the transport rate at bankfull discharge (in this case 2-year return period flow), we have to calculate the depth for which bankfull discharge is attained. The maximum possible value of depth is D, from which the bankfull discharge depth is calculated by based on iterative process using Equation 37.

$$\boldsymbol{Q = \frac{1}{n} A R^{2/3} S^{1/2}} \quad \textbf{37}$$

Where,

R = the hydraulic radius of given section i.e., ratio of Area to wetted perimeter (m)

A = the area of the cross section up to bankfull discharge depth (m^2)

S = the average slope of the river at the point (-)

n = Manning's coefficient for river reach based on its sediment characteristics i.e., n=0.050 for boulder reach, n=0.040 for gravel reach, n=0.035 for sand reach and n=0.050 for silt considering bedform roughness.

After the depth calculations, respective values of hydraulic radius, perimeter, flow velocities are calculated. These calculated hydraulic parameters are then used for sediment transport calculations.

8.3 Sediment transport of river reaches

Meyer-Peter & Müller Transport Formula was used in this study for calculating the sediment flux across the defined cross-section (Equation 38). This formula is useful for calculating the sediment transport in gravel bed rivers.

$$\boldsymbol{q_s = 13.3\sqrt{\Delta g D_m^3}\sqrt{(\theta - 0.047)^3}} \quad \textbf{38}$$

Where,

q_s = sediment transport rate per unit width ($m^3/s/m$)

$$\theta = \frac{u^2}{C^2 \Delta D_m} = Shields\ Parameter$$

C = Chezy Coefficient

D_m=median grain size diameter (D_{50})

The value of θ is dependent on the median grain size diameter of sediment. Since, the sediment size varies along the longitudinal profile of the river with coarse grained sediment mostly occurring in the steep upward zone of the river, and fines mostly on the lower flat slope reaches, the transport rate varies along the longitudinal profile. To address the variation of transport rate across the longitudinal profile of the river a correlation study on slope vs D_{50} grain size was done. The results show low level of correlation based on observed R^2 value Figure 60. The contribution of the Upper Siwalik in generation of the course (more abrasion resistant sediment) was observed to be high in the field observation. Based on this another correlation study was done using multivariate statistical approach between the slope, D50 and catchment area percentage of Upper Siwalik region. The results showed the improved correlation among variables Figure 61.

The final equation for calculating D_{50} based on the slope and area contribution of Upper Siwalik is given below Equation 39.

$$\boldsymbol{D_{50} = 7.151 + 17.910 \times S + 0.271 \times US - 0.2158 \times S \times US} \quad \textbf{39}$$

Where,

D_{50} is the median sediment size in mm

S is the percentage average slope of the given reach

US is the percentage contribution area of Upper Siwalik in total

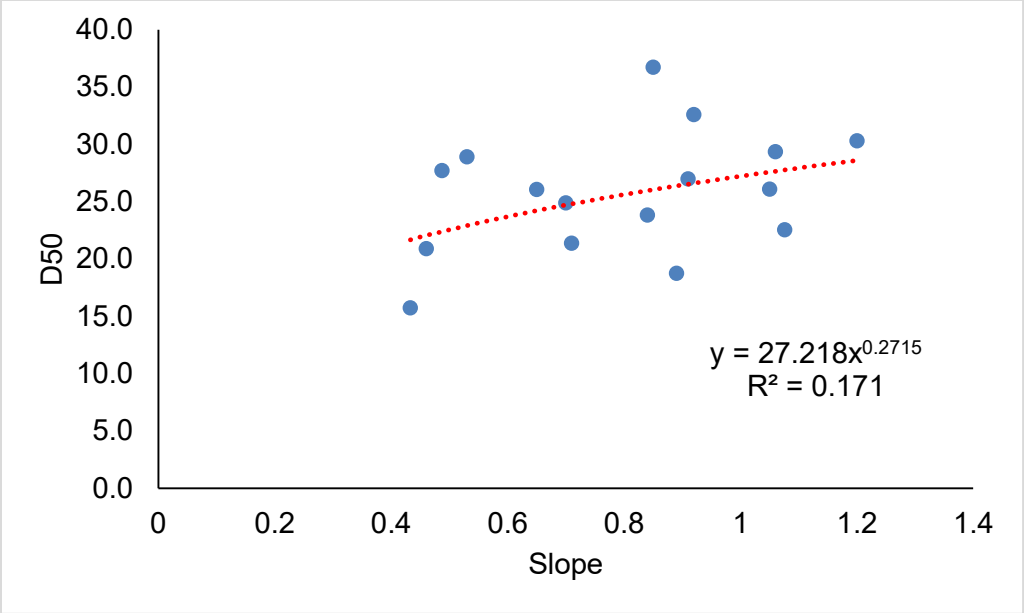


Figure 60: Slope vs D50 relation from selected rivers

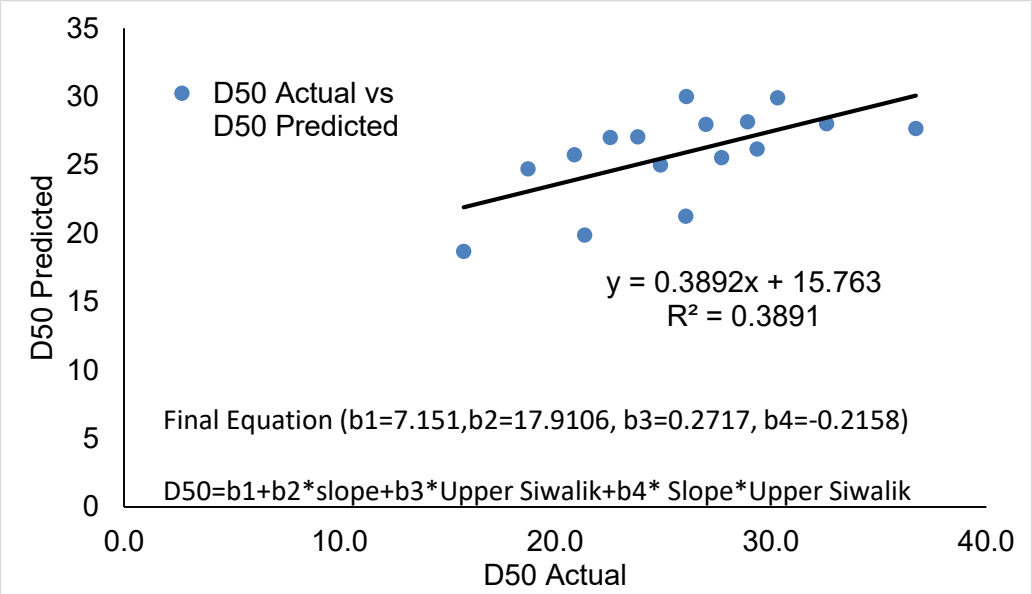


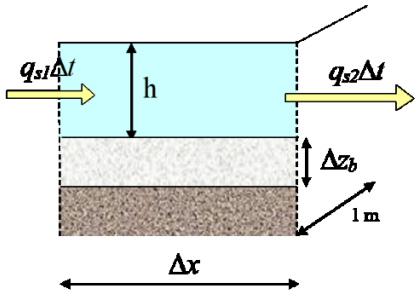
Figure 61: Multiple Linear Regression for D50, slope and Upper Siwalik

In the case of Bagmati and Kamala Rivers, which are perennial rivers, a fractional transport approach was adopted to compute the sediment transport of the reaches. The sediment transport capacity of sediment particles larger than 1 mm were first estimated and the particle size distribution of the transported sediment were computed proportionately to their transport rates. Finaly, the parameter values from hydraulic computations and sediment transport principles were

combined to calculate the erosion and deposition rate per year each pre-defined reaches of all river systems in Province 2.

8.4 Annual harvestable rate of sediment from river reaches

The river reaches in the lower Chure, Bhawar and Terai are first divided into several reaches, based on their planform and longitudinal slope. Then a simple sediment budget approach (Wishart et al., 2008) has been used to determine the sediment flux in the defined river reaches.



$$\frac{\partial z_b}{\partial t} = -\frac{\partial q_{Sb}}{\partial x}$$

Figure 62: Exner equation describing the mass conservation principle in sediment transport

A sediment continuity approach (Shown in in Figure 62) is used to model the conservation of mass between sediment in the bed of a channel and sediment that is being transported. This principle can be used to calculate the erosion or deposition in the given section. q_{s1} and q_{s2} are the sediment flux in and out of the control section of length Δx . In case of $q_{s1} > q_{s2}$, the influx of sediment is greater than the outflux, thus net gain in the control section and deposition occurs. For $q_{s1} < q_{s2}$, there is net loss in the control section and erosion occurs. The values of q_{s1} and q_{s2} has to be determined for the calculation of the deposition or erosion in the control section Figure 63. Similar approach has been used by Tamrakar & Maharjan (2020) to investigate the sediment dynamics and stability of Karra Khola in Hetuda.

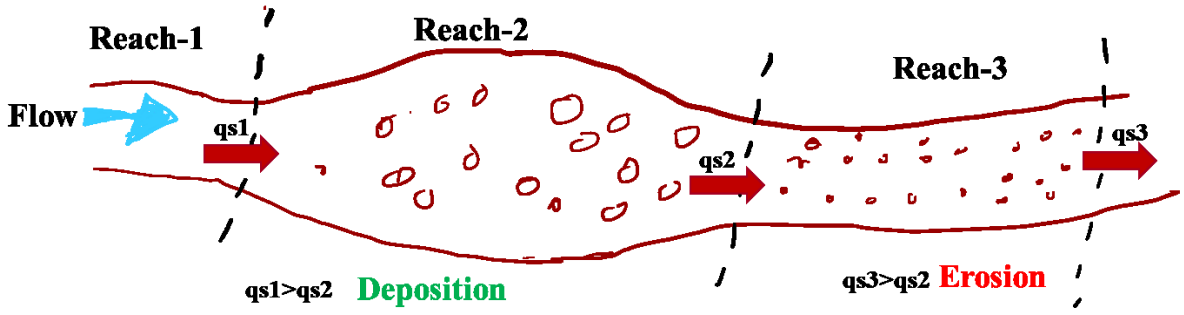


Figure 63: Depiction of erosion and deposition in different reaches

The geophysical study has shown that on average 10 m thick layer beneath river bed contains material suitable for the construction purpose (except for Khado River). However, this entire layer cannot be recommended for extraction on an annual basis because this exceeds the annual depositional volume by an order of magnitude. So, the harvestable amount of sediment from each reaches was estimated based on the computed volume of deposition. The depositional volume was multiplied by a factor of 0.3. The factor was determined combining mainly two elements. The first element is that the Meyer-Peter & Müller (1948) sediment transport formula is known to estimate sediment transport rates 2 – 2.5 times higher (Wong & Parker, 2006). The second element is that the estimated volume also contains uncertainties arising from the choices of parameters related to the hydrology, topography and sediment of the river reaches. So, only 50% of the estimated volume is considered for the abstraction considering these uncertainties. 38,888.79 Mm3 of sediment volume is estimated as the annual extraction volume from the river bed of river systems of Province 2. The details of the volume that can be extracted from the river systems of Province-2 are shown in Table 14. Similarly, the details of estimated sediment volume of extraction from river bed of river reaches of the river systems are presented in Appendix-A and Table D-28, Appendix D.

Table 14: Estimated annual harvestable sediment volume from river systems of Province-2, Nepal

River Systems	Number of reaches	Harvestable Volume (Mm3/year)
Badahar-Gagan Khola	10	1.60
Bagmati Main	4	12.10
Bagmati Nadi-Chadi Khola	12	4.33
Bagmati Nadi-Mansumara-Bagahi Nadi	8	1.14
Balan Nadi	55	7.80
Baluwa-Bilauti Nadi	4	0.02
Banke Hardi Khola	15	3.78
Bataha Khola	8	1.40
Bhalubahi-Bakhariya Nadi	13	1.95
Bigahi Khola	18	1.74
Bihul Nadi	5	0.00
Dhansar Khola	3	0.40
Dudhaura Khola	17	6.30
Ghurmi Khola	14	2.91
Jaladh Nadi	13	2.23
Jhim Nadi	15	10.35
Kamala Main	5	8.81
Kamala Nadi-Charnath Khola	5	1.02

River Systems	Number of reaches	Harvestable Volume (Mm3/year)
Khadak Nadi	17	0.07
Khado Khola	18	1.00
Lakhandehi Khola	52	8.00
Lal Bakaiya Nadi	21	6.65
Lamaha-Jhanj Khola	7	4.41
Mahuli Khola	10	0.54
Maraha Khola	24	4.97
Pasaha Khola	9	2.46
Pauda Khola	17	0.91
Paurai	4	0.04
Ratu Khola	22	4.81
Thute Sikhar Bas Khola	34	5.47
Tilabe Nadi	27	1.57
Trijuga Southern	3	0.00
Other Reaches	12	1.53
Grand Total	**501**	**110.29**

9 Impacts of riverbed sediment mining

9.1 Physical Environment

Most of the rivers in Province 2 originate from Chure and the area has a tropical to subtropical climate where the rainy season starts from June and ends in September. In the dry season, the dry and cold northwest wind bears little moisture. Since the whole area lies in the tropical region, April, May, June and July are the hottest months, whereas November, December, January and February are the colder months. The ambient air quality is expected to be within the National Ambient Air Quality Standards (NAAQS) of Nepal as there are no major industries and significant traffic volumes along the river side. The nearest industrial center is located in Hetauda and Rajbiraj. Most of the rivers are sandwiched by roads. The land is dominated by forests, agricultural lands and associated residential areas. The quality of noise levels in the area is expected to be within permissible standards. However, crusher plants and parallel roads are found on the bank of the rivers make noise. The river passes from the Churiya to Gangetic Plain in Terai region and flash floods and high sediment transport are common during monsoon. The river bank cutting is common to all rivers. Ground water is plenty on the lower parts (below 300 m).

9.2 Biological Environment

The forest in the entire catchment of rivers is broadly classified as sal, khayer, sisau, and terai hardwood. Forests are mostly dominated by Sal wood. In the nearby banks of rivers, there are primarily Sisau, Khayer, Yellow Tik. Sal forest has a high economic contribution in this area. Hence this area is the richest in forest biodiversity. All banks of rivers have plenty of non-timber forest products. About two dozen non timber forest product species are considered as high potential for economic value. Several species use their leaves, fibre, fruits for different respectives purposes and many plants with high herbal values. There are several forests protected by the government and community (Samudayik Ban) themselves. The forests serve as a good wild animal habitat for animals such as monkeys, jackals, squirrels, ghorals, chituwa (leopards), bagh (tigers), other birds and numerous other small insect types. There are several natural wetlands near the banks of the river.

9.3 Social Environment

The Chure river side is fragile and fertile land. There are several settlements on the banks of all rivers. Some of them have no land ownership certificate also. Most of people earning is agriculture, daily wages and as temporary foreign migrant workers, servicemen and business

entrepreneurs small to large. There are some sugar and other factories along the highway. Many people are employed in these factories. The sand and aggregate mining activity is increasing in almost all rivers. This helps income generation or opportunity of employment to the nearby resident people.

9.4 Environmental and social impacts

9.4.1 Beneficial impact

There is increase in income generation due to local employment of low income people in crusher related job self-entrepreneurship (tea stall etc due to river material transporter flow) and revenue generation to local government from river mining, forest etc. The sediment mining can also help in maintaining a passage of floods in rivers which have been clogged due to excess material deposition, thus reducing damages to the humans and infrastructures.

9.4.2 Adverse impact

The unregulated and excessive riverbed mining practices can have adverse environmental and social impacts during all their major phases - extraction, processing and transport. The impacts are explained as follows:

9.4.2.1 Physical impacts of river mining

The physical impacts of of the sediment mining from the river bed is mainly observed in the river channels and its corridors. This is usually the case when the extracted volume of the sediment from the river bed is more than the river system can naturally replenish. The following physical impacts common due to riverbed sediment mining:

- A decrease in bedload downstream of the mining area resulting in degradation of the riverbed downstream.
- Increase of river gradient at the site of excavation resulting in degradation of the riverbed upstream.
- Lowering of the river bed results in lowering of the groundwater table in the flood plain, thus impacting the agriculture practices. Similarly, lowered bed levels also result in difficulty of maintaining the intake of water for irrigation schemes.
- Erosion of material from bridge foundations thus damaging the bridge infrastructure. Bridge of Ratu River was damaged due to settlement of bridge pier caused by lowering of riverbed due to riverbed gravel mining (Shown in Figure 64).
- A change in stream course, causing bank erosion and shifting of the river course. The shifting of the river course cause loss of land and pose threat to human and infrastructures in the flood plain.



Figure 64: Damage to the East-West Highway bridge over Ratu River Caused by the settlement of the pier. The river bed has lowered by at least 2.5 m due to riverbed sediment mining. A newly constructed bridge can be observed behind the damaged bridge.

9.4.2.2 Biological impacts

Most of the Rivers systems of study area are ephemeral. Ephemeral streams are not suitable for the aquatic species unlike perennial rivers. Their role in ecosystem of the Chure, Bhawar and Terai is not well known. However, the riverbank erosion and shifting of the river channels cause direct loss of riverbank and floodplain habitat. In the case of perennial rivers like Bagmati and Kamala, the physical changes in the river channels and water quality have negative effects on instream biota, food webs, and fish and fisheries.

9.4.2.3 Socio-economic impacts

Riverbed sediment mining in Province-2 is one of the major sources of income, employment and local government revenue. However, the labour status in this sector is poorly monitored and regulated. Workers are usually informally employed, exploited and receive very low wages. The income opportunities also may detract young people from education (school) towards working in crusher related job.

Other negative socio-economic impacts of river sand mining may include, for example, damage to roads by heavy vehicle loads, and noise and dust during transport and from crusher plants. The vehicles may also damage farmer canal (paini) in the river banks thus impacting agriculture.

9.5 Good practices for gravel mining

The common sediment extraction methods are: river bed mining, mining of river deposits from active channel, wet and dry pit excavation from the immediate flood plain or terraces (Shown in Figure 65). Whereas the common extraction techniques practiced are: skimming a shallow layer, by pitting, by trenching, by capture in pre-dug pits, by removal of selected bed material (boulders), etc. The riverbed sediment extraction from the thalweg of the river channel must be avoided because of its maximum impact to the river channel. Such practice shall be only allowed when the river channel is clogged with sediment, for achieving the safe passage of the flood. Sediment extraction by skimming a shallow layer is preferred for extraction from the deposits in the active channel (Shown in Figure 66). Pitting and trenching must be avoided because of its higher physical impact to the upstream and the downstream (shown in Figure 67).

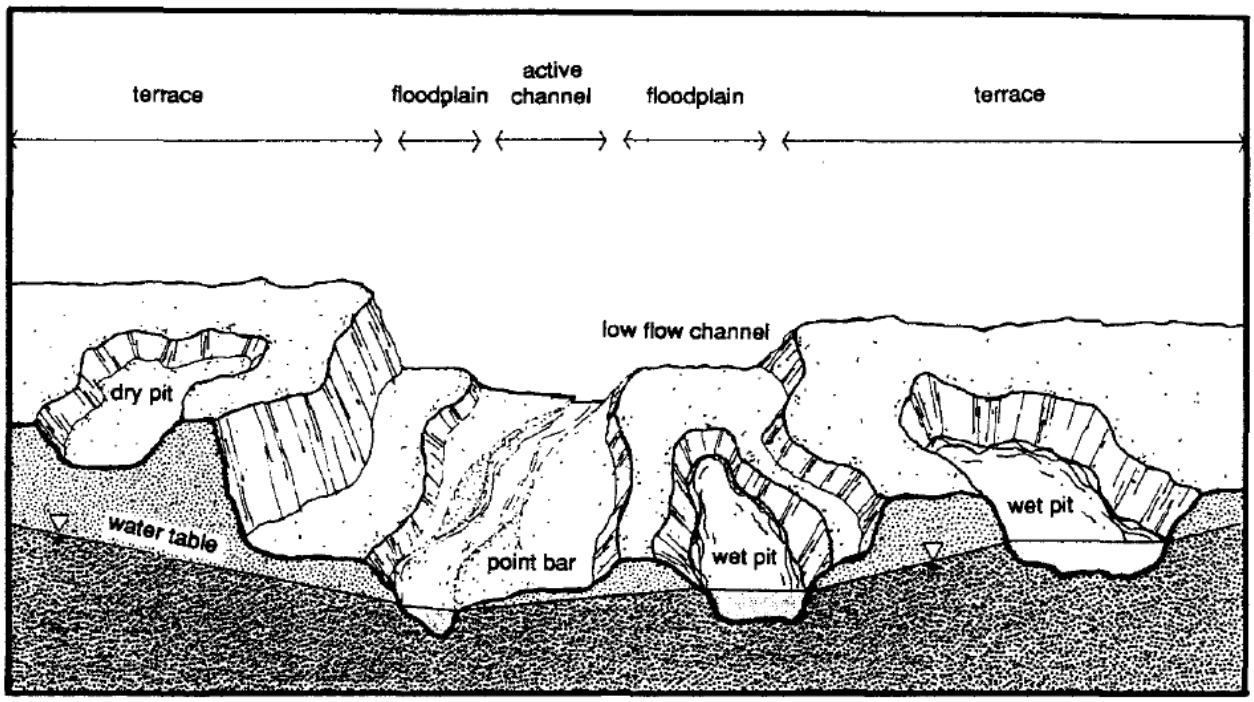


Figure 65: Commonly adopted gravel mining practices (*Source:* Kondolf, 1993)

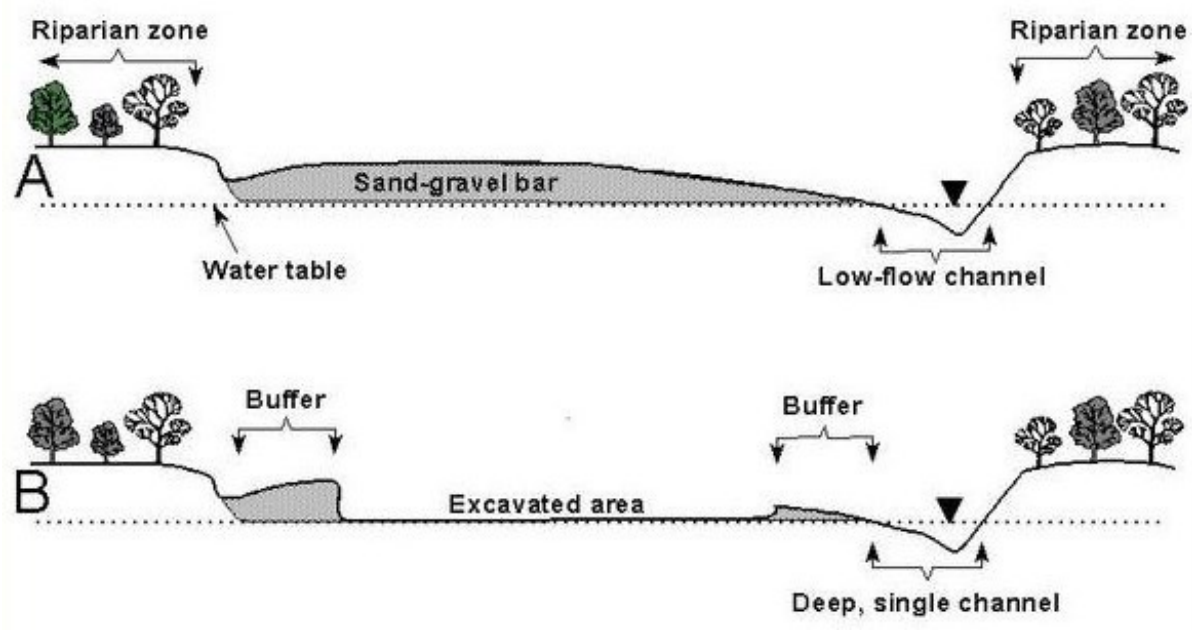


Figure 66: Sediment extraction by bar skimming (Source: http://threeissues.sdsu.edu/three_issues_sandminingfacts02.html)

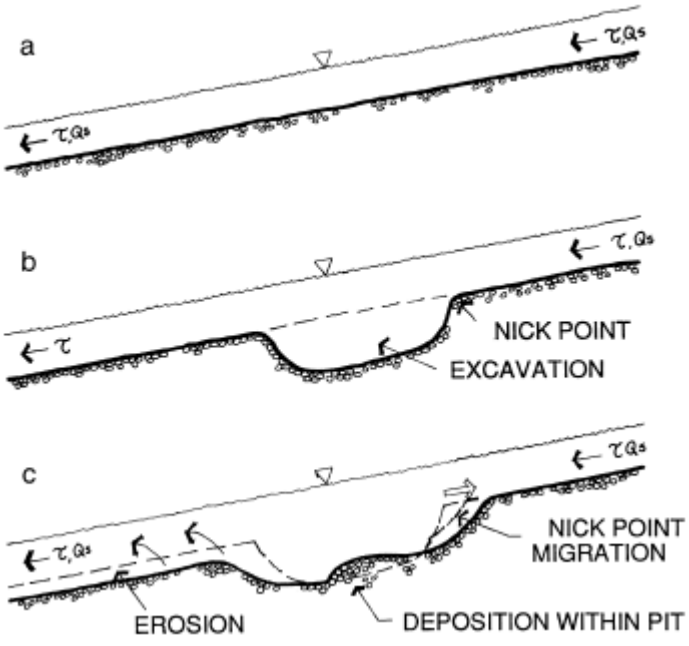


Figure 67: The upstream and downstream effects of mining by pit or trench excavation (Source: M. G. Kondolf, 1997).

Dry pits are preferred over wet pits, while extracting sediment from the flood plains and terreces, because of their minimum interference with the ground water table. Sediment extraction by both manual methods and using heavy machinery were observed during the field visit (Figure 68).

Manual extraction methods provide most employment, and minimise pollution risks to the water environment. So they must be encouraged over extraction using heavy machinery.



Figure 68: a) Sediment extraction by manual methods near observation point Bakaiya-2; b) Sediment extraction by using machines at the observation point Bakaiya-5.

10 Conclusions and Recommendations

10.1 Conclusions

The annual extraction volume of sediment from the river beds of River Systems, located in Province-2, is estimated using the sediment budget method. The method is based on the annual replenishing rate of the river. From the study, the annual sediment extraction volume from 39 river systems of Province-2 is estimated as 110.3 Mm^3. Only two River systems: Kamala and Bagmati Rivers, which originate from the Mahabharata range are perennial rivers. These perennial rivers resulted in the highest amount of harvestable sediment volumes. A 12.5 km long reach of Bagmati River, starting 2.5 km downstream of the exiting bagmati irrigation barrage, resulted in 9 Mm^3/year harvestable volume, which is highest amongst all river reaches. On an average, the sediment up to the depth of 10 m below the river bed in the Bhawar region consisted of a materials deemed suitable for construction works. However, this volume exceeds the annual replenish rate of the river by more than 10 times. So excavation of the entire depth is deemed unsustainable. The details of the harvestable sediment from the river reaches is presented in Appendix-A.

The geological composition of the catchments influenced the size and type of materials in the river bed. The Upper Siwalik, which consisted of the unconsolidated deposits, produced materials that are more resistant to abrasion. So, the river systems consisting of Upper Siwalik geology in the catchment were observed steeper, in the Bhawar region, and they transported gravels to a longer distance from the source. The Middle and the Lower Siwalik is mostly dominated by sand stone and mud stone, which can disintegrate easily into sand or silt during the transport process. So, the river systems dominated by the Middle and the Lower Siwalik geology are observed milder, in the Bhawar region, and the river bed material is dominated by sand.

10.2 Recommendation

The annual harvestable volume of sediments from river system is estimated based on a sediment budget method. The method is applied to this study with some limitations. So based on the experience and insights gained during this study the following recommendations are made:

- The sediment budget method determines the replenishing rate of the river reaches by computing the erosion and deposition of the river bed of the reaches. The results obtained from this study should be validated in the field before its application. The validation can be performed by measuring the average bed level changes along the river reach. The bed

level changes can be estimated by performing the topographic survey of the river reach before and after the monsoon period.

- The sediment budget method is principally governed by the sediment transport characteristics of the river reaches. The available sediment transport formulations in the literature, including the one used in this study, are derived in idealized laboratory experiments. The hydraulics in natural rivers are very different from these experimental conditions. So field measurements and study of sediment transport of River Systems of Chure-Bhawar region are recommended. A good field based understanding of the phenomena will help to improve the results of the sediment budget method.
- The sediment yield from the catchment has a key influence in the replenishing rate of the river. The sediment yield models available in the literature do not consider all dominant processes (mainly mass wasting phenomena) for sediment yield from the Chure region. So a study of sediment yield estimation from Chure region is also recommended.
- Most of the rivers originating from the Chure region are ephemeral. The rainfall in the catchments and the flow in the rivers in this region are not monitored. So, the duration of flows and floods in these, which heavily influence the estimation of erosion/ deposition, is unknown. So, installation of flow and rainfall monitoring stations are recommended in the River Systems of Chure region to determine the flow and flood characteristics of the river reaches.
- The sediment transport and morphdynamics in the braided rivers are highly variable both longitudinally and lateral. Morphological modelling using at least 2-D numerical model is required for understanding the morphological complexities of such river reaches. Such understanding would help in predicting the impacts of the sediment mining.
- The methods does not include the cumulative impacts of the sediment mining from different reaches and other human interventions in the same river. So a detailed study including such aspects is required estimate the sustainable harvestable sediment volume from the River Systems.

11 References

Abidin, M. H. B. Z., Ahmad, R. B. S. and F. B., Wijeyesekera, D. C., & Baharuddin, M. F. B. T. (2012). Integral Analysis of Geoelectrical (Resistivity) and Geotechnical (Spt) Data in Slope Stability Assessment. *Academic Journal of Science*, *1*(2), 305–316. Retrieved from https://www.researchgate.net/publication/234054357_Integral_Analysis_of_Geoelectrical_Resistivity_and_Geotechnical_SPT_Data_in_Slope_Stability_Assessment

Adhikari, D. P., & Koshimizu, S. (2005). Debris flow disaster at Larcha, upper Bhotekoshi Valley, central Nepal. *The Island Arc*, *14*(4), 410–423. https://doi.org/10.1111/j.1440-1738.2005.00495.x

Bhandari, B. P., & Dhakal, S. (2019a). Evolutional Characteristics of Debris Flow in the Siwalik Hills of Nepal. *International Journal of Geosciences*, *10*(12), 1049–1067. https://doi.org/10.4236/ijg.2019.1012060

Bhandari, B. P., & Dhakal, S. (2019b). Topographical and geological factors on gully-type debris flow in Malai River catchment, Siwaliks, Nepal. *Journal of Nepal Geological Society*, *59*, 89–94. https://doi.org/10.3126/jngs.v59i0.24994

Bhandari, B. P., & Dhakal, S. (2020). Spatio-temporal dynamics of landslides in the sedimentary terrain: a case of Siwalik zone of Babai watershed, Nepal. *SN Applied Sciences*, *2*(5), 854. https://doi.org/10.1007/s42452-020-2628-0

Bilham, R., Blume, F., Bendick, R., & Gaur, V. (1998). Geodetic constraints on the translation and deformation of India: Implications for future great Himalayn earthquakes. *Current Science*, *74*(3), 213–229.

Dhakal, Subodh. (2015). Evolution of Geomorphologic Hazards in Hindu Kush Himalaya (pp. 53–72). https://doi.org/10.1007/978-4-431-55242-0_4

Dhakal, Susmita, Cui, P., Rijal, C. P., Su, L., Zou, Q., Mavrouli, O., & Wu, C. (2020). Landslide characteristics and its impact on tourism for two roadside towns along the Kathmandu Kyirong Highway. *Journal of Mountain Science*, *17*(8), 1840–1859. https://doi.org/10.1007/s11629-019-5871-3

Dhital, M. R. (2015). *Geology of the Nepal Himalaya*. Cham: Springer International Publishing. https://doi.org/10.1007/978-3-319-02496-7

Efthimiou, N., Lykoudi, E., & Karavitis, C. (2017). Comparative analysis of sediment yield estimations using different empirical soil erosion models. *Hydrological Sciences Journal*, *62*(16), 2674–2694. https://doi.org/10.1080/02626667.2017.1404068

Ettazarini, S., & Jakani, M. El. (2017). ASSESSMENT OF SOIL LOSS RISK USING INTEGRATED REMOTE SENSING AND GEOGRAPHIC INFORMATION SYSTEM (GIS) TECHNIQUES IN THE ARGANA BASIN , MOROCCO, *320*, 186–194.

Foster, G. R., McCool, D. K., Renard, K. G., & Moldenhauer, W. C. (1981). Conversion of the universal soil loss equation to SI metric units. *Journal of Soil and Water Conservation*, *36*(6), 355–359.

Gangopadhyay, S. (2013). *Engineering Geology*. Oxfor University Press.

Ganseer, A. (1964). *Geology of the Himalayas*. New York: Interscience.

Griffiths, G. A., & McKerchar, A. I. (2008). Dependence of flood peak magnitude on catchment area. *Journal of Hydrology (New Zealand)*, *47*(2), 123–131. Retrieved from http://www.jstor.org/stable/43944969

Hagen, T. (1969). Report on the Geological Survey of Nepal, Vol.1: Preliminary reconnaissance. *Denkschriften Der Schweizerischen Naturforschenden Gesellschaft Memoires de La Societe Helvetique Des Sciences Naturelles*, *84*(1), 185.

IAEG. (1992). Homepage of IAEG. Retrieved December 10, 2010, from http://www.iaeg.info

Keller, G. V., & Frischknecht, F. C. (1966). *Electrical methods in geophysical prospecting*. Oxford, UK: Pergamon Press Inc.

Kondolf, G. M. (1993). The reclamation concept in regulation of gravel mining in California. *Journal of Environmental Planning and Management*, *36*(3), 395–406. https://doi.org/10.1080/09640569308711954

Kondolf, G. M. (1997). PROFILE: Hungry Water: Effects of Dams and Gravel Mining on River Channels. *Environmental Management*, *21*(4), 533–551. https://doi.org/10.1007/s002679900048

Kondolf, M. G. (1997). Hungry Water: Effects of Dams and Gravel Mining on River Channels. *Environmental Management*, *21*(4), 533–551. https://doi.org/10.1007/s002679900048

Loke, M. H. (2012). *2-D and 3-D electrical imaging surveys*. *Tutorial*.

Lowrie, W., & Fichtner, A. (2020). *Fundamentals of Geophysics*. Cambridge University Press. https://doi.org/10.1017/9781108685917

Meyer-Peter, E., & Müller, R. (1948). Formulas for Bed-Load Transport. *International Association for Hydraulic Structures Researach - Zweite Tagung - Second Meeting - Deuxième Réunion*.

Neitsch, S. L., Arnold, J. G., Kiniry, J. R., Srinivasan, R., & Williams, J. R. (2002). Soil and Water Assessment Tool User's Manual. *TWRI Report TR-192*, 412.

Pandey, A., Mishra, S. K., & Gautam, A. K. (2015). Soil Erosion Modeling Using Satellite Rainfall Estimates. *Journal of Water Resource and Hydraulic Engineering*, *4*(4), 318–325. https://doi.org/10.5963/JWRHE0404002

Pandey, K. K., Abhash, A., & Prakash Tripathi, R. (2020). Revised Dicken's method for flood frequency estimation of Upper Ganga basin. *Journal of Hydrology*, *586*, 124904. https://doi.org/10.1016/j.jhydrol.2020.124904

Pazdirek, O., & Blaha, V. (1996). Examples of resistivity imaging using ME-100 resistivity field acquisition system. In *EAGE 58th Conference and Technical Exhibition*. Housten, the Netherlands.

Popescu, M. E. (1994). A suggested method for reporting landslide causes. *Bulletin of the International Association of Engineering Geology*, *50*(1), 71–74. https://doi.org/10.1007/BF02594958

Redolfi, M., Tubino, M., Bertoldi, W., & Brasington, J. (2016). Analysis of reach-scale elevation distribution in braided rivers: Definition of a new morphologic indicator and estimation of mean quantities. *Water Resources Research*, *52*(8), 5951–5970. https://doi.org/10.1002/2015WR017918

Renard, K., Foster, G., Weesies, G., McCool, D., & Yoder, D. (1997). Predicting soil erosion by water: a guide to conservation planning with the Revised Universal Soil Loss Equation (RUSLE). *Agricultural Handbook No. 703*. https://doi.org/DC0-16-048938-5 65–100.

Renard, K. G., & Freimund, J. R. (1994). Using monthy precipitation data to estimate R-factor in the revised USLE. *Journal of Hydrology*, *157*(October 1993), 287–306.

Rinaldi, V. A., & Cuestas, G. A. (2002). Ohmic Conductivity of a Compacted Silty Clay. *Journal of Geotechnical and Geoenvironmental Engineering*, *128*(10), 824–835. https://doi.org/10.1061/(ASCE)1090-0241(2002)128:10(824)

Sakai, & H. (1983). Geology of the Tansen Group of the Lesser Himalaya in Nepal. *Mem. Fac. Sci. Kyushu University*, *25*, 27–74. Retrieved from http://ci.nii.ac.jp/naid/80001912241/en/

Sasaki, Y. (1992). Resolution of resistivity tomography inferred from numerical simulation. *Geophysical Prospecting*, *40*(4), 453–463. https://doi.org/10.1111/j.1365-2478.1992.tb00536.x

Sharma, K. P., & Adhikari, N. R. (2004). *Hydrological Estimations in Nepal*. DHM, GON.

Siddiqui, F. I., & Osman, S. B. harom A. B. S. (2012). Integrating Geo-Electrical and Geotechnical Data for Soil Characterization. *International Journal of Applied Physics and Mathematics*, *2*(2), 104–106. https://doi.org/10.7763/ijapm.2012.v2.63

Sinha, R., Gupta, A., Mishra, K., Tripathi, S., Nepal, S., Wahid, S. M., & Swarnkar, S. (2019). Basin-scale hydrology and sediment dynamics of the Kosi river in the Himalayan foreland. *Journal of Hydrology*, *570*, 156–166. https://doi.org/10.1016/j.jhydrol.2018.12.051

Sudha, K., Israil, M., Mittal, S., & Rai, J. (2009). Soil characterization using electrical resistivity tomography and geotechnical investigations. *Journal of Applied Geophysics*, *67*(1), 74–79. https://doi.org/10.1016/j.jappgeo.2008.09.012

Tamrakar, N. K., & Maharjan, S. (2020). SEDIMENT DYNAMICS AND STABILITY STATUS OF THE KARRA KHOLA, HETAUDA DUN VALLEY, CENTRAL NEPAL SUB-HIMALAYA. *International Journal of Engineering Technologies and Management Research*, *7*(11), 50–68. https://doi.org/10.29121/ijetmr.v7.i11.2020.815

Telford, W. M., Geldart, L. P., & Sheriff, R. E. (1990). *Applied Geophysics*. Oxford, UK: Cambridge University Press.

Tezel, O., & Ozcep, F. (2003). Relationships of electrical resistivity and geotechnical parameters. In *Proc. Conf. on Earth Sciences and Electronics*. Istanbul, Turkey.

TU-CDES. (2016). *Landslide Inventory Charchterization and Engineering Design for Mitigation Works of Chure Area in Ten Districts*.

Uddin, K., Shrestha, H. L., Murthy, M. S. R., Bajracharya, B., Shrestha, B., Giliani, H., et al. (2014). Development of 2010 national land cover database for the Nepal. *Journal of Environmental Management*, (September). https://doi.org/10.1016/j.jenvman.2014.07.047

Upreti, B. . (1999). An overview of the stratigraphy and tectonics of the Nepal Himalaya. *Journal of Asian Earth Sciences*, *17*(5–6), 577–606. https://doi.org/10.1016/S1367-9120(99)00047-4

Varnes, D. J. (1978). Slope movement types and processes. *Landslides : Analysis and Control*. Retrieved from http://ci.nii.ac.jp/naid/10019933719/en/

Wischmeier, W., Smith, D. D., Wischmer, W. H., & Smith, D. D. (1978). Predicting rainfall erosion losses: a guide to conservation planning. *U.S. Department of Agriculture Handbook No. 537*, 1–69. https://doi.org/10.1029/TR039i002p00285

Wishart, D., Warburton, J., & Bracken, L. (2008). Gravel extraction and planform change in a wandering gravel-bed river: The River Wear, Northern England. *Geomorphology*, *94*(1–2), 131–152. https://doi.org/10.1016/j.geomorph.2007.05.003

Wong, M., & Parker, G. (2006). Reanalysis and Correction of Bed-Load Relation of Meyer-Peter and Müller Using Their Own Database. *Journal of Hydraulic Engineering*, *132*(11), 1159–1168.

Yoshino, K., & Ishioka, Y. (2005). Guidelines for soil conservation towards integrated basin management for sustainable development: A new approach based on the assessment of soil loss risk using remote sensing and GIS. *Paddy and Water Environment*, *3*(4), 235–247. https://doi.org/10.1007/s10333-005-0023-5

Zhody, A. A. R., Eaton, G. P., & Mabey, D. R. (1974). *Application of surface geophysics to ground-water investigations*. https://doi.org/10.3133/twri02D1